Dissertation
Submitted to the
Combined Faculties for the Natural Sciences and for Mathematics
of the Ruperto-Carola University of Heidelberg, Germany
for the degree of
Doctor of Natural Sciences

presented by

Ekaterina Korotkevich
born in Novosibirsk, Russia
Oral-examination: July 17, 2015

Symmetry breaking in mouse development

Referees: Prof. Dr. Oliver Gruss
Dr. Alexander Aulehla

This work was carried out at the European Molecular Biology Laboratory in Heidelberg from October 2011 to May 2015 under supervision of Dr. Takashi Hiiragi.

Summary

Unlike many other species, where the body plan is already pre-patterned in the oocyte or upon fertilization, in the early mouse embryo there is no asymmetry up to 8-cell stage when all cells in the embryo have the same morphology and developmental potential. As development proceeds initially identical cells of the embryo segregate into two distinct cell lineages: trophectoderm (TE) and the inner cell mass (ICM) (Wennekamp et al., 2013; Rossant and Tam, 2009; Yamanaka et al., 2006). While both apical-basal cell polarity (Hirate et al., 2013; Alarcon, 2010) and cell-cell adhesion (Stephenson, Yamanaka and Rossant, 2010) are required for this differentiation, the decisive cue that breaks symmetry between the cells and is sufficient for specifying the first cell fate remains to be identified (Wennekamp et al., 2013).

To understand the mechanism underlying the symmetry breaking in the mouse embryo, in this study I have established a new experimental system in which an blastomere isolated at the 8-cell stage (1/8th blastomere) recapitulates the first lineage segregation between TE and ICM during its development into 4/32th mini-blastocyst. Using live-imaging and quantitative image analysis, I identified that inheritance of the apical domain during 1/8th-to-2/16th-cell stage division allows for predicting the process leading to TE fate specification. The majority of 8-cell blastomeres undergo asymmetric division defined by the differential segregation of the apical domain among daughter cells. In the 8-cell stage embryo, the apical domain, emerging at the center of the contact-free surface of the blastomere, recruits microtubule organizing centers to the sub-apical region, thereby forming one of the acentrosomal spindle poles and inducing the asymmetric division. After asymmetric 8-to-16-cell stage division, all cells that inherit the apical domain express a TE marker, Cdx2. In contrast, apolar cells can either acquire ICM fate, as previously described, or, if positioned on the embryo surface, form a new apical domain and turn on Cdx2. Thus, contrary to the previous model (Johnson and Ziomek, 1981b), cell fate is determined by its position within the embryo, but not by the division pattern. Finally, using 1/8th blastomere, I showed that cell contact, not mediated by Cdh1, facilitates cellular symmetry breaking and directs the apical domain formation in the center of the

contact-free surface, and that the inheritance of this apical domain predicts the acquisition of TE fate.

Zusammenfassung

Anders als bei anderen Spezies in denen die Grundauslegung der Körperachsen bereits in der Oozyte oder während der Befruchtung festgelegt werden, entsteht im Mausembryo bis zum 8-Zell Stadium keine Asymmetrie. Alle Zellen besitzen die gleiche Morphologie und das gleiche Entwicklungs-Potenzial. Während die Entwicklung fortschreitet, differenzieren sich ursprünglich gleichartige Zellen des Embryos in zwei eigenständige Zelllinien; das Trophektoderm (TE) und die Innere Zell Masse (inner cell mass - ICM) (Wennekamp et al., 2013; Rossant and Tam, 2009; Yamanaka et al., 2006). Für diese Differenzierung sind die apikale-basale Zellpolarität (Hirate et al., 2013; Alarcon, 2010) sowie die Zell-Zell Adhäsion (Stephenson, Yamanaka and Rossant, 2010) gemeinsam erforderlich, wobei der ausschlaggebende, Symmetrie brechende Initiator für eine erste Spezifizierung des Zellschicksals noch nicht identifiziert wurde (Wennekamp et al., 2013).

Um den Mechanismus zu verstehen der diesem Symmetrie-Bruch zugrunde liegt, habe ich in dieser Studie ein neues experimentelles System entwickelt, in welchem eine isolierte 1/8 Embryonale Zelle in ihrer Entwicklung zum 4/32 Zell Stadium die erste Zelllinien Differenzierung zwischen TE und ICM wiederspiegelt. Unter Verwendung von Lebendzellbeobachtung (Live-Imaging) und quantitativer Bild Analyse habe ich festgestellt, dass die Vererbung der apikalen Domäne während der 1/8 zur 2/16 Zellteilung eine Vorhersage über die Vorgänge zulässt, die zu einer Spezifikation der TE Zelllinien führen. Der größte Teil der 8-Zell Stadium Blastomeren durchlaufen eine asymmetrische Zellteilung, wenn man die unterschiedliche Verteilung der apikalen Domäne an die Tochterzellen zugrunde legt. Die in der Mitte der zellkontaktfreien Oberfläche, im 8-Zell Stadium entstehende apikale Domäne lokalisiert Mikrotubuli-Organisationszentren und somit auch einen der Spindelpole an die Sub-Apikale Region, wodurch eine asymmetrische Zellteilung induziert wird. Alle Zellen, die nach der asymmetrischen 8- zu 16-Zell Teilung eine apikale Domäne erben, exprimieren Cdx2, ein TE Marker. Im direkten Vergleich zeigt sich dass nicht- polare Tochterzellen nicht unbedingt ein ICM Zellschicksal annehmen müssen. Viele sind an der Oberfläche des Embryos positioniert, akquirieren eine apikale Domäne und schalten schlussendlich Cdx2 Expression an. Im

Gegensatz zu dem bestehenden Model (Johnson and Ziomek, 1981b), wird das Zellschicksal durch die Position im Embryo festgelegt und nicht von der Zellteilung bestimmt. Schlussendlich konnte durch die Verwendung von 1/8 Blastomeren demonstriert werden, dass Cdh1 unabhängiger Zellkontakt den zellulären Symmetrie-Bruch hervorruft, sowie die Bildung der apikalen Domäne im Zentrum der Zellkontakt freien Oberfläche verursacht. Des Weiteren kann durch den Erhalt einer induzierten apikale Domäne eine Vorhersage für ein TE-Zellschicksal getroffen werden.

Table of contents

Summary 1

Zusammenfassung 3

Table of contents 5

Abbreviations 9

1. Introduction 13

- **Symmetry breaking** 15
  - Symmetry breaking in early development 15
  - Cell polarization 18
  - Asymmetric division 22
- **Mouse as a model system** 25
  - Advantages of the mouse as a model organism 26
  - Mouse pre-implantation development 26
- **Symmetry breaking in mouse development** 28
  - The first cell fate decision in mouse development 28
  - Current models of cell fate specification in the early mouse embryo 33
  - Current problems in understanding early mouse development 36

2. Specific aim and experimental strategy 39

3. Material and Methods 45

- **Molecular work** 47
  - Genomic DNA extraction 47
  - Plasmid DNA extraction 47
  - Nucleic acid concentration and purity determination 47
  - Sequencing of DNA 48
  - E. coli transformation 48
  - Agarose gel electrophoresis and gel extraction of DNA 48
  - Molecular cloning 49
  - In vitro transcription 50
- **Cell culture** 52
- **Animal work** 52
  - Mouse lines 52
  - Genotyping 53

Mouse embryo work **55**
- Mouse embryo recovery 55
- Microinjection 55
- Micromanipulation 56

PI(4,5)P$_2$ uncaging **57**
Phytochrome system **57**
Microbeads **57**
Immunofluorescence **58**
Live imaging **59**
Image analysis **59**
- Spindle orientation 59
- Apical domain 60
- SAS4 spots 61
- Cdx2 expression 62
- Cell envelopment 62

Statistical analysis **63**

4. Results 65

Identification of the apical domain as a possible symmetry breaking cue **67**
- 1/8th blastomeres polarize without adhesion 67
- The majority of polarized 1/8th blastomeres divide asymmetrically 69
- Inheritance of the apical domain predicts TE fate 69

The 8-to-16-cell stage division is preferentially asymmetric **72**
- Possible factors influencing spindle orientation in the 8-cell stage embryo 72
- Apical domain forms in the center of the contact-free surface 74
- Apical domain recruits MTOCs to the sub-apical region 76

A cell's fate is determined by its position within the embryo **79**
- Apolar blastomeres in 16-cell stage embryo can repolarize and adopt TE fate 79
- The spatial context influences repolarization frequency 81

Requirement and sufficiency of the apical domain for TE fate specification **82**
- Disruption of the apical domain results in a failure to form trophectoderm 82
- Induction of the apical domain in an apolar 1/8th blastomere 84
- Cdh1-independent cell contact facilitates and directs apical domain formation 86
- Induced apical domain predicts spindle orientation and TE-fate specification 87

5. Discussion 91

Cdh1-independent contact facilitates and directs the apical-basal polarization of the 1/8th blastomere 93
Predominant asymmetric divisions of 8-cell stage blastomeres 94
Apical domain predicts TE fate 95
A cell's fate is specified according to its position within the embryo 96
Perspectives 97

6. References 101

Acknowledgements 121

Abbreviations

1,2-POG – 1-palmitoyl-2-oleoyl-sn-glycerol
aPKC – atypical protein kinase C
BAC – bacterial artificial chromosome
Baz – Bazooka
Bem1 – Bud emergence protein 1
bp – base pairs
Brat – Brain tumour
BSA – bovine serum albumin
Cdc42 – cell division control protein 42
Cdh1 – Cadherin 1
Cdx2 – Caudal type homeobox 2
CRISPR – clustered regulatory interspaced short palindromic repeat
DAPI – 4,6-diamidino-2-phenylindole
Dlg – Discs large
DMSO – dimethyl sulfoxide
DN – dominant-negative
DNA – deoxyribonucleic acid
DPBS – Dulbecco's phosphate-buffered saline
E – embryonic day
ECM – extracellular matrix
EDTA – ethylenediaminetetraacetic acid
e.g. – *exempli gratia*, for example
EGFP – enhanced green fluorescent protein
Elf5 – E74-like factor 5
EMK1 – ELKL Motif Kinase
Eomes – Eomesodermin
ES – embryonic stem
Fc – fragment crystallizable
Gai – Guanine nucleotide-binding protein G(i) subunit alpha
Gata3 – GATA binding protein 3
GTPase – guanosine triphosphatase

H2B – histone 2B

hCG – human chorionic gonadotropin

HEPES – 4-(2-hydroxyethyl)-1-piperazineethanesulfonic acid

H-KSOM – KSOM with HEPES

hUtrCH –human Calponin homology domain of Utrophin

i.e. – *id est*, that is

ICM – inner cell mass

Insc – Inscuteable

IRES – internal ribosomal entry site

IU – international unit

KSOM – potassium simplex optimization medium

LAP – localization and affinity purification

LGN – Leu-Gly-Asn repeat-enriched

MAP4 – microtubule-associated protein 4

Mira – Miranda

mRNA – messenger RNA

MT – microtubule

MTOC – microtubule organizing center

Mud – Mushroom Body Defect

Myr – myristoylation signal

mz – maternal-zygotic

NEBD – nuclear envelope breakdown

NuMA – Nuclear Mitotic Apparatus

Oct4 – Octamer-binding transcription factor 4

Palm – palmitoylation signal

PAR – partitioning defective

PCR – polymerase chain reaction

PI3K – phosphoinositide 3-kinase

PI(4,5)P_2 – phosphatidylinositol 4,5-bisphosphate

Pins – Partner of Inscuteable

PI(3,4,5)P_3 – phosphatidylinositol (3,4,5)-trisphosphate

PMMA – polymethyl methacrylate

PLL – poly-L-lysine

PON – Partner of Numb

Pou5f1 – POU domain, class 5, transcription factor 1
Pros – Prospeto
PVP – polyvinylpyrrolidone
RNA – ribonucleic acid
RhoA – Ras homolog gene family member A
rpm – rounds per minute
RT – room temperature
Sall4 – Sal-like protein 4
SAS4 – spindle assembly defective-4
SEM – standard error of the mean
shRNA – small hairpin RNA
Sox2 – SRY-box 2
TAE – Tris-acetate- EDTA
TALEN – transcription activator-like effector nuclease
TE – trophectoderm
Tead4 – TEA domain family member 4
TF – transcription factor
WT – wild type
w/v – weight per volume
Yap1 – yes-associated protein 1
ZFN – zinc finger nuclease

1. Introduction

Symmetry breaking

Symmetry breaking is a crucial biological process that breaks uniformity to generate complexity and functional diversity. It acts at different levels: cells, tissues, organs and organisms. Generally, asymmetry at a smaller scale generates asymmetry at a higher level. For example, in migrating cells differential dynamics of actin reorganization along the axis of cell movement breaks cell symmetry to generate the front and the rear of a cell (Cramer, 2010). Left-right symmetry breaking in a vertebrate body is achieved by directional fluid flow resulting from the chiral nature of cytoskeleton elements (Okada et al., 2005). In development of multicellular organisms, symmetry breaking is essential in order to produce cells with distinct morphology and functions (Munro and Bowerman, 2009; Prehoda, 2009; Petricka, Van Norman and Benfey, 2009). In majority of cases this is accomplished by asymmetric division of beforehand polarized cells. Given the importance of the symmetry breaking in generation of multicellular organisms it is an intriguing field for many of developmental biologists.

Symmetry breaking in early development

In development of various multicellular species symmetry breaking occurs at different times and by different mechanisms, though the eventual outcome is the same for all of them – generation of cells with distinct fates. In some species like *Drosophila melanogaster* the main axes of the future body are defined already in the oocyte (Roth and Lynch, 2009; Huynh and St Johnston, 2004; Riechmann and Ephrussi, 2001). During oogenesis a large number of mRNAs (bicoid, nanos, oskar and gurken), produced by nurse cells, are transported along cytoskeleton elements into the oocyte. Differential localization of these mRNAs in the oocyte is mediated by directional transport (Clark, Meignin and Davis, 2007), anchoring in a specific region of the cell (Vanzo and Ephrussi, 2002; Delanoue et al., 2007) and selective stabilization (Zaessinger, Busseau and Simonelig, 2006). Regulated translation of positioned mRNAs leads to the establishment of morphogen gradients (Cook et al., 2004;

Wilhelm et al., 2003). After fertilization nuclei first undergo a series of divisions without cytokinesis, and only later on are separated by membrane invagination (Foe and Alberts, 1983; A. Mazumdar and M. Mazumdar, 2002). The resulting cells contain different amounts and combination of morphogenes and therefore adopt distinct fates (Fig. 1.1a). In other species symmetry is broken upon fertilization. For example in *Caenorhabditis elegans* sperm entry triggers a rapid reorganization of initially symmetric cell cortex generating polarity along the future anterior-posterior axis (Munro, Nance and Priess, 2004). This results in differential segregation of fate determinants along the anterior-posterior axis (Cheeks et al., 2004) and asymmetric positioning of the mitotic spindle (Grill et al., 2003; 2001). As a result, the zygote undergoes asymmetric division generating two daughter blastomeres, AB and P1, different in size and committed to distinct fates (Sulston et al., 1983; Fig. 1.1b). These examples demonstrate that despite the differences in mechanisms of symmetry breaking there are two crucial processes when generating diversity in development: cell polarization and asymmetric division.

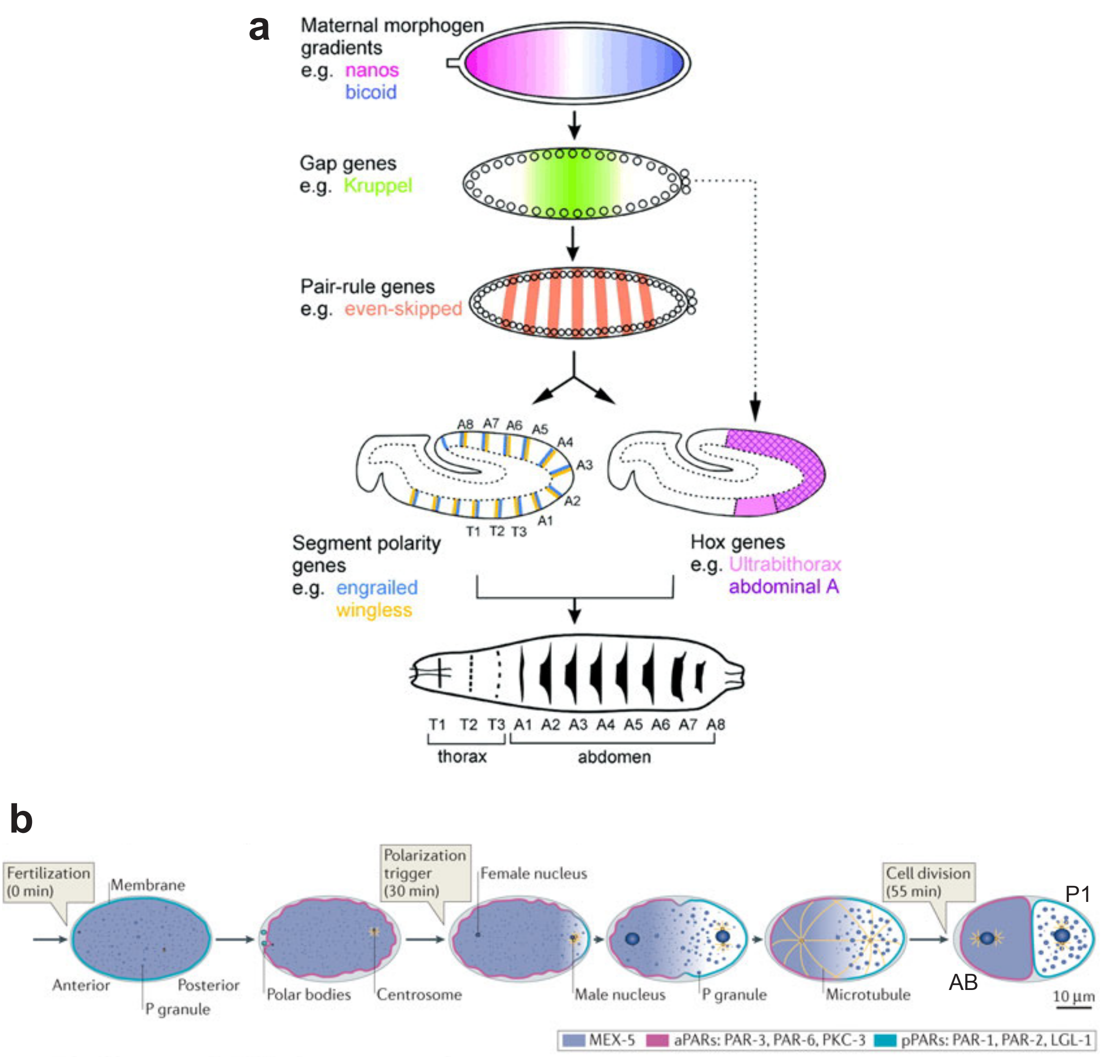
a
Maternal morphogen gradients
e.g. nanos
bicoid
Gap genes
e.g. Kruppel
Pair-rule genes
e.g. even-skipped
A8 A7 A6 A5
A4
A3
A2
A1
T1 T2 T3
Segment polarity genes
e.g. engrailed
wingless
Hox genes
e.g. Ultrabithorax
abdominal A
T1 T2 T3 A1 A2 A3 A4 A5 A6 A7 A8
thorax
abdomen
b
Fertilization (0 min)
Membrane
Anterior
Posterior
P granule
Polar bodies
Centrosome
Polarization trigger (30 min)
Female nucleus
Male nucleus
P granule
Microtubule
Cell division (55 min)
P1
AB
10 μm
MEX-5
aPARs: PAR-3, PAR-6, PKC-3
pPARs: PAR-1, PAR-2, LGL-1

Figure 1.1: Symmetry breaking in *Drosophila* and *C. elegans* development.

a, Symmetry breaking in *Drosophila* early development. Polarization of the *Drosophila* egg occurs during oogenesis when a number of mRNAs, such as bicoid and nanos, localize differentially. After the egg is fertilized, translation and diffusion of these mRNAs sets up morphogen gradients regulating the expression of hunchback and caudal, which in turn regulate expression of several zygotic genes and specification of the body segments. Adapted from (Sanson, 2001). **b**, *C. elegans* development from fertilization until the first division. Fertilization of the oocyte initiates contractions of the cell cortex leading to polarized localization of PAR proteins. PAR proteins, in turn, direct the subsequent segregation of fate determinants and the position of mitotic spindle, resulting in asymmetric division. Adapted from (Hoege and Hyman, 2013).

Cell polarization

Cell polarization leads to generation of spatially segregated regions with different protein, lipid and/or mRNAs composition. Differential segregation of molecular components is essential for cells to establish discrete domains enabling execution of distinct functions or to generate qualitatively different cells after asymmetric division. Cell polarity in budding yeast, anterior–posterior polarity in *C. elegans* one-cell embryo and apical–basal polarity in epithelial cells are well-known examples of cell polarity (Thompson, 2012; Fig. 1.2).

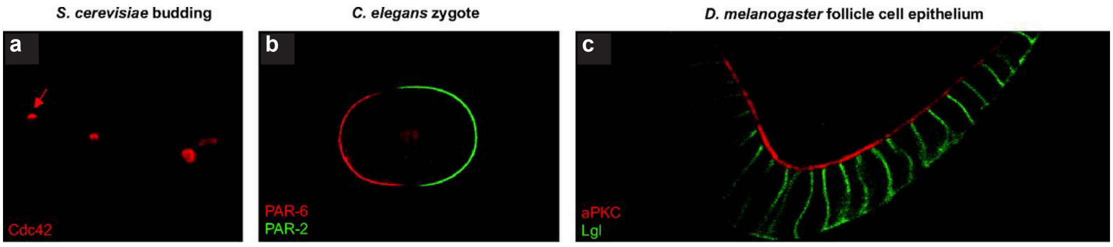

Figure 1.2: The localization of polarity determinants in various species.

a, Local Cdc42 accumulation in budding yeast. **b,** Non-overlapping localization of PAR proteins in worm zygote. **c,** Epithelial polarity in *Drosophila* follicle. Adapted form (Thompson, 2012).

Cell polarity in various species is underlain by a diversity of complex molecular mechanisms. A concept of local activation and global inhibition unify a wide range of cell polarity mechanisms (Turing, 1952; Goehring and Grill, 2013). The core elements in this concept comprise symmetry breaking, local signal amplification and long-range inhibition. Symmetry breaking can be induced by an internal cue, e.g. bud scar in *Saccharomyces cerevisiae* (Chant et al., 1991); or by an external one, e.g. chemo-attractant gradient for mammalian neutrophils (Servant et al., 2000). Remarkably, cells also have the ability to polarize spontaneously without any internal or external stimuli (Wedlich-Soldner and Li, 2003; Wedlich-Soldner, 2003; Irazoqui, Gladfelter and Lew, 2003). Local amplification of initial infinitesimal variations in polarity protein concentrations is typically achieved by a positive feedback loop (Drubin and Nelson, 1996; Altschuler et al., 2008). To stabilize and maintain cell polarity the process of local activation is usually coupled to a long-range inhibition. A constrained region of activation is generated when an inhibitor spreads faster than an activator. Additional known mechanisms that reinforce polarity are directed transport (Marco et al., 2007; Wedlich-Soldner, 2003) and mutual inhibition (Hao, Boyd and Seydoux, 2006; Hutterer et al., 2004). In principle, polarity could be generated under very simple conditions: with a limited amount of single type of molecules by a positive feedback loop (Altschuler et al., 2008). In majority of biological systems, however, cell polarity is achieved by a complex network of positive and negative feedback loops, making the system considerably more robust in a wide range of conditions (Chau et al., 2012).

In many contexts evolutionarily conserved partitioning defective (PAR) proteins play a central role in cell polarity (Fig. 1.3). In response to specific cues, PAR proteins adopt asymmetric cortical localization, with the PAR-aPKC complex comprising Par-3, Par-6 and atypical protein kinase C (aPKC) distributed in a complementary pattern to that of Par1. For example in *C. elegans* one-cell embryo PAR-aPKC complex is restricted to the anterior of the embryo, while Par1 is restricted to the posterior (Cuenca et al., 2003; Rose and Kemphues, 1998; Fig. 1.3a). In epithelial cells PAR-aPKC complex is localized to the apical domain, whereas Par1 localization is restricted to the basolateral domain (Benton and St Johnston, 2003; Fig. 1.3d). This non-overlapping localization of PAR proteins in cells is maintained by active mutual exclusion from the specific regions of the cell cortex (Nance and Zallen, 2011; Hao, Boyd and Seydoux, 2006; Benton and St Johnston, 2003). Asymmetrically localized PAR proteins influence a varity of key cellular processes, including distribution of cell fate determinants, spindle positioning and tight junction formation (Cheeks et al., 2004; Benton and St Johnston, 2003; Hutterer et al., 2004; Suzuki et al., 2004).

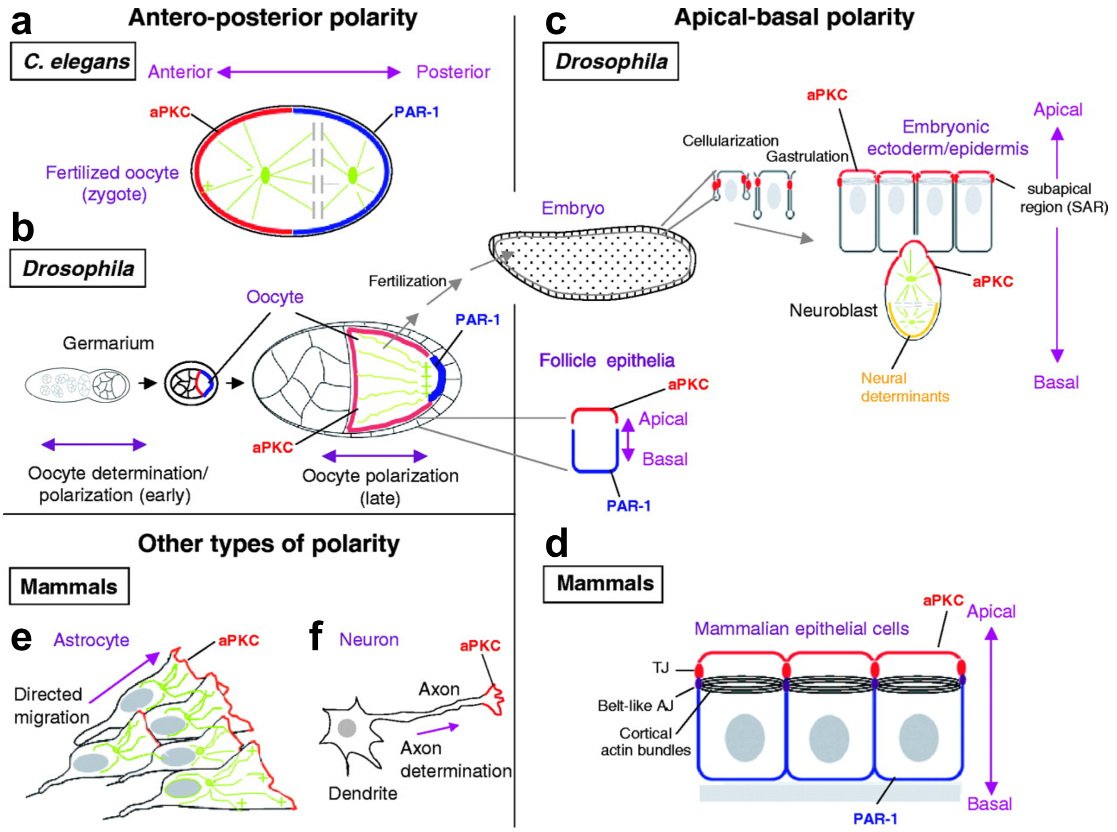
a
Antero-posterior polarity
C. elegans
Anterior
Posterior
aPKC
PAR-1
Fertilized oocyte
(zygote)
b
Drosophila
Oocyte
Fertilization
PAR-1
Germarium
aPKC
Oocyte determination/
polarization (early)
Oocyte polarization
(late)
c
Apical-basal polarity
Drosophila
aPKC
Apical
Embryonic
ectoderm/epidermis
Cellularization
Gastrulation
subapical
region (SAR)
Embryo
aPKC
Neuroblast
Neural
determinants
Basal
Follicle epithelia
aPKC
Apical
Basal
PAR-1
Other types of polarity
Mammals
e
Astrocyte
aPKC
Directed
migration
f
Neuron
aPKC
Axon
Axon
determination
Dendrite
d
Mammals
aPKC
Apical
Mammalian epithelial cells
TJ
Belt-like AJ
Cortical
actin bundles
Basal
PAR-1

Figure 1.3: PAR polarity in various systems.

a, Anterior-posterior polarization of the *C. elegans* zygote. **b,** Anterior-posterior polarization of *Drosophila* oocyte. **c,** Apical-basal polarity of *Drosophila* epithelium. **d,** Apical-basal polarity in mammalian epithelial cells. **e,** Polarization of mammalian astrocytes. **f,** Polarization of a mammalian neuron. Red lines and dots indicate the localization of the PAR-aPKC complex; blue lines represent distribution of PAR-1. Adapted from (Suzuki and Ohno, 2006).

Small GTPases are another group of cell polarity regulators that is conserved throughout most, if not all, eukaryotic organisms. For instance, cell division control protein 42 (Cdc42) is a master regulator of cell polarity in budding yeast. Local accumulation of Cdc42 on plasma membrane defines the site of polarized growth and formation of the bud or shmoo (Fig. 1.4a). Predominantly, two distinct positive feedback loops are hypothesized to be involved in the process of Cdc42 polarization, namely actin (Wedlich-Soldner, 2003) and Bud emergence protein 1 (Bem1; Irazoqui, Gladfelter and Lew, 2003) mediated pathways (Fig. 1.4b). Cdc42 also plays an important role in cell polarity by interacting with PAR-aPKC complex and regulating its localization in other contexts such as worm embryonic blastomeres (Aceto, Beers and Kemphues, 2006), *Drosophila* neuroblast (Atwood et al., 2007) and epithelial cells (Hutterer et al., 2004).

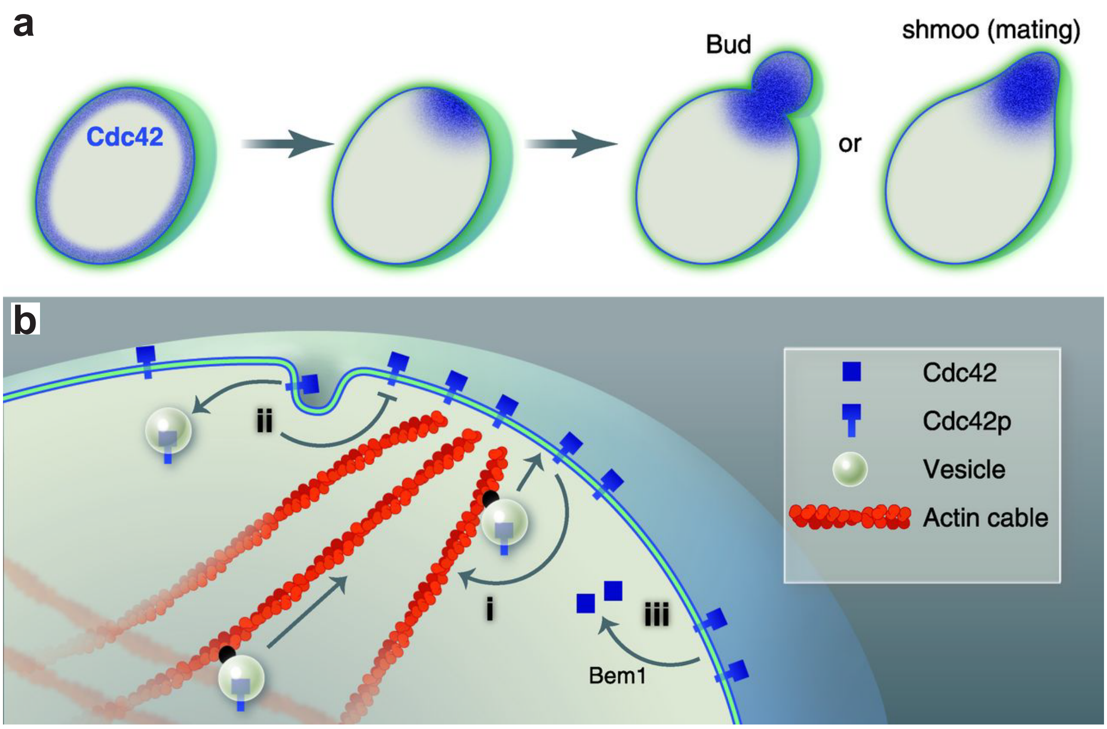

Figure 1.4: Cell polarization in budding yeast.

a, Cdc42 polarization in budding yeast. Either spontaneously or in response to an extracellular cue Cdc42 distribution changes from uniform to localized causing polarized growth. **b,** Mechanisms of Cdc42 polarization. Cdc42 polarized distribution is generated by (i) positive, actin-dependent feedback, (ii) endocytosis, and (iii) positive feedback mediated by Bem1. Adapted from (Mogilner, Allard and Wollman, 2012).

The localization of key regulatory molecules to specific cortical sites is typically mediated by cytoskeleton, mainly by actin filaments and microtubules (Li and Gundersen, 2008). In general, actin filaments facilitate the symmetry breaking process and a fast response to the polarizing cues, while microtubules work on stabilization and maintenance of asymmetry and hence are important for long-lasting cell polarity. In these processes orientated organization of cytoskeletal filaments allows for directed transport of molecules or organelles by motor proteins to specific sites in the cell. For example, actin cables in budding yeast are involved in the symmetry breaking by delivering Cdc42 to the growth site (Wedlich-Soldner, 2003). In epithelial cells trafficking of relevant proteins to the apical domain along oriented microtubules is important for the maintenance of polarity (Akhtar and Streuli, 2013). Actomyosin contractility can also lead to asymmetric redistribution of specific molecules. For instance, in *C. elegans* actomyosin contractions result in polarized localization of PAR proteins (Munro, Nance and Priess, 2004). Another actin-based mechanism involved in cell polarization is endocytosis. In budding yeast endocytosis allows to recycle Cdc42 molecules that diffused from the polarized cap (Marco et al., 2007). Thus, a variety of cytoskeleton-based processes are involved in cell polarization.

Despite the complexity of the signaling network and differences between various systems significant progress has been made in identifying key mechanisms and molecules involved in the establishment of cell polarity. Comparison of general mechanisms participating in cell polarity in phylogenetically distant cell types reveals a common hierarchy of processes: symmetry breaking, local signal amplification and maintenance of asymmetry. A set of conserved molecular players involved in cell polarity – PAR proteins, small GTPases and cytoskeleton – was also identified. Further work will help to uncover the full spectrum and more details of molecular mechanisms governing cell polarity in diverse systems.

Asymmetric division

Asymmetric division is an essential mechanism for generating diverse cell types in embryonic development and adult organisms. Asymmetric divisions have been described in numerous systems, such as *C. elegans* early embryo development, *Drosophila* nervous system and mammalian epithelia (Morin and Bellaïche, 2011; Jörg Betschinger and Jürgen A Knoblich, 2004). For asymmetric division to occur, the cell needs to polarize and distribute fate determinants along polarity axis. When the spindle is aligned with the polarity axis the division results in differential distribution of fate determinants in the two daughter cells, thus giving rise to cells with distinct fates.

As discussed above, in most known systems the polarity axis is established by the PAR-aPKC complex (Nance and Zallen, 2011; Suzuki and Ohno, 2006). The cues from the polarized cortex direct the mitotic spindle via spindle orientation complex consisting of Gai, Leu-Gly-Asn repeat-enriched protein (LGN) and Nuclear Mitotic Apparatus protein (NuMA) (Gotta et al., 2003; Srinivasan et al., 2003; Bowman et al., 2006; Izumi et al., 2006; Siller, Cabernard and Doe, 2006). NuMA is a microtubule-binding protein that recruits the dynein-dynactin motor complex to the cell cortex. This complex exerts a pulling force on astral microtubules to recruit and maintain one centrosome at the apical pole, thereby aligning the mitotic spindle along the apical-basal polarity axis (Couwenbergs et al., 2007; Nguyen-Ngoc, Afshar and Gönczy, 2007; Morin and Bellaïche, 2011).

One of the best studied examples of asymmetric division is *Drosophila* neuroblast – a stem cell-like progenitor of central nervous system (Fig. 1.5). *Drosophila* neuroblasts delaminate from a monolayered epithelium called the ventral neuroectoderm, and divide asymmetrically to generate a small ganglion mother cell and a large cell that remains a neuroblast (Wodarz, 2005; Jörg Betschinger and Jürgen A Knoblich, 2004). In neuroblasts Bazooka (Baz, *Drosophila* homolog of Par3), Par6 and aPKC together with Inscuteable (Insc), Partner of Inscuteable (Pins; *Drosophila* homolog of LGN) and Gαi are localized apically (Wodarz et al., 1999; 2000; Petronczki and J A Knoblich, 2001; Schober, Schaefer and J A Knoblich, 1999; Schaefer et al., 2000). Numb, Brain tumour (Brat) and Prospeto (Pros) accumulate at the basal plasma membrane in late prometaphase. This accumulation is facilitated by adaptor proteins Partner of Numb (PON) and Miranda (Mira) (Joerg Betschinger, Mechtler and Juergen A Knoblich, 2006; Lee et al., 2006; Lu et al., 1998; Ikeshima-Kataoka et al., 1997; Shen, L. Y. Jan and Y. N. Jan, 1997; Schuldt et al., 1998; Doe et al., 1991). When the basal determinants are localized, the mitotic spindle is set up in an apical–

basal orientation. This process is mediated by Pins through its binding to the microtubule-associated dynein-binding protein Mushroom Body Defect (Mud; *Drosophila* homolog of NuMA), which forms a cortical attachment site for astral microtubules, allowing the correct spindle alignment with the polarity axis (Izumi et al., 2006; Bowman et al., 2006; Siller, Cabernard and Doe, 2006). Additionally, this process is controlled by interaction of Pins with Discs large (Dlg) at the cortex, which, in turn, interacts with kinesin Khc-73 at the microtubule plus ends (Siegrist and Doe, 2007; 2005). The subsequent division results in two cells of unequal size and the basal determinants being inherited only by the smaller daughter cell (Fig. 1.5).

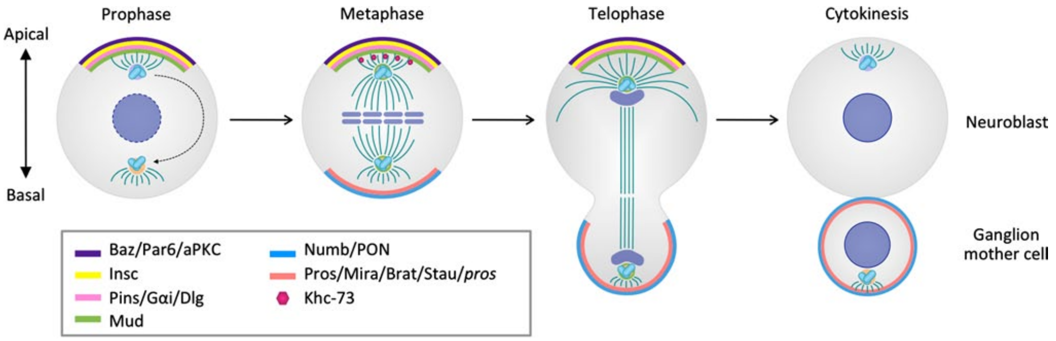

Figure 1.5. Asymmetric cell division of *Drosophila* neuroblast.

Polarized localization of apical proteins (PAR, Insc, Pins and Gαi) is established during prophase. In metaphase the spindle is orientated along the axis of apical-basal polarity and Numb, Brat, Pros, PON and Mira proteins are localized at the basal cortex. Division results in asymmetric segregation of cell fate determinants into two daughter cells: one large cell that keeps the identity of a neuroblast and one small cell that differentiates into a neuron or glia. Adapted from (Gómez-López, Lerner and Petritsch, 2014).

In conclusion, symmetry breaking is a fundamental process that occurs universally in biology. Cell polarization and asymmetric division are the two common mechanisms crucial for symmetry breaking at the cell and multicellular organism levels. A combination of genetic, biochemical and live imaging studies of model organisms, such as budding yeast, fruit fly and nematode, together with computational modeling resulted in a fruitful insight into mechanisms of the symmetry breaking process. The common principals underlying symmetry breaking, such as local activation and global inhibition, and a number of molecular players, e.g. cytoskeleton, Cdc42, PAR proteins and LGN/NuMA/Gαi complex, have been identified. Nevertheless, as asymmetry in biology is ample and diverse, there are plenty of exciting challenges lying ahead and the knowledge obtained so far will aid in elucidating the symmetry breaking mechanisms in other systems.

Mouse as a model system

In many aspects mammalian model organisms have advantages over other non-mammalian species. They are much closer to humans genetically and physiologically. When investigating complex physiological systems such as immune, endocrine and nervous systems, as well as diseases that affect these systems, a mammalian model organism is a good choice. Mammalian model organisms should also be used when studying curtain aspects of development, as several steps of mammalian development are drastically different from non-mammalian species (O'Farrell, Stumpff and Su, 2004). One prominent feature of the mammal development is that in all mammals, except for monotremes, it takes place inside the mother’s uterus (Behringer, Eakin and Renfree, 2006). As there is very little amount of yolk in the oocyte majority of mammals evolved placenta – a tissue that connects the embryo with the mother, nourishing the fetus throughout development (Brawand, Wahli and Kaessmann, 2008). The early phase of development when embryo is not attached to the mouse’s uterus is called pre-implantation development. As apparently there are no analogs of pre-implantation development in non-mammalian species (O'Farrell, Stumpff and Su, 2004), it is essential to use a mammalian model organism to understand the early mammalian development.

Advantages of the mouse as a model organism

Mouse is a frequent choice of many scientists as a mammalian model system due to its small size and easiness to maintain in the laboratory. Mice do not require a lot of space and are relatively cheap to maintain. They have a short generation time (around 2 months) and a large litter size (6-10 offspring). In addition, the mouse genome has been sequenced (Mouse Genome Sequencing Consortium et al., 2002) and a variety of tools have been developed to easily manipulate the genome and create transgenic animals. Transgenic mice are conventionally generated by injections of DNA into zygote pronucleus (Gordon and Ruddle, 1981; Wagner et al., 1981), injection of genetically modified embryonic stem (ES) cells into the blastocyst (Gossler et al., 1986) or transduction of single-cell embryo using viral vectors (Lois et al., 2002). Gene-targeting can be achieved through an array of techniques such as homologous recombination in ES cells (Capecchi, 2005; Thomas and Capecchi, 1987) and employment of engineered site-specific nucleases (zinc finger nucleases (ZFNs), transcription activator-like effector nucleases (TALENs) and clustered regulatory interspaced short palindromic repeat (CRISPR)/Cas RNA guided nuclease system) (Gaj, Gersbach and Barbas, 2013; Meyer et al., 2010; Qiu et al., 2013; H. Wang et al., 2013). In addition, gene expression can be controlled in space and time by chemicals or genetically encoded light-switchable molecules (X. Wang, X. Chen and Yang, 2012; Danielian et al., 1998). Currently thousands of unique inbred strains and genetically engineered mutant animals are available for research. All these reasons undoubtedly make the mouse an excellent model to study mammals.

Mouse pre-implantation development

In mice as well as in the majority of other mammals pre-implantation development occurs in the female reproductive tract and serves to prepare the embryo for implantation into the uterus. It starts with fertilisation followed by several rounds of cell division and results in a blastocyst composed of two cell types: the inner cell mass (ICM) and the trophectoderm (TE; Fig. 1.6). ICM cells will eventually give rise to the embryo proper itself, while TE cells will develop into extra embryonic tissues that form the placenta (Wennekamp et al., 2013; Takaoka and Hamada, 2011; Johnson, 2009; Rossant and Tam, 2009).

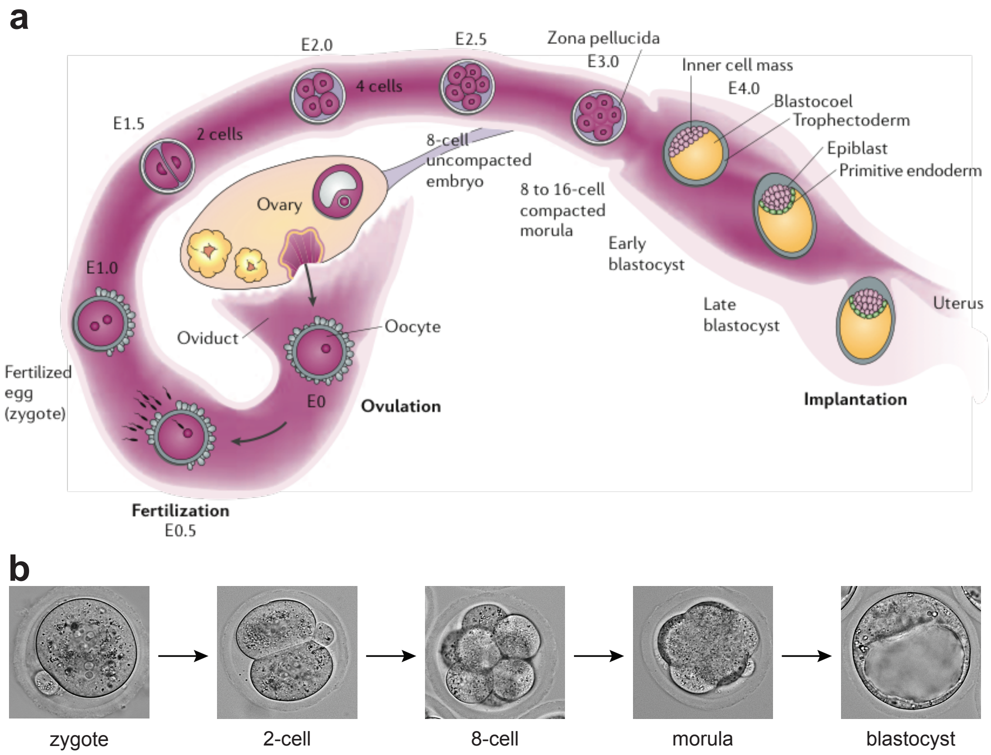
a
E2.0
E2.5
Zona pellucida
E3.0
Inner cell mass
E4.0
Blastocoel
Trophectoderm
E1.5
4 cells
2 cells
8-cell
uncompacted
embryo
Epiblast
Primitive endoderm
Ovary
8 to 16-cell
compacted
morula
Early
blastocyst
E1.0
Late
blastocyst
Uterus
Oviduct
Oocyte
Fertilized
egg
(zygote)
E0
Ovulation
Implantation
Fertilization
E0.5
b
zygote
2-cell
8-cell
morula
blastocyst

Figure 1.6: Mouse pre-implantation development.

a, A schematic representation of the steps in the mouse pre-implantation development starting with fertilization of the oocyte (embryonic day 0, E0) and finishing with implantation at around E4.5. Adapted from (Wang and Dey, 2006). **b,** Images of mouse pre-implantation embryos at different stages obtained with wide field microscope.

Before blastocyst formation two crucial morphological events occur. At 8-cell stage the embryo undergoes compaction – the process of cells flattening upon each other mediated by an increase in blastomere contractility and E-cadherin dependent intercellular adhesion (Maître et al., 2015, *in press;* Johnson, Maro and Takeichi, 1986). Concomitant with compaction each blastomere of the 8-cell embryo develops apical-basal polarity (Ziomek and Johnson, 1980; Ducibella et al., 1977).

At the 32-cell stage, fluid starts to be pumped into intercellular space to from a cavity known as the blastocoel, a process driven by Na^+/H^+ exchanger (Kawagishi et al., 2004; Manejwala, Cragoe and Schultz, 1989). Blastocoel appearance marks blastocyst formation. Throughout early pre-implantation development mouse embryos are enclosed in a glycoprotein envelope, called zona pellucida, which prevents premature attachment of the embryo to the uterus. At late blastocyst stage the embryo hatches from this glycoprotein envelope employing a small trypsin-like protease and then implants into the uterus, thereby ending pre-implantation stage (Perona and Wassarman, 1986).

Symmetry breaking in mouse development

Mammalian development is strikingly different from other species. Unlike many other organisms, where the body plan is already pre-patterned in the oocyte (Roth and Lynch, 2009) or at fertilization (Munro and Bowerman, 2009), mammalian embryo has no asymmetry during the first few days after fertilization. In mouse the symmetry breaking process starts much later in development, at the morula stage, and eventually results in separation of future placental cells from the pluripotent cells generating embryo proper (Wennekamp et al., 2013; Beddington and Robertson, 1999).

The first cell fate decision in mouse development

Up to 8-cell stage all cells in the mouse embryo have the same morphology, equal developmental potential (Kelly, 1977) and undistinguishable gene expression pattern (Guo et al., 2010). First asymmetry appears at the cell level in the late 8-cell stage embryo when cells develop apical-basal polarity (Ziomek and Johnson, 1980; Ducibella et al., 1977). During this time a set of proteins and membrane lipids change their position within the cell from uniform distribution to either apical (Ezrin, aPKC, Pard6b, Par3; Louvet et al., 1996; Pauken and Capco, 2000; Vinot et al., 2005; Plusa, 2005) or basolateral localization (phosphatidylinositol (3,4,5)-trisphosphate

(PI(3,4,5)P3), ELKL Motif Kinase (EMK1; mouse homolog of Par1), Cadherin 1 (Cdh1, also known as E-cadherin); Halet, Viard and Carroll, 2008; Vinot et al., 2005; Vestweber et al., 1987; Fig. 1.7). As cleavage proceeds, asymmetry between cells emerges. As a result of asymmetric divisions apolar and polar cells appear. They are positioned on the inside or outside of the embryo, respectively (Johnson and McConnell, 2004). One day later, at around 32-cell stage, the process of symmetry breaking ends with the establishment of two distinct cell lineages: ICM and TE (Rossant and Tam, 2009; Yamanaka et al., 2006).

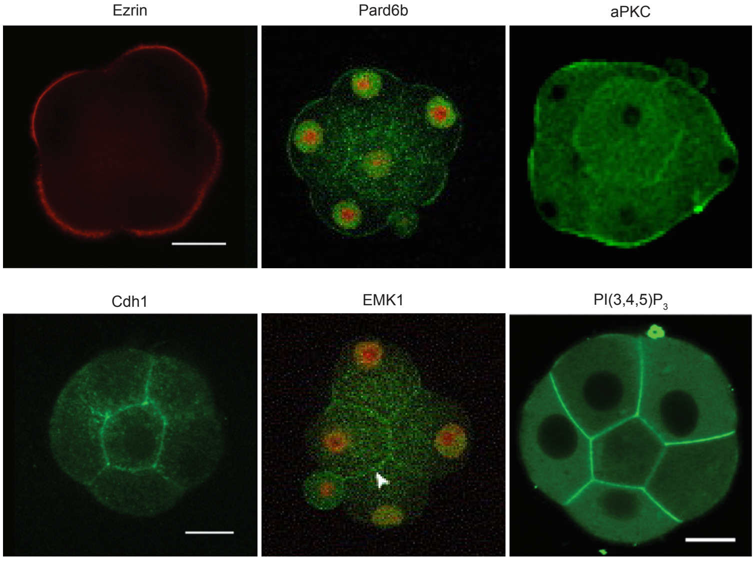

Figure 1.7: Apical-basal polarity in mouse 8-cell stage embryo.

At 8-cell stage every blastomere of the embryo acquires apical-basal polarity. Ezrin, Pard6b and aPKC are localized apically, while Chd1, EMK1 and PI(3,4,5)P$_3$ are restricted to the basolateral domain. Scale bars, 20 µm. Adapted from (Dard et al., 2009; Vinot et al., 2005; Liu et al., 2013; Halet, Viard and Carroll, 2008).

There is growing evidence that TE is the first fate to be specified in the mouse pre-implantation embryo (Dietrich et al., 2015, *in revision*; Dietrich and Hiiragi, 2007). TE is an epithelium with tight junctions that surrounds the inner cell mass and the cavity (Collins and Fleming, 1995). It is characterized by expression of Caudal type homeobox protein 2 (Cdx2), GATA binding protein 3 (Gata3), Eomesodermin

(Eomes) and E74-like factor 5 (Elf5; Fig. 1.8). Cdx2 acts upstream of Eomes and Elf5 (Donnison et al., 2005) and in parallel with Gata3 (Ralston et al., 2010). Cdx2 is required for proper lineage segregation and TE function, but not for the initial lineage decision (Strumpf et al., 2005; Ralston and Rossant, 2008). At the morula stage Cdx2 expression is heterogeneous, i.e. the expression level is variable and not correlated to cell position or to the expression of other markers and becomes restricted to the outside cells only at the blastocyst stage (Fig. 1.9). TEA domain family member 4 (Tead4) transcription factor (TF) acts upstream of Cdx2 (Nishioka et al., 2009). Tead4 is expressed in all cells of the embryo and its differential activity in inside and outside cells is controlled by Hippo signaling pathway via phosphorylation of its co-factor Yes-associated protein 1 (Yap1). In outside cells the Hippo pathway is repressed by cell polarity, hence Yap1 is not phosphorylated and can be translocated to the nucleus where its binding to Tead4 promotes *Cdx2* expression (Fig. 1.10).

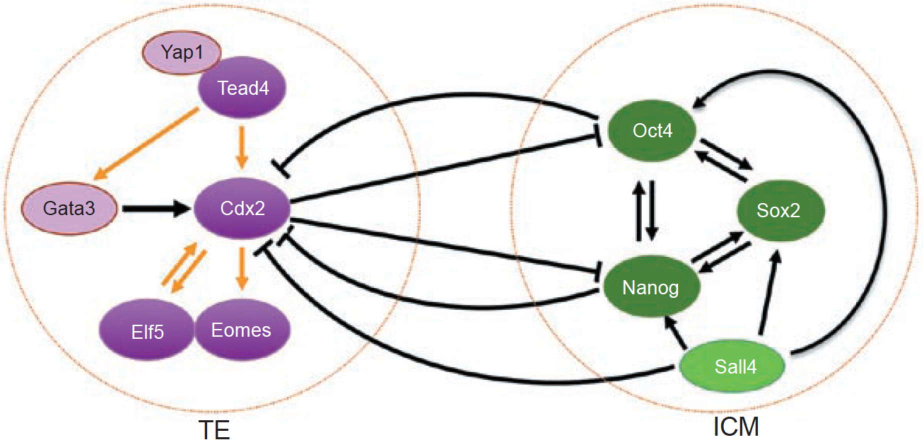

Figure 1.8: Transcriptional network specifying ICM vs. TE.

Cdx2, Elf5 and Eomes are TE-specific transcription factors. Tead4, together with its co-factor Yap1, up-regulates expression of *Cdx2* and *Gata3*. Cdx2 activates *Eomes* and *Elf5*, while Elf5 and Gata3 enhance *Cdx2* activity. Oct4, Nanog, and Sox2 are the core TFs promoting ICM cell fate. Sal-like protein 4 (Sall4) activates the core ICM TFs and suppresses *Cdx2* expression. A double negative feedback loop between Cdx2 and Oct4-Nanog ensures establishment of appropriate cell fate in individual blastomeres. Adapted from (L. Chen et al., 2010).

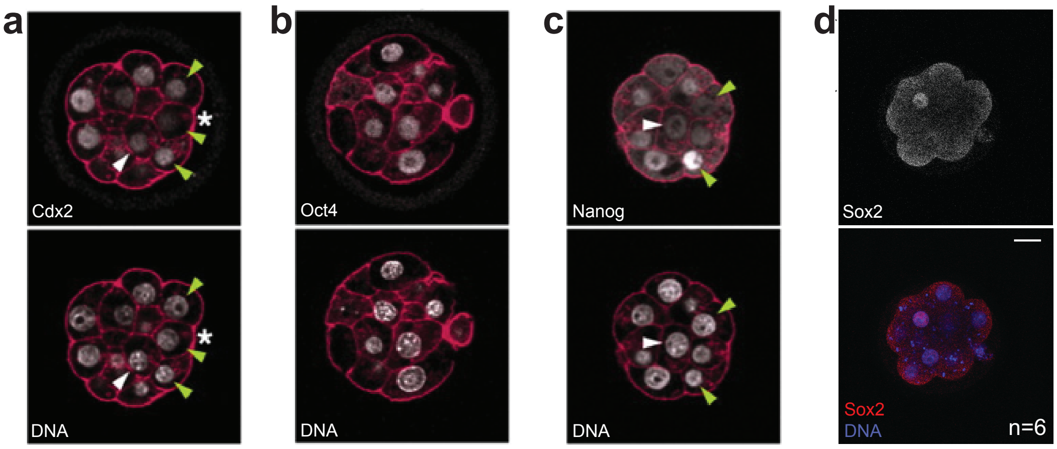
a
b
c
d
Cdx2
Oct4
Nanog
Sox2
DNA
DNA
DNA
Sox2
DNA
n=6

Figure 1.9: Expression pattern of key TF in the late morula.

a, Heterogeneous levels of Cdx2 protein. **b,** Uniform level of Oct4 protein in all cells of the embryo. **c**, Heterogeneous level of Nanog protein. Cell membrane is marked by actin (red); white and yellow arrowheads indicate inside and outside cells of interest, respectively. Adapted from (Dietrich and Hiiragi, 2007). **d,** *Sox2* is expressed only in the inside cell of morula. Scale bar**,** 20 µm. Adapted from (Wicklow et al., 2014).

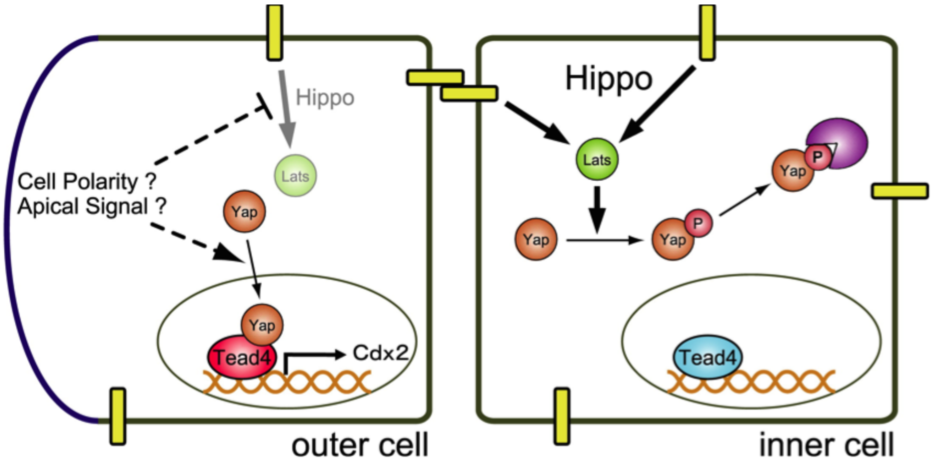
Hippo
Cell Polarity ?
Apical Signal ?
Lats
Yap
Yap
Tead4
Cdx2
outer cell
Hippo
Lats
Yap
Yap
P
Yap
P
Tead4
inner cell

Figure 1.10: Role of Hippo signaling in cell fate specification in the mouse pre-implantation embryo.

In the outside cells, Hippo signaling is suppressed by cell polarity allowing nuclear accumulation of Yap. Tead4 binds nuclear Yap and induces *Cdx2* expression that promotes TE differentiation. In the inside cells, Hippo signaling is activated by cell–cell contacts, which phosphorylates and inhibits nuclear localization of Yap, thereby suppressing *Cdx2* expression. Adapted from (Nishioka et al., 2009).

The second cell lineage in the blastocyst is ICM – a pluripotent cell population characterized by expression of Octamer-binding transcription factor 4 (Oct4, also known as POU domain, class 5, transcription factor 1 (POU5F1); Nichols et al., 1998), Nanog (Mitsui et al., 2003) and SRY-box 2 protein (Sox2; Wicklow et al., 2014) transcription factors (Fig. 1.8). At morula stage *Oct4* is equally expressed in all cells of the embryo, while *Nanog* expression at this stage is heterogeneous (Dietrich and Hiiragi, 2007). In the late blastocyst Cdx2 represses *Oct4* and *Nanog* expression in the trophectoderm, thereby restricting it to ICM blastomeres (Strumpf et al., 2005; Fig. 1.8). Surprisingly, it was recently reported that Sox2 is a unique early marker of ICM, expression of which could be observed only in the inside cells already at the morula stage (Fig. 1.9). It was also shown that *Sox2* is regulated by Hippo pathway, although it is not clear whether *Sox2* expression is regulated by Hippo pathway components in the same way as *Cdx2* (Wicklow et al., 2014).

It was shown that both cell polarity and cell-cell adhesion are required for the proper cell lineage segregation (Alarcon, 2010; Stephenson, Yamanaka and Rossant, 2010). Experiments where *Pard6b* expression was down-regulated by shRNA demonstrated that apical domain is necessary for the *Cdx2* expression and TE fate specification (Alarcon, 2010; Fig. 1.11a). Another study on maternal-zygotic (mz) *Chd1*$^{-/-}$ revealed that cell-cell adhesion is also essential for the correct allocation of TE and ICM cells (Stephenson, Yamanaka and Rossant, 2010; Fig. 1.11b). Despite the recent progress in our understanding of early mammalian development, it remains unknown what is the crucial factor that is sufficient for induction of the first developmentally relevant difference between the cells in the mouse embryo.

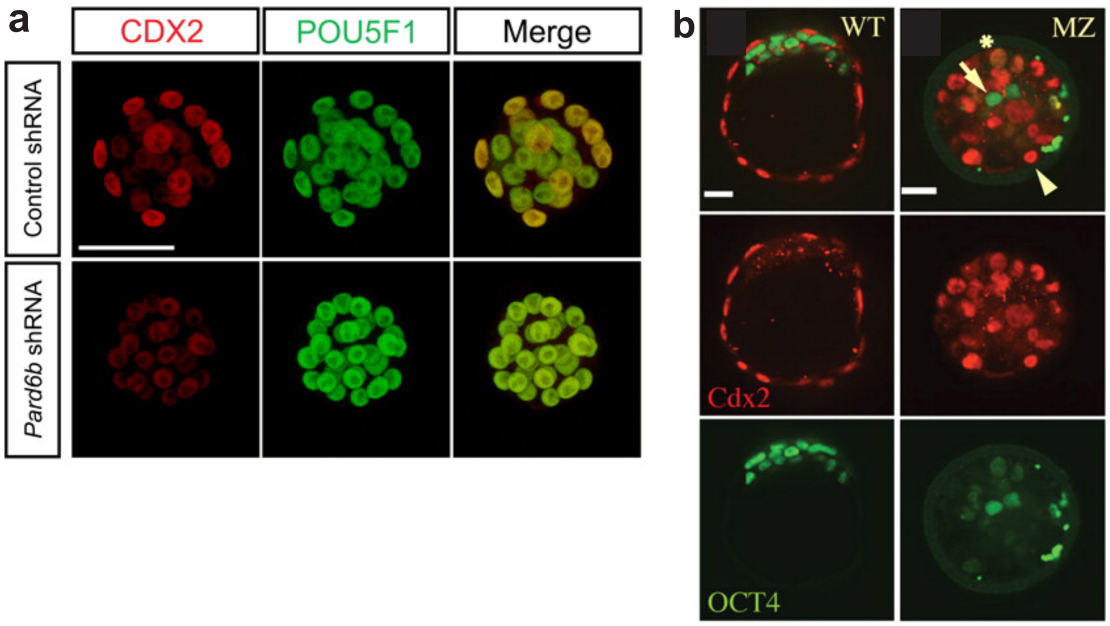

Figure 1.11: Cell polarity and cell-cell adhesion are required for proper allocation of TE and ICM cells.

a, Double immunostaining for Cdx2 (red) and Oct4 (Pou5f1, green) proteins in embryos injected with control or Pard6b shRNA plasmid. Down-regulation of *Pard6b* expression significantly diminishes the level of Cdx2 protein in all cells of the embryo. Adapted from (Alarcon, 2010). **b,** In mouse embryos lacking maternal and zygotic Cdh1 formation of the epithelial layer is disrupted, nevertheless individual cells initiate TE- and ICM-like fates. The number of Cdx2-positive cells in embryos is significantly higher in mz mutants in comparison to wild type embryos. Scale bars, **a** – 50 µm, **b** – 20 µm. Adapted from (Stephenson, Yamanaka and Rossant, 2010).

Current models of cell fate specification in the early mouse embryo

Currently there are two predominant hypotheses explaining the mechanism of ICM and TE cell fate specification (Fig. 1.12). The inside-outside model puts forward that cells adopt fate according to their position in the late morula (Tarkowski and Wróblewska, 1967). Cells that are on the inside of the embryo become ICM, while the cells that end up outside adopt the TE fate (Fig. 1.12a). The cue that cells use to sense their position in the embryo and subsequently to define their fate remains elusive. Potential candidates for positional information could be the difference between inside and outside cells in apical-basal polarity, in amount of contact with the neighbouring cells, in cell shape and volume or in metabolism.

The second model – cell polarity model – argues that the critical factor in initiating lineage divergence is the inheritance of the apical domain (Johnson and Ziomek, 1981b). According to this model there are two possible types of division – symmetric and asymmetric. Symmetric division generates two polar cells, while asymmetric divisions generate one polar and one apolar cell. Those cells that inherit the apical domain during 8-to-16-cell stage division become TE, while apolar cells are destined to become ICM (Fig. 1.12b). Even though spindle orientation and subsequent position of the division plane are crucial for this model, the factors that direct spindle alignment are still unidentified. To date, the direct link between the division plane, the inheritance of the apical domain and the cell fate remains to be demonstrated.

Inside-outside and cell polarity models are supported by a number of experiments. Yet curtain aspects of the mouse embryo development are difficult to reconcile with one or the other model. The inside-outside model was tested in several studies where labeled blastomeres were repositioned to the inside or outside of the embryo, resulting in their preferential differentiation into ICM or TE, respectively (Suwińska et al., 2008; Hillman, Sherman and Graham, 1972; Kelly, 1977). Although inside-outside model is consistent with the regulative nature of the early mouse embryo (ability of the embryo to form a blastocyst even after removal, addition or relocation of cells up to around 30-cell stage; Nagashima et al., 1984; Tarkowski, 1961; Suwińska et al., 2008; Kelly, 1977; Hillman, Sherman and Graham, 1972) and with the recent findings on Hippo pathway (Nishioka et al., 2009), it cannot be reconciled with the heterogeneity of crucial transcription factors (Dietrich and Hiiragi, 2007; Ralston and Rossant, 2008). The cell polarity model is supported by a number of observations, e.g. disruption of the apical-basal polarity by small interfering RNA against Pard3b or domainant negative (DN) form of aPKC in one blastomere of the 4-cell stage embryo directs its progeny inside the embryo (Plusa, 2005). Despite this supporting evidence the original cell polarity model cannot be reconciled with the regulative capacity of the mouse pre-implantation embryo or with the heterogeneity of the crucial transcription factors (Dietrich and Hiiragi, 2007; Ralston and Rossant, 2008). Thus, these two hypotheses propose fundamentally different cues and mechanisms for cell lineage allocation and none of these models alone can fully explain cell lineage segregation in the early mouse embryo.

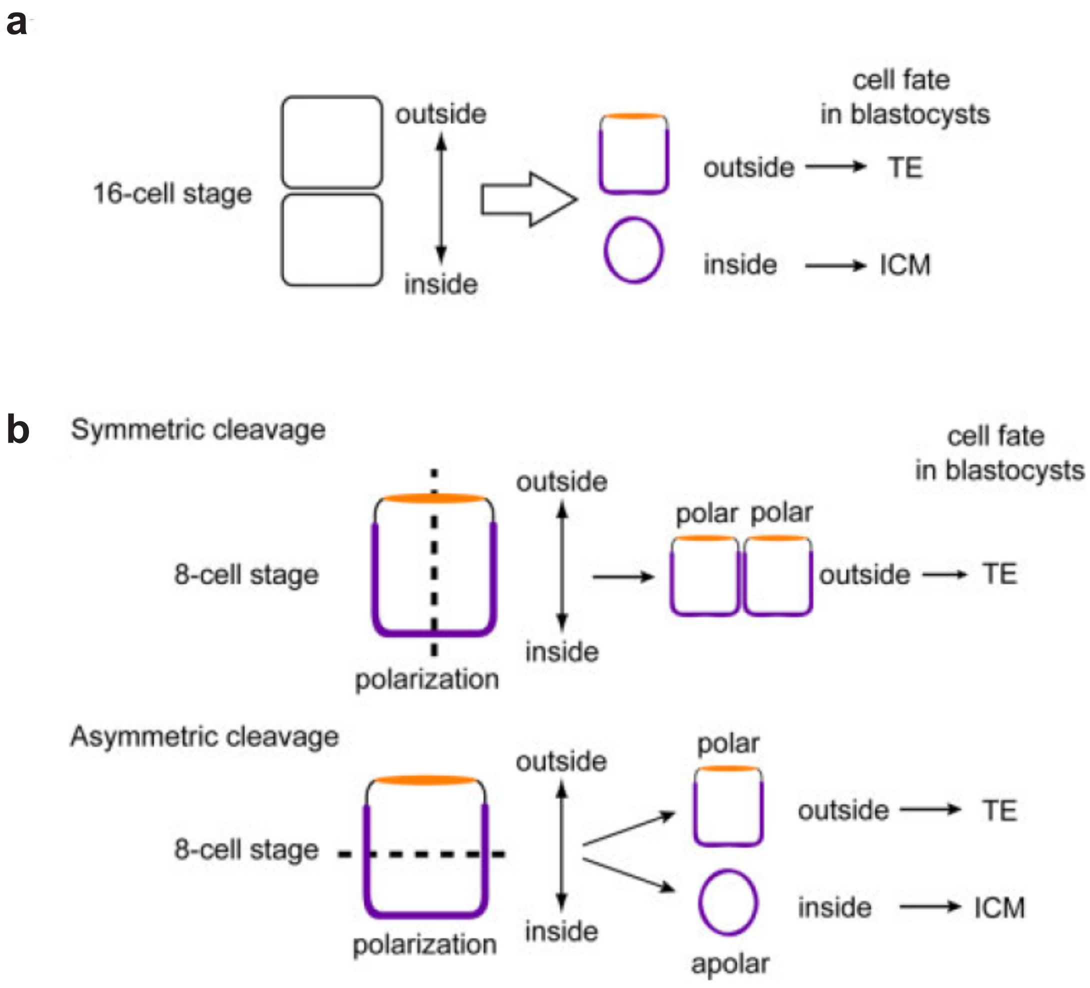
a
16-cell stage
outside
inside
cell fate
in blastocysts
outside
TE
inside
ICM
b
Symmetric cleavage
8-cell stage
polarization
outside
inside
polar polar
cell fate
in blastocysts
outside
TE
Asymmetric cleavage
8-cell stage
polarization
outside
inside
polar
apolar
outside
TE
inside
ICM

Figure 1.12: Classical models of cell lineage specification in early mouse embryo.

a, The inside–outside model. Differentiation into ICM and TE depends on inside or outside position of the cell. **b,** The cell polarity model. Cells inheriting apical domain become TE, apolar cells adopt ICM fate. Adapted from (Yamanaka et al., 2006).

Current problems in understanding early mouse development

The early mouse development is a very dynamic process, with the embryo rotating inside the zona pellucida and individual cells changing their position in relation to each other as cleavage proceeds (Watanabe et al., 2014; Yamanaka, Lanner and Rossant, 2010). Furthermore, no stereotypic division patterns can be observed and the cleavages are only roughly synchronized in time (Lehtonen, 1980). It was also reported that expression levels of the key TFs are heterogeneous. Moreover, the early mammalian development is highly regulative, and cell fate can be reversed up to the early blastocyst stage (Stephenson, Yamanaka and Rossant, 2010; Rossant and Lis, 1979; Rossant and Vijh, 1980). Additionally, cell lineage segregation appears to be influenced by many interdependent factors, such as cell shape, cell mechanics, apical-basal polarity and cell–cell adhesion. Thus, changing one factor (e.g. cell-cell adhesion) inevitably influences other factors (e.g. cell shape, cell polarity) as well (Fig. 1.13). Altogether, this complexity of the early mouse development has made it difficult to identify the crucial symmetry breaking cue and to fully understand the mechanism underlying the segregation of TE and ICM lineages.

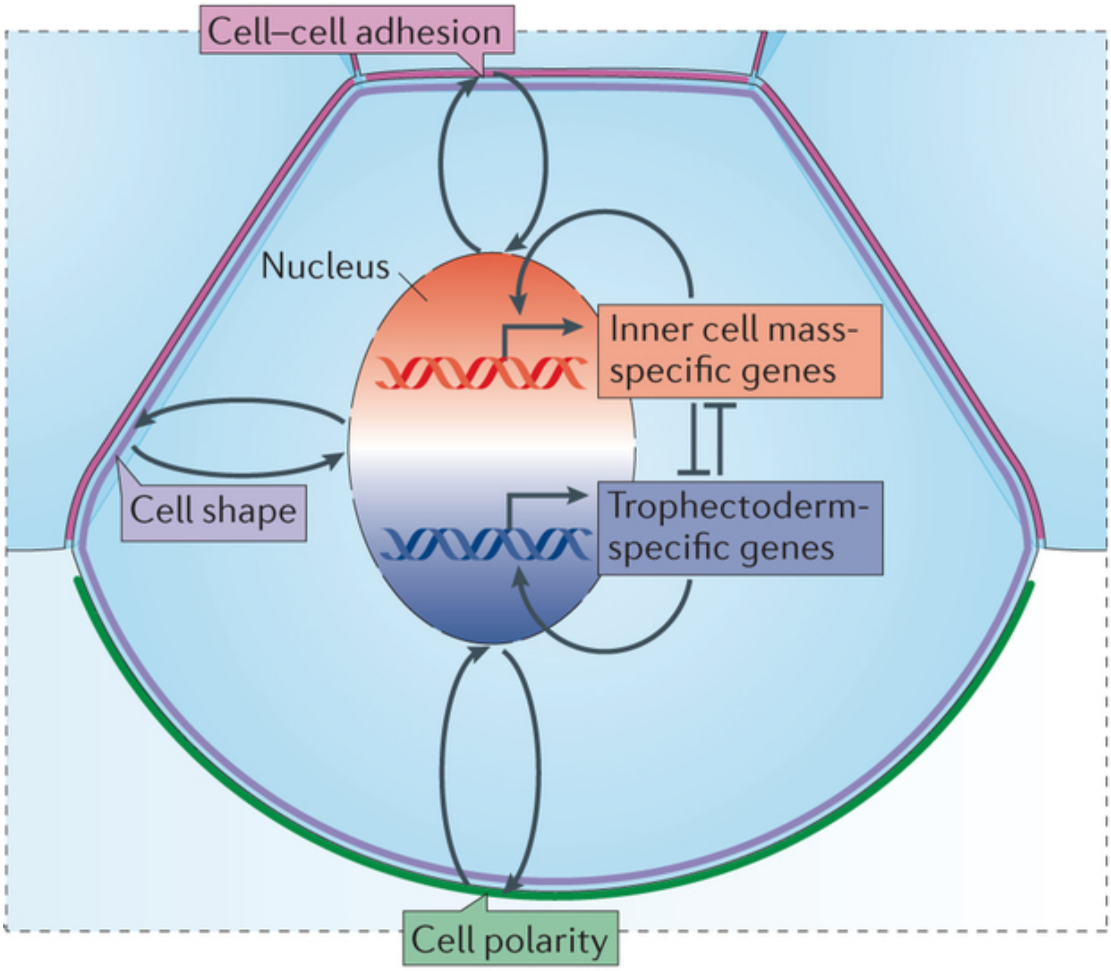
Cell–cell adhesion
Nucleus
Inner cell mass-specific genes
Cell shape
Trophectoderm-specific genes
Cell polarity

Figure 1.13: The interaction of various factors in the early mouse embryo.

Cell fate is determined by interaction of various factors. Factors such as cell shape, cell–cell adhesion and apical-basal polarity, can influence the activity of gene expression. Gene expression, in turn, can modify the physical parameters of the cell, thereby directing its position in the embryo to fit its gene expression profile. Adapted from (Wennekamp et al., 2013).

2. Specific aim and experimental strategy

Due to the complexity of the mouse pre-implantation development, discussed in Introduction, up to date the mechanism of cell lineage segregation remains not fully understood. To unravel the mechanism underlying the establishment of the first two cell lineages in mouse embryo it is crucial to identify the signal initiating this process. Knowing the initial cue will allow elucidating the down-stream events and eventually controlling cell fate specification. Therefore, the aim of this study is to identify the symmetry breaking cue in the mouse embryo that initiates the ICM vs. TE lineage segregation.

Given the interactions among various cellular factors (e.g. cell polarity, shape, size and cell adhesion) potentially influencing cell lineage segregation, it is crucial to use an experimental system with the minimum level of such interactions. Therefore, I took an advantage of a “reduced” system, which utilizes the ability of blastomeres isolated from 8-cell stage embryo (1/8th blastomeres) to recapitulate morphogenesis and patterning of the blastocyst (Johnson and Ziomek, 1983; Dietrich and Hiiragi, 2007). When isolated 1/8th blastomeres continue to develop and after 2 rounds of divisions form a 4/32th mini-blastocyst, which consists of TE- and ICM-like cells as assessed by their position (inside or outside) and expression of lineage specific genes, e.g. *Cdx2* (Fig. 2.1a). Due to this unique capacity, in vitro development of 1/8th blastomeres to 4/32th mini-blastocyst can be used as a simplified experimental system to study the blastocyst lineage segregation.

An asymmetric 2/16th pair consists of one polar blastomere enveloping its apolar sister, with Cdx2 expression level always higher in the former (Dietrich and Hiiragi, 2007). This indicates that the TE cell fate is invariably specified at the 2/16th-cell stage under this experimental setting, in contrast to the variability in Cdx2 expression observed in the whole 16-cell stage embryo (Dietrich and Hiiragi, 2007; Ralston and Rossant, 2008). This finding suggests that the symmetry is already broken between the 2/16th sister cells and therefore allows me to focus on the 1/8th-to-2/16th-cell stage transition to investigate the symmetry breaking mechanism.

Lineage segregation during the 1/8th-to-2/16th-cell stage transition can be monitored by live-imaging the development of 1/8th blastomeres expressing fluorescent markers for different cellular structures (e.g. membrane, nucleus, spindle, apical domain). It is also possible to track the cell fate specification during development using transgenic mouse lines expressing fluorescently labelled lineage-specific genes, e.g. Cdx2-EGFP (McDole and Zheng, 2012). Notably, this system would make it possible for me to manipulate or ectopically induce a given cellular parameter (e.g. cell shape, volume, apical-basal polarity and cell adhesion) without affecting other factors, and to test which one is most crucial and sufficient for the symmetry breaking during mouse embryogenesis (Fig. 2.1b). The goal of this study is thus to understand the mechanism underlying the symmetry breaking and to test controlling the cell fate specification during the blastocyst development.

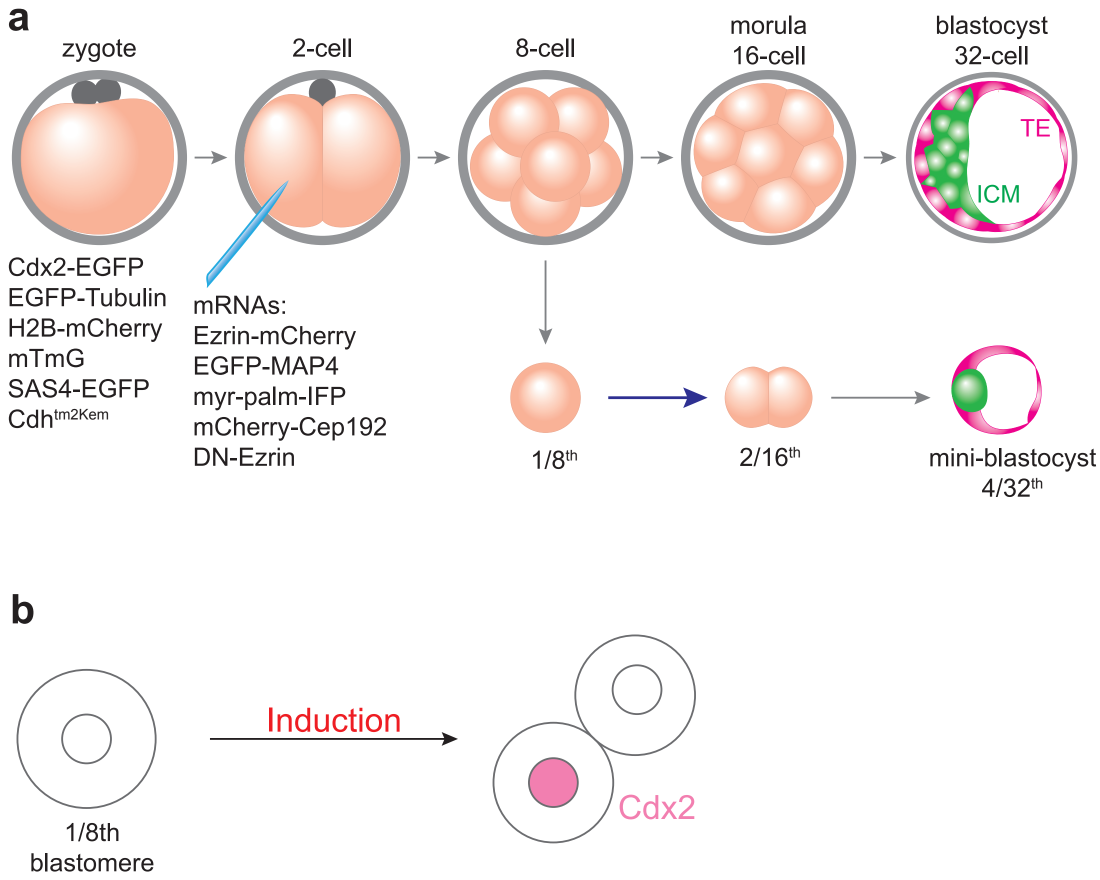
a
zygote
2-cell
8-cell
morula
16-cell
blastocyst
32-cell
TE
ICM
Cdx2-EGFP
EGFP-Tubulin
H2B-mCherry
mTmG
SAS4-EGFP
Cdh^tm2Kem
mRNAs:
Ezrin-mCherry
EGFP-MAP4
myr-palm-IFP
mCherry-Cep192
DN-Ezrin
1/8th
2/16th
mini-blastocyst
4/32th
b
Induction
1/8th
blastomere
Cdx2

Figure 2.1: Experimental design.

a, A simplified experimental system to study symmetry breaking in mouse development. 1/8th blastomeres are isolated from the 8-cell stage transgenic embryo into which mRNAs encoding fluorescent reporters are microinjected at the 2-cell stage. *In vitro* development of 1/8th blastomere to 4/32th mini-blastocyst recapitulates the TE vs. ICM lineage segregation. **b,** Controlling the symmetry breaking by manipulating a cellular parameter in the 1/8th blastomere.

3. Material and Methods

Molecular work

Genomic DNA extraction

Genomic DNA (gDNA) was isolated from mouse tails. After overnight digestion of tissue with Proteinase K (0.5 mg/ml Proteinase K (Sigma, P2308), 50 mM Tris-HCl pH 8.0 (Sigma, T2663), 100 mM EDTA pH 8.0 (Fluka, 03690), 100 mM NaCl (Sigma, S5150), 1% sodium dodecyl sulfate (Serva, 39575.02)), the supernatant was mixed with equal volume of 2-propanol to precipitate gDNA. The pellet was dried overnight and dissolved in Tris-EDTA buffer (Qiagen) at 65°C, 15 min, 450 rpm (Eppendorf, Thermomixer comfort).

gDNA extraction for this study was done by Stefanie Salvenmoser and Ramona Bloehs.

Plasmid DNA extraction

Plasmid DNA was isolated from bacteria cultured overnight in LB medium supplemented with suitable antibiotic at 37°C and 230 rpm using the QIAprep Spin Miniprep Kit (Qiagen) or the HiSpeed Plasmid Maxi Kit (Qiagen), depending on the required amount and concentration, according to manufacture's protocol.

Nucleic acid concentration and purity determination

DNA or RNA concentration was determined by measuring absorption of ultraviolet light of a 260 nm wavelength using a spectrophotometer (Life Technologies, NanoDrop 8000). 1 absorbance unit of light at a wavelength of 260 nm corresponds to a concentration of 50 µg/ml for double-stranded DNA or 40 µg/ml for single-stranded RNA. The ratio of absorbance at 260 nm and 280 nm was used to assess the purity of DNA and RNA. A ratio of ~1.8 was accepted as "pure" for DNA, while RNA was concidered "pure" when a ratio was ~2.0.

Sequencing of DNA

DNA sequencing was performed by GATC Biotech (Konstanz, Germany).

E. coli transformation

1 µg of plasmid DNA or 20 µl of a ligation reaction were added to 50 µl competent *E. coli* DH5α (Life Technologies, 18265-017). When non-methylated plasmid was required *E. coli* JM100 were used (Agilent Technologies, 200239). After 1h incubation on ice, samples were heat-shocked at 42°C for 90 sec (Eppendorf, Thermomixer comfort) and then cooled down on ice for 2 min. Afterwards, 800 µl of SOC medium (Sigma, S1797) was added to bacteria and samples were further incubated at 37°C and 500 rpm for 1 h (Eppendorf, Thermomixer comfort), followed by plating on LB-agar plates supplemented with suitable antibiotic and overnight incubation at 37°C.

Agarose gel electrophoresis and gel extraction of DNA

DNA fragments after PCR or restriction reaction were mixed with loading dye (Life Technologies, R0611) and separated by electrophoresis in 1-1.5% (w/v) agarose (Lonza, 50004) gel supplemented with 0.03 µl/ml DNA stain (Serva, 39804.01) in the TAE buffer (Life Technologies, B49), applying 5 V/cm. DNA fragments were visualized with ultraviolet light on video-based gel documentation system (Intas, GEL Stick "Touch"). As standards for fragment size and DNA amount 100 base pairs (bp) or 1000 bp DNA ladder (Life Technologies, SM0323, SM0313) were used, depending on the expected size of the DNA fragments. When required, DNA fragments were extracted from agarose gels using a gel extraction kit (Qiagen, 28704) according to the manufacturer's protocol.

Molecular cloning

To construct specific plasmids, standard cloning technique employing restriction enzymes was used. All restriction enzymes were purchased from New England Biolabs. Whenever available, high-fidelity versions of the restriction enzymes were used. Insert was cut out from the donor plasmid or produced by PCR. PCR was conducted with Phusion High-Fidelity DNA Polymerase (Life Technologies, F-530S) according to the enzyme manufacturer's protocol. After each restriction digest and PCR, DNA fragments were isolated by agarose gel electrophoresis and subsequent gel extraction. Ligation of the DNA fragments was performed using T4 DNA ligase (New England Biolabs, M0202S) at 16°C for 16 h, followed by heat shock transformation of *E. coli* and subsequent culturing to obtain the desired plasmid.

pCS2- mOrange2-hUrtCH: DNA sequence coding for mOrange in pCS2-mOrange-hUtrCH plasmid (a gift from William Bement, Laboratory of Cell and Molecular Biology, University of Wisconsin-Madison, Madison, USA) was cut out with BamHI and BsrGI and replaced by mOrange2 sequence cut out from pmOrange2 vector (Clontech, 632548) with the same restriction enzymes.

pGEM-H2B-mCherry: PCR amplified cDNA coding for H2B from pCMV-H2B-Venus plasmid (a gift from Anna-Katerina Hadjantonakis, Sloan-Kettering-Institute, New York, USA) was inserted into pGEM-G4S-mCherry plasmid (generated by Sebastian Wennekamp, Hiiragi lab, EMBL, Heidelberg, Germany) cut with XmaI and AccI restriction enzymes. The primers used were as follows:
H2B-F-AccI: CAGTGTCGACATGCCAGAGCCAGCGA
H2B-R-XmaI: CAGTCCCGGGGTGGCGACCGGTGGAT

pCS2-flag-mEzr-Δact: flag-mEzr-Δact fragment was cut from pIND-flag-mEzr-Δact plasmid (a gift from Richard Fehon, The University of Chicago, Chicago, USA) with SpeI and Not1I and inserted into pSC2+ backbone (a gift from Nihan Kara, Cold Spring Harbor Laboratory, Cold Spring Harbor, USA) cut with XbaI and NotI restriction enzymes.

pCS2-PhyB-mCherry-CAAX: PhyB-mCherry-CAAX sequence was amplified by PCR using pHR-PhyB-mCherry-CAAX plasmid (Delquin Gong, Orion Weiner lab, University of California, San Francisco USA) as a template and inserted into pSC2+ backbone cut with BamHI and XbaI restriction enzymes. The primers used were as follows:
PhyBBamHIfw: TCGAGGATCCATGGTATCAGGTGTTG
PhyBXbaIrv: GGGGTCTAGATTACATGATAACACACTTGG

pCS2-Isect-YFP-Pif: Isect-YFP-Pif sequence was amplified by PCR using pMSCV-Isect-DHPH-yfp-Pif plasmid (Delquin Gong, Orion Weiner lab, University of California, San Francisco USA) as a template and inserted into pSC2+ backbone cut with BstBI and XbaI restriction enzymes. The primers used were as follows:
IsectBstBIfw: TTGATTCGAAATGGATATGTTGACCCC
TimXbaIrv: GCGGTCTAGATTAGTCAACATGTTTATTGCTTTC

pCS2-Tim-YFP-Pif: Tim-YFP-Pif sequence was amplified by PCR using pAL190 plasmid (Delquin Gong, Orion Weiner lab, University of California, San Francisco USA) as a template and inserted into pSC2+ backbone cut with BstBI and XbaI restriction enzymes. The primers used were as follows:
TimBstBIfw: TCGATTCGAAATGCTCTCCATGACC
TimXbaIrv: GCGGTCTAGATTAGTCAACATGTTTATTGCTTTC

In vitro transcription

Prior to *in vitro* transcription reaction the plasmids were linearized using restriction enzymes (Table 3.1). mRNA was produced in vitro using mMessage mMachine transcription kits (Ambion, AM1340, AM1348, AM1344, AM1345). Polyadenylation was carried out using Poly(A)Tailing Kit (Ambion, AM1350).

Table 3.1:

Construct	Source	Lineari-zation enzyme	Kit	Polyaden-ylation	mRNA concentration used for experiments
pCS2-EGFP-hUtrCH	William Bement, Laboratory of Cell and Molecular Biology, University of Wisconsin-Madison, Madison, USA	NsiI	SP6	+	30 ng/µl
pCS2-mOrange2-hUrtCH	-	NsiI	SP6	+	60 ng/µl
pGEM-H2B-mCherry	-	SphI	SP6	+	50 ng/µl
pGEMHE-EGFP-MAP4	Jan Ellenberg lab, EMBL, Heidelberg, Germany	SphI	T7	-	130 ng/µl
pRN3-Ezrin-mCherry	Sophie Louvet-Vallée, CNRS, UMR7622-Laboratoire de Biologie Cellulaire du Développement, Paris, France	SfiI	T3	-	150 ng/µl
pGEMHE-myr-palm-IFP670	Judith Reichmann, Jan Ellenberg lab, EMBL, Heidelberg, Germany	PacI	T7 ULTRA	+	30 ng/µl
pc31-mCherry-Cep192	Melina Schuh, MRC, Cambridge, UK	NotI	T7	+	140 ng/µl
pCS2-flag-mEzr-Δact	-	NsiI	SP6	+	300 ng/µl
pCS2-PhyB-mCherry-CAAX	-	NotI	SP6	+	300 ng/µl
pCS2-Isect-YFP-Pif	-	NotI	SP6	+	40 ng/µl
pCS2-Tim-YFP-Pif	-	NotI	SP6	+	40 ng/µl

Cell culture

NIH-3T3 cells stably transfected with pHR-PhyB-mCherry-CAAX and pHR-iSH-YFP-Pif (a gift from Delquin Gong, Orion Weiner lab, University of California, San Francisco USA) were cultured as previously described (Toettcher et al., 2011).

Animal work

All animal work was performed in the Laboratory Animal Resources at the European Molecular Biology Laboratory, according to the permission by the institutional veterinarian overseeing the operation (ARC number TH11 00 11). The animal facilities are operating according to international animal welfare rules (Federation for Laboratory Animal Science Associations guidelines and recommendations). Mouse colonies were maintained in specific pathogen-free conditions with 12-12 h light-dark cycle.

Mouse lines

The following mouse lines were used in this study: (C57BL/6xC3H) F1 for wild-type (WT), Cdx2-EGFP knock-in (McDole and Zheng, 2012), R26-EGFP-Tuba (Abe et al., 2011), R26-H2B-mCherry (Abe et al., 2011), mTmG (Muzumdar et al., 2007), Cdh1^{tm2Kem} (Boussadia et al., 2002), ZP3-Cre (de Vries et al., 2000) and SAS4-EGFP BAC transgenic mice.

To generate SAS4-EGFP mice the SAS4 gene was modified on a bacterial artificial chromosome by recombineering (Testa et al., 2003). The stop codon of the SAS4 coding sequence in the RP11-756A22 BAC was replaced with the ‘localization and affinity purification’ (LAP) tag (Poser et al., 2008). The LAP tagging cassette consists of EGFP sequence followed by an internal ribosome entry site and the neomycin-kanamycin resistance gene for eukaryotic and bacterial expression (Fig. 4.7a). The correct placement of the tagging cassette was confirmed by PCR amplifying the integrations site with the following primers: TGCTCTACGGCTGATGTGTC (hSASS4-F) and TGCAAACGGTCATCAAGAAA (hSASS4-R), producing a 3500 bp fragment. To generate a transgenic ES cell line the modified BAC was transfected into R1/E ES cells that were selected for BAC integration with 250 µg/ml G418 (Life Technologies, 10131035). The ES cells were subsequently injected into C57BL/6 blastocysts that were transferred into pseudo-pregnant CD1 female mice. The resultant pups were examined for the presence of BAC integration by genotyping.

Generation of the modified BAC was done by our collaborators Nicolas Berger and Frank Buchholz (Medical Systems Biology, UCC, University Hospital and Medical Faculty Carl Gustav Carus, TU Dresden, Germany). ES cell injection was performed at the EMBL transgenic facility by Yvonne Petersen. Part of the analysis of the newly established mouse line was carried out by Aurélien Courtois (Hiiragi lab, EMBL, Heidelberg, Germany).

Genotyping

Cdx2-eGFP knock-in, R26-EGFP-Tuba, R26-H2B-mCherry, mTmG, Cdh1^{tm2Kem} and ZP3-Cre mice were genotyped according to protocols described previously.
The primers used were as follows:

Cdx2-EGFP mice:
Cdx2-Fw: ATGGTTCCGTTCCCTGGTTC
GFP-R: GCGGACTTGAAGAAGTCGTGCTGCTT
Cdx2-Ex3: AGGCTTGTTTGGCTCGTTACA C

R26-EGFP-Tuba and R26-H2B-mCherry mice:
R26-P3: TCCCTCGTGATCTGCAACTCCAGTC
R26-P4: AACCCCAGATGACTACCTATCCTCC
R26-P6: GCTGCAGGTCGAGGGACC

mTmG mice:
oIMR7318: CTCTGCTGCCTCCTGGCTTCT
oIMR7319: CGAGGCGGATCACAAGCAATA
oIMR7320: TCAATGGGCGGGGGTCGTT

Cdh1^{tm2Kem}mice:
Cdh1-KO for: CTTATACCGCTCGAGAGCCGG A
Cdh1-KO rev: GTGTCCCTCCAAATCCGATA
tm2kem-deleted F: GAATTCTGAACATCATTATCAGTATTTA
tm2kem-deleted R: TGACACATGCCTTTACTTTAGT

ZP3-Cre mice:
Cre_upper: TGCTGTTTCACTGGTTGTGCGGCG
Cre_lower: TGCCTTCTCTACACCTGCGGTGCT

SAS4-EGFP-BAC mice were genotyped using CTGCTAAATTCGAACGCCAGC (SAS4_F) and CGTCCATGCCGAGAGTGATC (SAS4_R) primers producing a 828 bp fragment.

mzChd1$^{-/-}$ embryos were generated by mating Cdh1$^{floxed/floxed}$ Zp3Cre$^{tg/+}$ females with Cdh1$^{+/-}$ males. Embryos were recovered at the embryonic day 1.5 (E1.5) and one of the two blastomeres was injected with mRNAs encoding Ezrin-mCherry and Myr-palm-IFP. At the late 4-cell stage the zona pellucida was removed mechanically (Tsunoda et al., 1986) and embryos were dissociated to 1/4th blastomeres. Two non-injected 1/4th blastomeres were reaggregated to form 2/4th-embryos and cultured further in the incubator to determine the genotype of the embryos by their ability or inability to form blastocyst and 1/2-embryo-PCR according to the protocol described earlier (Boussadia et al., 2002). The remaining two 1/4th blastomeres were again dissociated at the 2/8th-cell stage into 1/8th blastomeres and used for experiments.

All genotyping work was carried out by Stefanie Salvenmoser and Ramona Bloehs.

Mouse embryo work

Mouse embryo recovery

To obtain mouse pre-implantation embryos, female mice were superovulated by intraperitoneal injection of 5 international unit (IU) of pregnant mare's serum gonadotropin (Intervet, Intergonan) followed by injection of 5 IU human chorionic gonadotropin (hCG; Intervet, Ovogest 1500) 48-50 hours later, and immediately mated with male mice. Zygotes were recovered at E0.5 by ripping the ampula of the ovuducts recovered from the pregnant female mice in hyaluronidase (300 µg/ml, Sigma, H4272) in KSOM with HEPES (H-KSOM; Zenith biotech, ZEHP-050) supplemented with 10 mg/mg PVP-40 (Sigma, P0930). 2- and 8-cell stage embryos were obtained by flushing the oviduct with H-KSOM medium at E1.5 and E2.5, respectively. After recovery embryos were washed in H-KSOM, transferred into 10µm drops of KSOM (Zenith biotech, ZEKS-050) covered with mineral oil (Sigma, M8410) in a tissue culture dish (Falcon, 353001) and cultured in a CO_2 incubator (Thermo Scientific, Heracell 240i) at 37°C with 5% CO_2.

Microinjection

Microinjection of *in vitro* produced mRNAs was performed using a microinjector (Eppendorf, FemtoJet) connected to a manipulator (Narishige, MON202-D) on an epifluorescent microscope (Zeiss, Observer.Z1) equipped with an incubation chamber. Microinjection needles (Warner Instruments, G100TF-6) and holding pipettes (Warner Instruments, GC100T-15) were prepared using a micropipette puller (Sutter Instrument, P-97) and a microforge (Narishige, MF-900). During microinjection the embryos were kept in 10 µl H-KSOM drop covered with mineral oil on a glass-bottom dish (MatTek, P506-1.5-14-F) at 32°C. To knock-down Pard6b expression 10 ng/µl of plasmid encoding shRNA against Pard6b (Sigma-Aldrich, TRCN0000054686) was injected into the male pronucleus of a zygote at 24-26 hours after hCG injection. Plasmids encoding non-target shRNA (Sigma-Aldrich, SHC002; Addgene, #1864) were used as a control interchangeably. For all other experiments mRNAs were injected into cytoplasm of the 2-cell stage embryos, one cell or both cells depending on the experimental condition, at 42-44 hours after hCG injection at a concentration shown in Table 3.1.

Micromanipulation

-Isolation of single blastomeres-

To dissociate embryonic cells, the zona pellucida was first removed either mechanically using holding pipette and a glass needle with help of Narishige manipulator (Tsunoda et al., 1986) or by 3-min incubation with pronase (0.5% w/v Proteinase K, Sigma, P8811, in H-KSOM supplemented with 0.5% PVP-40). Subsequently zona-free embryos were placed into custom-made KSOM medium without Ca^{2+} and Mg^{2+} for 10 min (Biggers, McGinnis and Raffin, 2000). Embryonic cells were dissociated into single cells by pipetting up and down with a narrow flame-polished glass capillary (Brand, 708744). All embryos without zona pellucida and isolated blastomeres were cultured in Petri dishes (Falcon, 351008) to minimize attachment to the bottom of the dish. For experiments when polarized 1/8th blastomeres were required embryos were dissociated at the late 8-cell stage, whereas for experiments when apolar blastomeres were needed embryos were first dissociated at late 4-cell stage and then examined by stereomicroscope (Zeiss, Discovery.v8) equipped with a heating plate (Tokai hit, MATS-UST2) every 30 min for 1/4th-to-2/8th-cell division. Non-polarized 1/8th blatomeres were recovered by dissociating 2/8th blastomeres right after division.

-Removal of cells from the 8-cell embryo-

To remove blastomeres from the 8-cell stage embryo, a slit was generated in the zona pellucida using the same method as described for zona pellucida removal (Tsunoda et al., 1986). Embryos were then transferred into 10 µl drop of KSOM without Ca^{2+} and Mg^{2+} for 15 min at 37°C to loosen the cell-cell adhesion, and 4 blastomeres were sucked out by glass pipette 15-20 µm in diameter, attached to Narishige micromanipulator.

PI(4,5)P_2 uncaging

Apolar 1/8th blastomeres were incubated in 50 µM caged phosphatidylinositol 4,5-bisphosphate (PI(4,5)P_2) or in 50 µM caged 1-palmitoyl-2-oleoyl-sn-glycerol (1,2-POG) solution in dimethyl sulfoxide (DMSO; Sigma, D2650) for 30-60 min at 37°C, 5% CO_2 and then used directly for local uncaging experiments with 405 laser on a double scanner confocal microscope (Olympus, FV1000). Caged PI(4,5)P_2 and 1,2-POG were kindly provided by Andre Nadler (Carsten Schultz lab, EMBL, Heidelberg, Germany).

Phytochrome system

NIH-3T3 cells stably transfected with pHR-PhyB-mCherry-CAAX and pHR-iSH-YFP-Pif or apolar 1/8th blastomeres microinjected with PhyB-mCherry-CAAX and Isect-YFP-Pif or Tim-YFP-Pif mRNAs were incubated in 4 µM phycocyanobilin (Frontier Scientific, P14137) in DMSO for 30-60 min at 37°C, 5% CO_2, then washed and used for the photoactivation experiments. Photoactivation was done on a confocal microscope (Zeiss, LSM780) using 561 nm laser and bleaching mode for local activation and externally installed 735 nm light-emitting diode (Thorlabs, M735L3) equipped with 721 nm longpass filter (Thorlabs, FGL9) constantly illuminating the whole sample for global inactivation. The external light-emitting diode was installed with help of Petr Strnad (Ellenberg lab, EMBL, Heidelberg, Germany).

Microbeads

To coat microbeads with poly-L-lysine (PLL) polystyrene microbeads (Corpuscular, 100255) were washed in sterile water and air-dried. Then the beads were incubated in 0.01% PLL solution (Sigma, P4832) for 10 min at room temperature (RT), followed by the solution removal with a glass micropipette, after which beads were air-dried overnight. To coat the microbeads with Cdh1, recombinant mouse Cdh1 Fc chimera protein (RnDsystems, 748-EC-050) was reconstituted at 100 µg/ml in sterile DPBS with Ca^{2+} and Mg^{2+} (Gibco, 14040-091). ProteinA-coated PMMA beads

(Microparticles, PMMA-Protein A-S2976B), 36 µm in diameter, were washed 2 times in DPBS-T. After centrifugation at 3000 g for 2 min, the washed beads (approx. 4x10^4 beads) were incubated in 25 µl of 0.8 µg/ml Cdh1 solution for 90 min at 4°C, 1400 rpm (Eppendorf, Thermomixer), followed by washing with DPBS-T twice. To block non-coated sites of the beads, they were incubated in 1% heat-inactivated BSA (80°C, 10 min; Sigma, A3311) overnight at 4°C. Polymethyl methacrylate (PMMA) beads (Microparticles, PMMA-R-B375), washed in 0.01% Tween20 in DPBS, were uses for non-specific adhesion of 1/8th blastomeres.

Immunofluorescence

Embryos were fixed in 4% paraformaldehyde (Electron Microscopy Sciences, 19208) in DPBS for 30 min at RT and then washed with 0.1% Tween20 (Sigma, P-7949) in DPBS (DPBS-T). Following permeabilization in 0.25% TritonX-100 (Sigma, T8787) in PBS for 30 min at RT, embryos were washed in DPBS-T and then blocked in DPBS-T for 1 h at RT. Embryos were then incubated with primary antibodies in DPBS-T overnight at 4°C, washed in DPBS-T and incubated with secondary antibodies for 2-3 h at RT. Immunostained embryos were washed in DPBS-T and transferred into 5 µl DAPI (Molecular Probes, D3571; 1:2000) in DPBS-T drop on a glass-bottom dish (MatTek, P356-1.5-20-C) covered with mineral oil for microscopy. All solutions except for paraformaldehyde were supplemented with 3% BSA (Sigma, A9647). The primary antibodies used were rabbit polyclonal anti-Pard6b (Santa Cruz, sc-67393, 1:100), rat anti-tyrosinated γ-Tubulin (AbD Serotec, MCA77G; 1:200,000), mouse anti-Pericentrin (BD, 611814; 1:200), rabbit anti-SAS4 (a gift from Renata Basto; 1:500). The secondary antibodies used were goat anti-rabbit Alexa Fluor 488 (Life Technologies, A11008; 1:200), goat anti-mouse Alexa Fluor 546 (Life Technologies, A21123; 1:200), goat anti-rat Alexa Fluor 633 (Life Technologies, A21094; 1:200).

Live imaging

Embryos or isolated blastomeres were placed into 2-10 µl KSOM drop on glass-bottom dish (MatTek, P356-1.5-20-C) or plastic-bottom dish (Ibidi, 81151) covered with mineral or silicone oil (Ibidi, 50051), respectively. Samples were imaged on LSM780 (Zeiss) with 10-20 min interval using C-Apochromat 40x water objective (Zeiss). 1/8th blastomeres in Fig. 4.1a were imaged on spinning disk microscope (Yokogawa, cv1000). To compensate for embryo drift during imaging, a tracking macro written and installed by Antonio Politi (Ellenberg lab, EMBL, Heidelberg, Germany) was used. Temperature and CO_2 levels were maintained at 37°C and 5%, respectively, in a specially designed microscope incubation chamber (EMBL mechanical workshop). In experiments where non-polarized 1/8th blastomeres expressing Cdx2-EGFP were imaged, 488 nm laser was turned on at the end of the 1/8th cell stage to minimize phototoxicity.

Image analysis

Spindle orientation

In the embryo spindle orientation was evaluated in R26-EGFP-Tuba embryos by measuring the angle between the spindle axis and the vector connecting the embryo center with the spindle center. The two spindle poles, defined by the EGFP-tubulin signal, determined the spindle axis. The embryo center was determined by segmenting the embryo based on EGFP-tubulin cytoplasmic signal using IMARIS (Bitplane, v. up to 7.7.1).

Spindle orientation in isolated blastomeres in relation to the apical domain was evaluated by measuring the angle between the spindle axis and the vector connecting the cell center with the center of the apical domain. For this blastomeres expressing Ezrin-mCherry and EGFP-MAP4 (microtubule-associated protein 4) were used. The apical domain center and the cell center were defined 10 min before nuclear envelope breakdown (NEBD), while the spindle axis was determined at the late metaphase/early anaphase. This measurement was performed only for those blastomeres that did not move substantially during this time. The cell center was defined by fitting a sphere into the blastomere using Fiji. To identify the apical domain center, coordinates of several points of the apical domain edge were first defined on z-slices in Fiji, into which a circle was fitted employing the Taubin method, in Matlab (Mathwork, R2010b). Using the coordinates of the cell center, the center of the fitted circle and the cell radius, the coordinates of the apical domain center were calculated. The random distribution of the spindle orientation is described by the function $\sin\alpha$ on the interval 0° – 90° (Watanabe et al., 2014).

Apical domain

In order to evaluate the relative position of the apical domain in the contact-free cell surface, embryos expressing Ezrin-mCherry and mG were imaged during the 8-cell stage. The blastomeres were segmented based on mG signal using Ilastik and Level-set algorithm, and accordingly the cell center and the center of the contact-free surface were determined. To create the map of the apical domain, defined by Ezrin signal, the longitude and latitude (φ, θ) were assigned to the individual voxels of the segmented blastomere surface, where direction of the north pole is specified by the vector going from the cell center to the center of the contact-free surface. The time dependent change of Ezrin intensity was drawn by mapping the normalized signal intensity $I(\varphi_1, \theta)$ and $I(\varphi_1+180°, \theta)$ as a function of θ, where φ_1 is a constant longitude. The north pole, where $\theta = 90°$, is located at the central position of the vertical axis, from which $I(\varphi_1, \theta)$ and $I(\varphi_1+180°, \theta)$ are mapped to the opposite direction along the vertical axis. To estimate the relative position of the apical domain in the contact-free surface the angle between the two vectors was measured: one vector connecting the cell center with the center of the contact free surface and another vector connecting the cell center with the center of normalized Ezrin signal. The center of Ezrin signal was calculated by measuring voxel intensity weighted sum of vectors of the contact-free surface. Ezrin signal was normalized to the membrane signal.

To assess the segregation of the apical domain between two daughter cells, in the embryo or in isolation, embryos or isolated blastomeres expressing Ezrin-mCherry and fluorescently tagged membrane were imaged during the 8-to-16-cell division. One hour after cytokinesis blastomeres were segmented as described above. The Ezrin intensity was measured on the cell membrane, and the map of the normalized intensity of Ezrin to its cytoplasmic background was created for individual daughters excluding blastomeres interface. Pixels on two Ezrin maps were classified using k-means method into two groups to determine the boundary between the background and the signal. The sum of intensities of non-background pixels was computed for both daughter blastomeres and their ratio was calculated.

To evaluate the distribution of the induced apical domain position in relation to the contact with a bead, an angle between the following two vectors was measured: first vector connecting the center of the apical domain with the cell center, and the second vector connecting the cell center with the bead center. For these measurements blastomeres expressing Ezrin-mCherry and Myr-palm-IFP were used. The center of the apical domain was determined as described above for the whole embryo 30 min before NEBD. Membrane signal was used to segment the cell membrane and determine the cell center as described above. The center of the bead was defined by fitting a circle into a bead in Fiji. Random distribution of the apical domain position is described by the function $\sin\alpha$ on the interval 0° – 180°.

SAS4 spots

To examine the position of SAS4 spots in relation to the apical domain, SAS4-EGFP and Ezrin-mCherry expressing embryos were used. SAS4 localization in blastomeres was analyzed 30 min before NEBD. SAS4 spots were segmented in Fiji and their geometrical center was projected on the blastomere surface. The center of the apical domain and its diameter were measured as described for the isolated blastomeres. The relative distance between the projected SAS4 spots and the apical domain center was calculated and projected SAS4 spots were plotted on the 1D graph, where 0 is the center of the apical domain and 1 is its edge.

To quantify the number of SAS4 spots in embryos injected with control or DN Ezrin mRNA, SAS4-EGFP embryos were used. SAS4 signal was segmented on maximum intensity projection of z-stack in Fiji and number of segmented spots was quantified.

Cdx2 expression

Nuclei of the embryos expressing Cdx2-GFP and H2B-mCherry were automatically segmented based on H2B signal using Ilastik v1.0 and tracked using StarryNite and AceTree software. Cdx2-GFP intensity was measured inside the segmented nuclei and linearly normalized. Normalization curve was determined using the R26-EGFP-Tuba embryos imaged under the same condition. For Pard6b knock-down experiment measurement of Cdx2-GFP intensity was done only for the last time point before 32- to 33-cell stage transition and Cdx2-GFP signal was normalized to the H2B-mCherry signal.

To evaluate the Cdx2 expression level in isolated blastomeres, signal intensity of the Cdx2-GFP and H2B-mCherry were measured in the middle of the nucleus of both daughter cells 30 min before 2/16th-to-4/32th-cell stage division in Fiji.

Cell envelopment

The degree of envelopment of one blastomere by another was determined by measuring the ratio of the two areas depicted in the Fig. 4.2e. Blastomeres interface of which was parallel to the imaging plane were excluded from the analysis.

Nuclei and cell membrane segmentation and tracking pipelines were developed by Ritsuya Niwayama.

Statistical analysis

Graphs were generated and statistical analyses were performed using Matlab. Spindle orientation distribution in relation to the apical domain and apical position distribution in relation to the contact with the bead were evaluated by the two-sample Kolmogorov–Smirnov test applied on the observed values against the theoretical values for random distribution. For statistical analysis data were first analyzed for normality using Shapiro-Wilks test. The statistical dependence between two variables was evaluated with Spearman's rank correlation coefficient. One-sided Fisher's exact test was used for statistical analysis of repolarization frequency in the whole and 1/2-embryos. For statistical analysis of Pard6b knock-down data Mann-Whitney U-test was used. In boxplot in Fig. 4.11d the central mark is the median, the edges of the box are the 25th and 75th percentiles, the whiskers extend to the most extreme data points not considered the outliers.

4. Results

Identification of the apical domain as a possible symmetry breaking cue

In order to identify the symmetry breaking cue, the development of 1/8th blastomeres expressing fluorescent markers for different cellular structures (membrane, nucleus, microtubules (MT), apical domain) and TE lineage marker (Cdx2), was monitored and examined for the earliest hallmark predicting cell fate.

1/8th blastomeres polarize without adhesion

During the development of initially apolar 1/8th blastomeres, which expressed fluorescently labelled hUtrCH (F-actin binding human Calponin homology domain of Utrophin; Burkel, Dassow and Bement, 2007) I observed the appearance of an increased amount of actin on one side of the cell cortex. Shortly before cell division this cortical actin formed a ring-shaped structure at the cell cortex (Fig. 4.1a). Immunostaining of these blastomeres with an antibody against aPKC demonstrated that this actin-ring corresponds to the periphery of the apical domain (Fig. 4.1b). Thus, it appears that the initially symmetric isolated blastomeres can polarize without cell-cell interaction.

To exclude the possible induction of polarization by adhesion to the culture dish, I systematically tested dishes that were not only suitable for microscopy, but either had non-adhesive surface or were coated with repellent chemicals such as polydimethylsiloxane, polyethylene glycol or silicone. The optimal dish identified in this screen was Ibidi non-treated plastic-bottom dish (Ibidi, 81151). 1/8th blastomeres cultured in these dishes displayed no sign of attachment to the bottom in the 10-h time period that is sufficient for cell polarization (N = 16). Therefore, all following experiments involving non-polarized 1/8th blastomeres were performed using this type of dish. When cultured in Ibidi dishes, it was observed that 66% of non-polarized 1/8th blastomeres acquired an apical domain, which can be identified with Ezrin – an apical domain marker (*N* = 21 of 32 cells examined; Fig. 4.1c).

As an alternative approach in preventing blastomere attachment to the dish, I used zona pellucida from hatched pre-implantation mouse embryos as a natural non-adhesive surface to culture isolated blastomeres. Initially, non-polarized isolated blastomeres expressing Ezrin-mCherry and EGFP-hUtrCH were placed individually into a zona pellucida and imaged until the cell division to 2/16th-cell stage occurred. With the use of these conditions, 38% blastomeres polarized before division (N = 3 of 8 cells examined; Fig. 4.1d). These results indicate that neither cell-cell contact, nor acellular adhesion are necessary for isolated blastomeres to polarize.

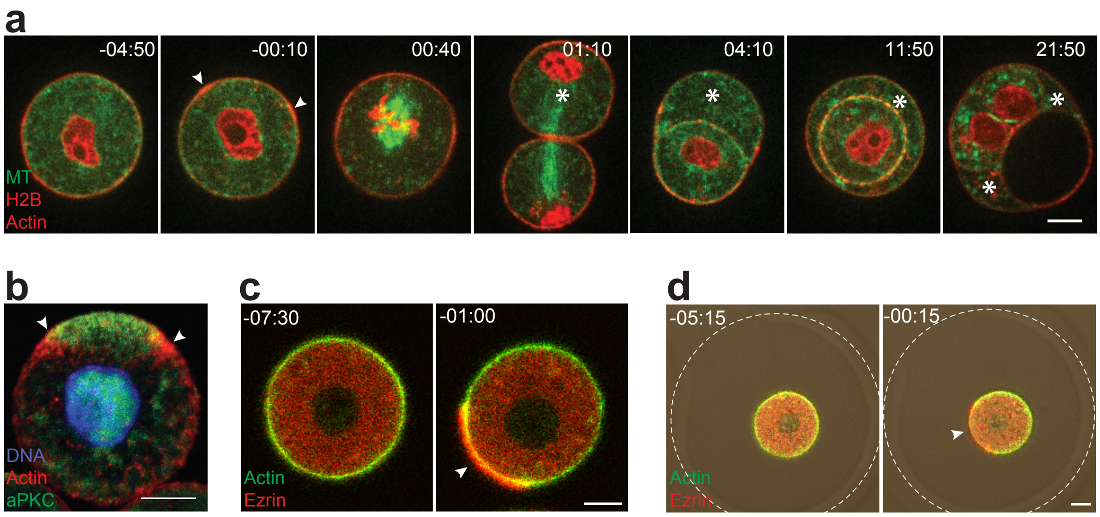

Figure 4.1: The apical domain can be self-organized in a 1/8th blastomere.

a, Development of a 1/8th blastomere microinjected with mOrange2-hUtrCH, H2B-mCherry and EGFP-MAP4 (MT) mRNAs. **b,** Immunostaining of polarized 1/8th blastomeres. **c,** Polarization of initially apolar 1/8th blastomere expressing EGFP-hUtrCH and Ezrin-mCherry cultured in non-adhesive dish. **d,** Polarization of an initially apolar 1/8th blastomere expressing EGFP-hUtrCH and Ezrin-mCherry cultured inside the zona pellucida. White arrowheads indicate the apical domain. Asterisks mark the blastomere that inherited the apical domain after division and its progeny. Broken circle labels zona pellucida. Time, post-NEBD (hh:mm). Scale bars, 10 µm.

The majority of polarized 1/8th blastomeres divide asymmetrically

Analysis of the development of polarized 1/8th blastomeres injected with Ezrin-mCherry and EGFP-MAP4 mRNAs revealed that the majority of these blastomeres formed the spindle in line with the apical-basal axis (80%, N = 20 of 25 cells examined, within 0-45°; $P < 10^{-6}$; Fig. 4.2a,b). Furthermore, measurements of Ezrin signal intensity on the membrane of both daughter cells right after division of the polarized 1/8th blastomeres, expressing Ezrin-mCherry and Myr-palm-IFP, showed that the majority of these blastomeres underwent asymmetric division, as defined in this study by the differential segregation of the apical domain (86%, N = 19 of 22 cells with the ratio of Ezrin segregation higher than 3:1; Fig. 4.2c,d). This finding is consistent with previous observations (Johnson and Ziomek, 1981b). Interestingly, many of the 2/16th couples after asymmetric division displayed an envelopment of the apolar cell by its polar sister cell (in 14 out of 16 examined couples the degree of envelopment was higher than 0.2; Fig. 4.2e), while couples generated by symmetric division did not exhibit such behavior. These results indicate that the majority of 1/8th blastomeres align the spindle along the polarity axis leading to differential segregation of the apical domain and that asymmetric division has an impact on the following morphogenesis.

Inheritance of the apical domain predicts TE fate

Remarkably, all daughter cells that inherited the apical domain as a result of an asymmetric division gave rise to cells differentiating into TE (Fig. 4.1a, Fig. 4.2a,c and Fig. 4.3a). Analyses of the development of transgenic Cdx2-EGFP 2/16th couples showed that the more a cell envelops its sister cell, the higher the level of Cdx2 it expresses compared to its sister cell ($N = 22$; $R = -0.6$, $P < 0.005$, Spearman correlation test; Fig. 4.3b). Given that in 2/16th couples, resulted from asymmetric divisions, polar cell envelops the apolar sister, there is a relationship between segregation of the apical domain and the expression levels of Cdx2 in the daughter cells, such that upon asymmetric division Cdx2 expression is higher in the polar sister cell.

Together these data suggest an intriguing possibility that the acquisition of the apical domain may allow predicting the following cell division pattern, morphogenesis and differentiation of its specific progeny into TE.

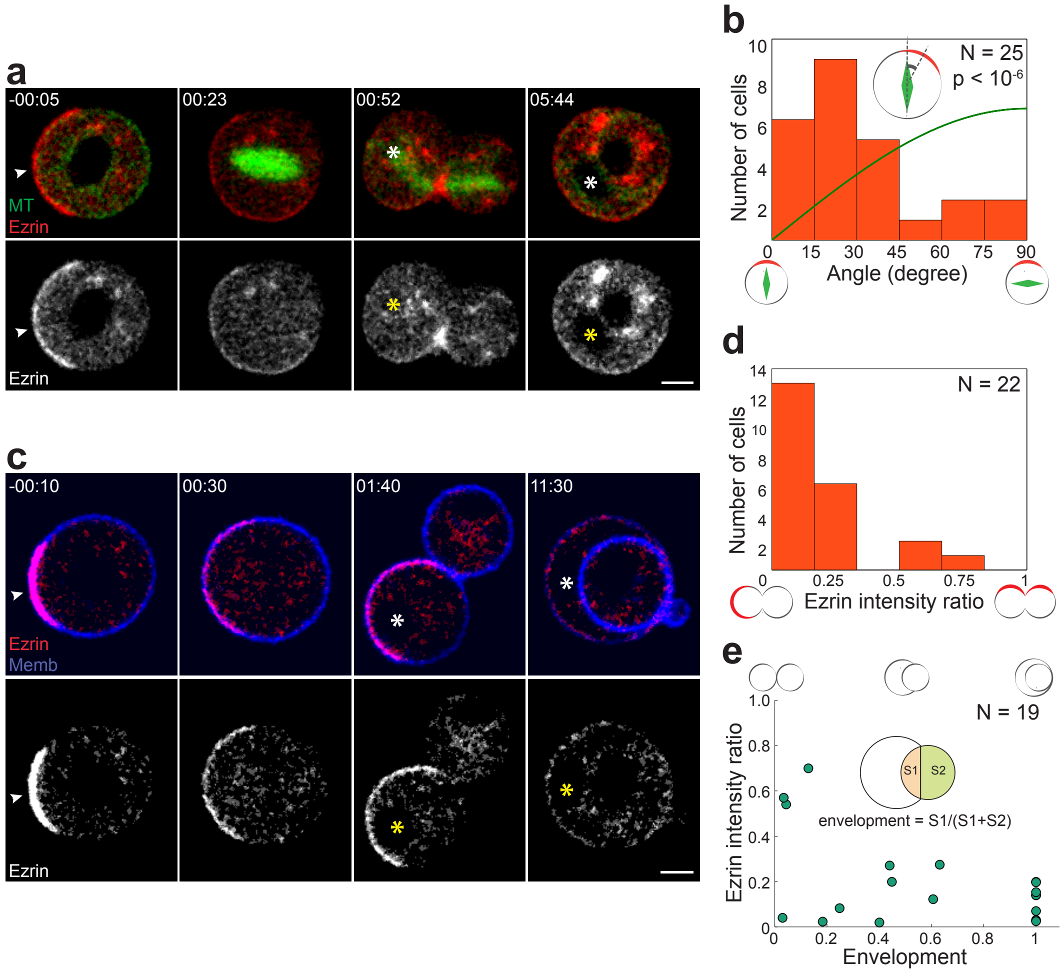

Figure 4.2: Predominantly asymmetric 1/8th-to-2/16th-cell stage divisions.

a, Time-lapse of a polar 1/8th blastomere expressing Ezrin-mCherry and EGFP-MAP4 (MT). **b,** Distribution of the spindle orientation relative to the apical domain in late metaphase 1/8th blastomeres. **c,** Development of a polarized 1/8th blastomere microinjected with Ezrin-mCherry and Myr-palm-IFP (Memb) mRNAs. **d,** Differential segregation of the apical domain after 1/8th-to-2/16th-cell stage division. **e,** Correlation between relative Ezrin intensity and the degree of envelopment. White arrowheads indicate the apical domain. Blastomeres that inherited the apical domain after division are marked with asterisk. Time, post-NEBD (hh:mm). Scale bars, 10 µm.

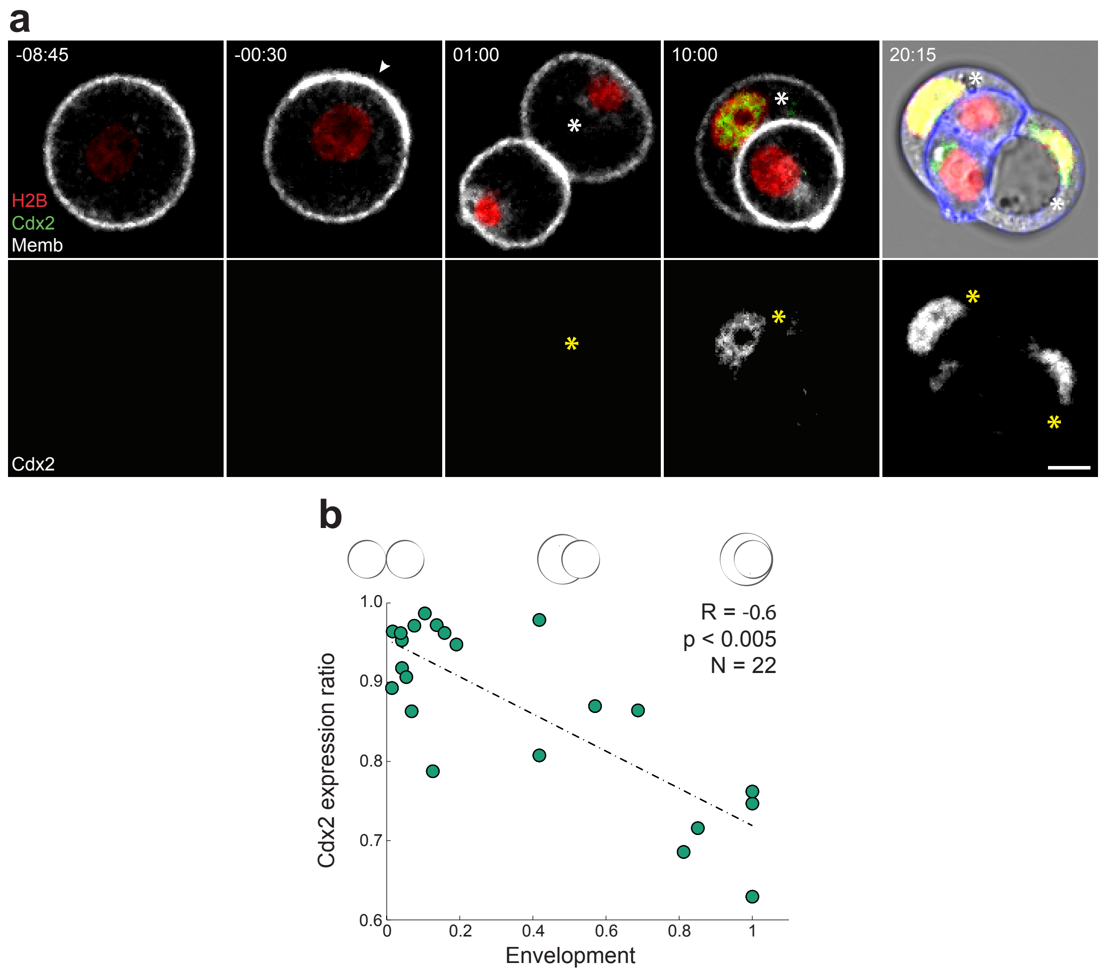
a
-08:45
-00:30
01:00
10:00
20:15
H2B
Cdx2
Memb
*
Cdx2
b
1.0
0.9
0.8
0.7
0.6
0
0.2
0.4
0.6
0.8
1
R = -0.6
p < 0.005
N = 22
Cdx2 expression ratio
Envelopment

Figure 4.3: Cdx2 expression pattern during development of 1/8th blastomere to mini-blastocyst.

a, Time-lapse images of the developing 1/8th blastomere expressing Cdx2-EGFP, R26-H2B-mCherry and Myr-palm-IFR (Memb). The polar daughter cell envelops its apolar sister and expresses Cdx2. White arrowhead indicates the apical domain. The blastomere that inherited the apical domain after division and its progeny are marked with asterisks. Time, post-NEBD (hh:mm). Scale bar, 10 µm. **b,** Correlation between the relative level of Cdx2 expression and the degree of envelopment.

The 8-to-16-cell stage division is preferentially asymmetric

While in isolation the 1/8th blastomeres exhibited a strong bias toward asymmetric division segregating the apical domain preferentially to one of the daughter cells, in the whole embryo it has been generally considered that the majority of blastomeres undergo "symmetric" divisions during 8-to-16-cell stage transition, as defined by the eventual cell position, on the inside or outside of the embryo (Johnson and McConnell, 2004; Johnson, Maro and Takeichi, 1986; Plusa, 2005). When the spindle orientation was examined in the whole 8-cell stage embryos, transgenic for EGFP-tubulin, by live imaging at high spatiotemporal resolution, in as many as 75% ($N = 98$ of 130 cells examined, $P < 10^{-22}$; Fig. 4.4a,b) of the blastomeres the spindle was oriented along the apical-basal axis (within 0-45°). Moreover, the majority of blastomeres in 8-cell stage embryos expressing Ezrin-mCherry underwent asymmetric division (74%; $N = 23$ of 31 cells with the ratio of Ezrin segregation higher than 3:1; Fig. 4.4c), which is consistent with my findings regarding 1/8th blastomere development and with several recent studies (Anani et al., 2014; Watanabe et al., 2014).

Possible factors influencing spindle orientation in the 8-cell stage embryo

To understand the mechanism underlying the preferential asymmetric division of 8-cell stage blastomeres, I first examined the correlation between different cellular parameters and spindle orientation in the 8-cell embryo. The relative timing of cell division, cell volume, sphericity and size of the apical domain were evaluated (Fig. 4.5). Among those, only the apical domain size showed a statistically significant correlation with spindle orientation ($R = 0.46$, $P < 0.002$, Spearman correlation test; Fig. 4.5a). Blastomeres with a smaller apical domain are more likely to undergo asymmetric division, while cells with bigger apical domain tend to divide symmetrically, in agreement with earlier report (Pickering et al., 1988).

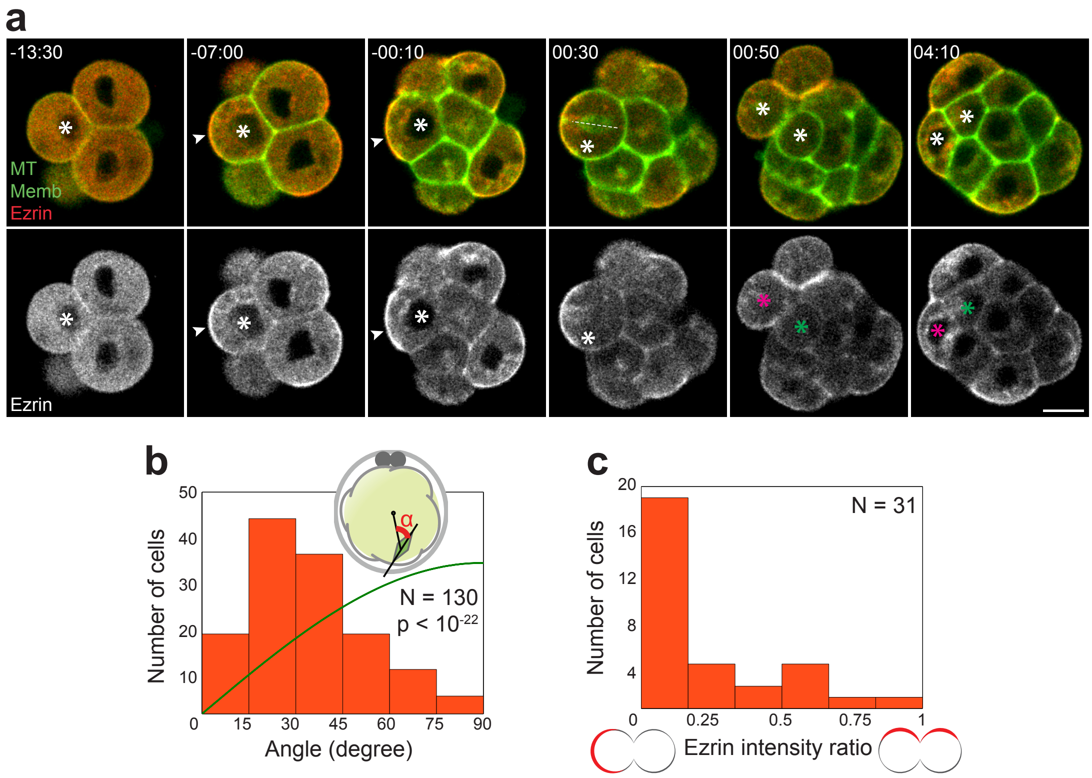
a
-13:30
-07:00
-00:10
00:30
00:50
04:10
MT
Memb
Ezrin
Ezrin
b
Number of cells
50
40
30
20
10
0
15
30
45
60
75
90
Angle (degree)
α
N = 130
p < 10^-22
c
Number of cells
20
16
12
8
4
0
0.25
0.5
0.75
1
Ezrin intensity ratio
N = 31

Figure 4.4: Predominantly asymmetric divisions in the 8-cell stage embryo.

a, Time-lapse images of the asymmetric 8-to-16-cell stage division in a R26-EGFP-Tuba (MT) x mG (Memb) embryo microinjected with Ezrin-mCherry mRNA. White arrowhead indicates the apical domain. Asterisks label the blastomere dividing asymmetrically and its progeny. Magenta asterisks mark the blastomere that inherited the apical domain; green asterisks label the apolar blastomere going inside the embryo. **b**, Distribution of spindle orientation in the 8-cell stage embryo. **c,** Differential segregation of the apical domain after 8-to-16-cell stage division. Time, post-NEBD (hh:mm). Scale bar, 20 μm.

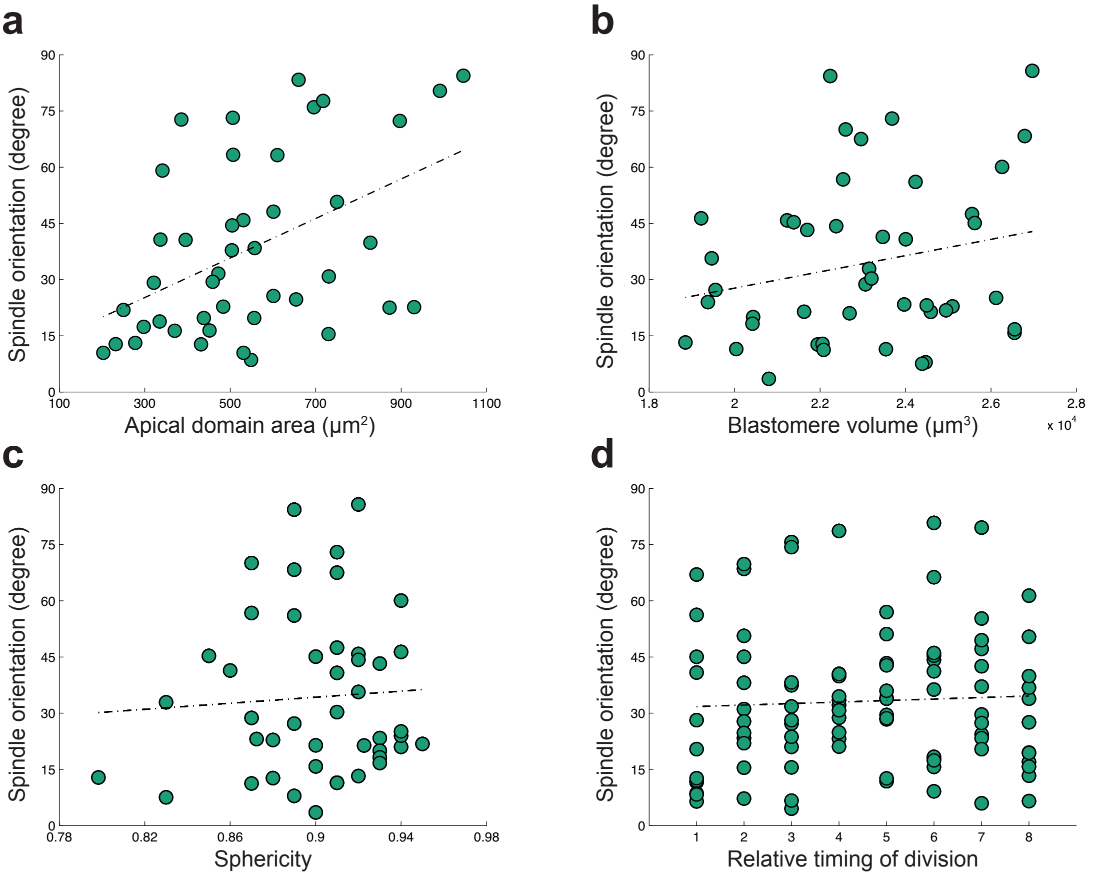

Figure 4.5: Correlation of spindle orientation with different parameters of 8-cell stage embryo blastomeres.

a, Correlation of the apical domain area and the spindle orientation in the 8-cell stage embryo. N = 43, R = 0.46, P < 0.002. **b,** Correlation of the blastomere volume with the spindle orientation. N = 45, R = 0.17, P = 0.26. **c,** Correlation between the sphericity of the cell in the embryo and the spindle orientation. N = 45, R = 0.04, P = 0.82. **d,** Correlation between relative timing of blastomere division and the spindle orientation in the embryo. N = 96, R = 0.07, P = 0.48. Spearman correlation test was used for all data sets.

Apical domain forms in the center of the contact-free surface

To understand how the apical domain could influence the spindle orientation, I first examined *de novo* apical domain formation in blastomeres of 8-cell stage embryo. Live-imaging of transgenic mG 8-cell stage embryos microinjected with Ezrin-mCherry and image analysis of the emerging apical domain (Fig. 4.6a) showed that in some blastomeres the apical domain formed directly in the center of the contact-free surface, while in others it was initially off-centered (Fig. 4.6b,c). Nevertheless, in both cases the center of the contact-free surface and the center of the apical domain converged towards the end of the interphase (Fig. 4.6b,c). Interestingly, timing of the apical domain emergence at 8-cell stage varied from 20 to 640 min before NEBD (N = 8), which cannot be explained by asynchronous divisions from 4-to-8-cell stage (Fig 4.6c).

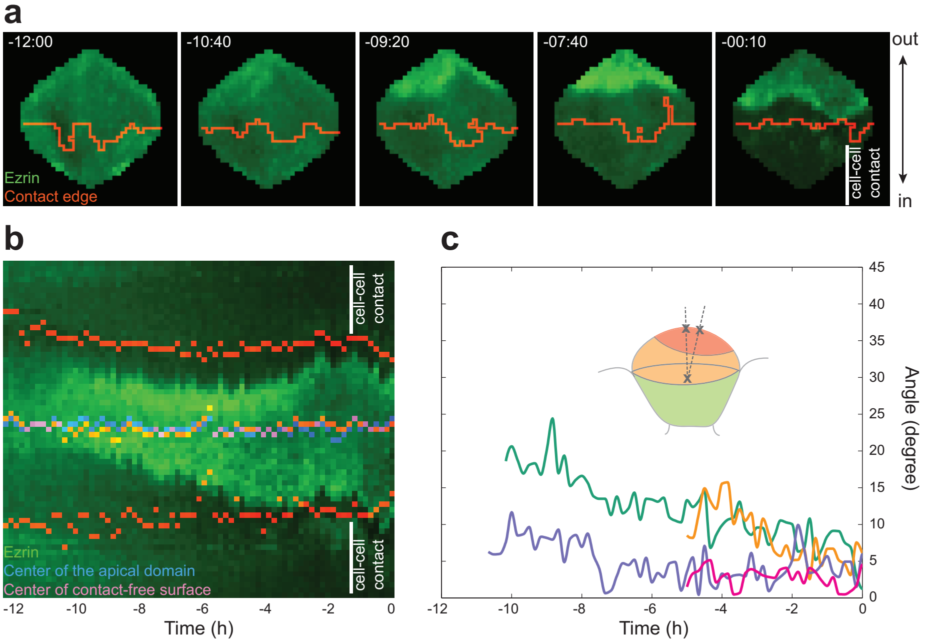
a
-12:00
-10:40
-09:20
-07:40
-00:10
out
in
Ezrin
Contact edge
cell-cell contact
b
cell-cell contact
cell-cell contact
Ezrin
Center of the apical domain
Center of contact-free surface
-12
-10
-8
-6
-4
-2
0
Time (h)
c
45
40
35
30
25
20
15
10
5
0
Angle (degree)
-12
-10
-8
-6
-4
-2
0
Time (h)

Figure 4.6: The apical domain is positioned in the center of the contact-free surface.

a, Map of a blastomere developing polarity in the 8-cell stage embryo. Red line depicts the border between cell-cell contact and contact-free surface. **b,** Kymograph of the formation of the apical domain in the blastomere of the 8-cell stage embryo. **c,** The center of the apical domain, as it grows, progressively approaches to the center of the contact-free surface. Time, post-NEBD (hh:mm).

Apical domain recruits MTOCs to the sub-apical region

In the pre-implantation mouse embryo, the spindle is self-assembled by the collective action of microtubule organizing centers (MTOCs) without centrioles. To fully characterize the dynamics of MTOCs localization, a BAC-transgenic mouse expressing SAS4-EGFP was generated (Fig. 4.7a). Up to the 4-cell stage, the distribution of MTOCs in the cytoplasm was random, whereas in an 8-cell stage embryo, clusters of MTOCs were observed mostly in the sub-apical region, which is consistent with previous findings (Courtois et al., 2012; Houliston, Pickering and Maro, 1987). To confirm the localization of SAS4 in the transgenic mouse line, 8-cell stage WT embryos were examined by immunostaining with antibodies against SAS4 and Pericentrin (Pcnt). The results showed enrichment of SAS4 spots at the apical side of the blastomere, that co-localized with Pcnt (Fig. 4.7b). In addition, live imaging of SAS4-EGFP embryos microinjected with another MTOC marker, Cep192, showed co-localization of these two markers at the apical side (Fig. 4.7c).

Recruitment of MTOCs to the sub-apical region where they formed a cluster coincided with the emergence of the apical domain (Fig. 4.8a,b). Upon nuclear envelope breakdown, MTOC cluster evolved into one pole of the spindle on the apical side (Fig. 4.8c), whereas the other pole was assembled by collective self-organization of MTOCs distributed on the basal hemisphere of the nuclear surface. When the apical domain was disrupted by DN Ezrin (Speck et al., 2002), formation of MTOC clusters was suppressed (Fig. 4.8d,e), indicating that the recruitment of MTOCs is dependent on the apical domain.

Collectively the apical domain forms at the center of the contact-free surface and recruits MTOCs to the sub-apical region. MTOCs may tether one of the spindle poles to the sub-apical region, thereby aligning spindle along apical-basal axis and allowing the preferential segregation of the apical domain to only one of the daughter cells.

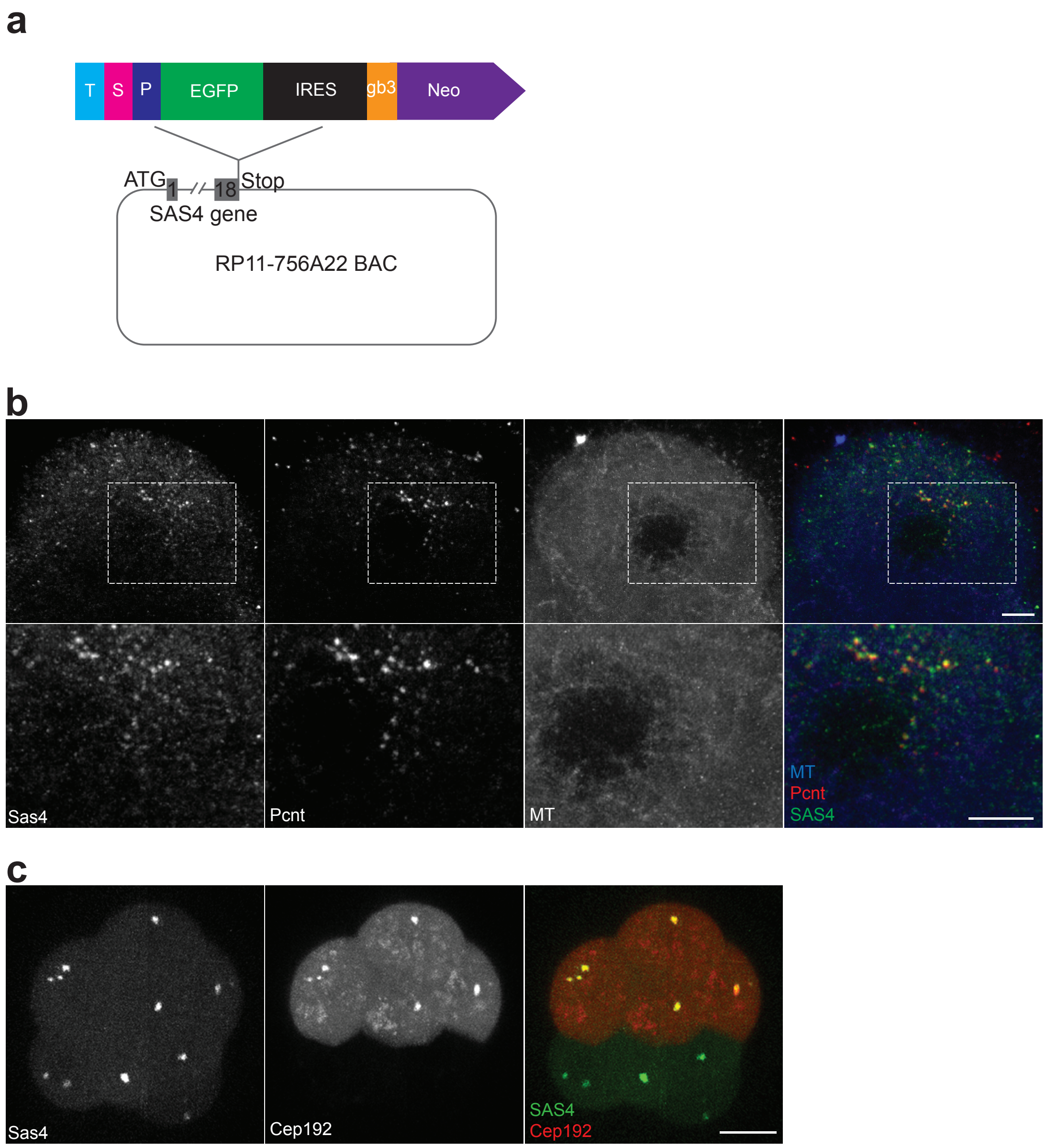
a
T
S
P
EGFP
IRES
gb3
Neo
ATG
1
18
Stop
SAS4 gene
RP11-756A22 BAC
b
Sas4
Pcnt
MT
MT
Pcnt
SAS4
c
Sas4
Cep192
SAS4
Cep192

Figure 4.7: Generation of SAS4-EGFP-BAC mouse line.

a, C-terminus tagging of SAS4 with LAP cassette. The cassette contains: TEV cleavage site (T), S-peptide (S), PreScission cleavage site (P), EGFP, an internal ribosome entry site (IRES), a bacterial promoter (gb3) and a neomycin resistance gene (Neo). **b,** Co-localization of SAS4 and Pcnt shown by immunostainin of the 8-cell stage mouse embryo. **c,** Co-localization of SAS4 and Cep192 in SAS4-EGFP embryos microinjected with Cep192-mCherry mRNA in one cell of the 2-cell embryo. Z-projected image of the 8-cell stage live embryo. Scale bars, **b** – 5 µm, **c** – 20 µm.

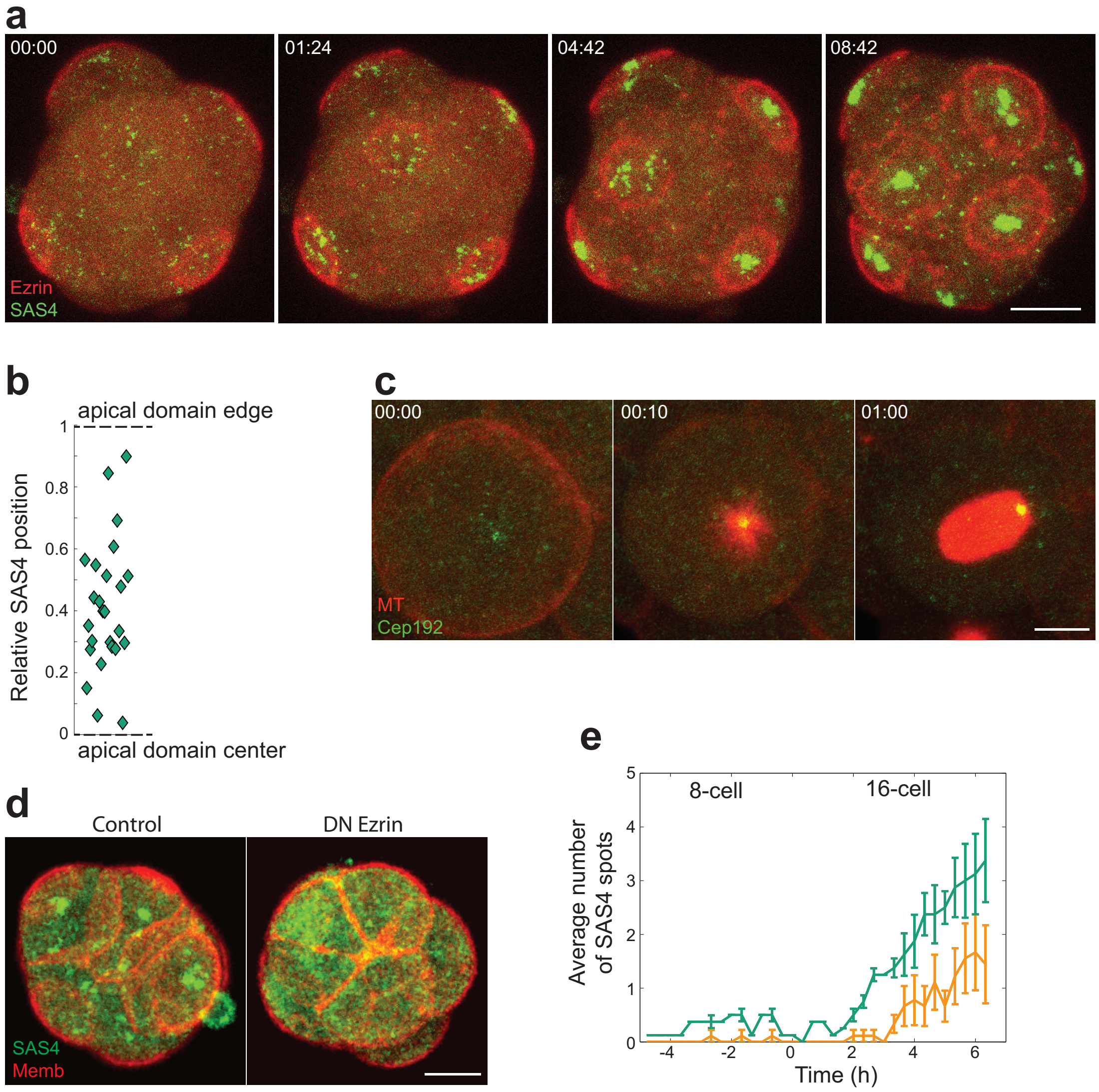
a
00:00
01:24
04:42
08:42
Ezrin
SAS4
b
apical domain edge
Relative SAS4 position
apical domain center
1
0.8
0.6
0.4
0.2
0
c
00:00
00:10
01:00
MT
Cep192
d
Control
DN Ezrin
SAS4
Memb
e
8-cell
16-cell
Average number of SAS4 spots
Time (h)
5
4
3
2
1
0
-4
-2
0
2
4
6

Figure 4.8: The apical domain recruits MTOCs to form one of the spindle poles.

a, Time-lapse images of the apical domain maturation in a SAS4-EGFP 8-cell stage embryo microinjected with Ezrin-mCherry mRNA. **b,** The relative position of SAS4 spots to the apical domain. **c,** Localization of Cep192 at the spindle pole in one blastomere of the 8-cell embryo expressing EGFP-MAP4 and Cep192-mCherry. **d,** The apical domain is required for recruiting MTOCs to the sub-apical region. DN Ezrin (with Myr-palm-IFP) or control (Myr-palm-IFP only) mRNA was injected into the 2-cell stage embryo. DN Ezrin suppressed formation of MTOC clusters at the 8-cell stage. **e,** Average number of SAS4 spots in embryos injected with control (green, N = 8 embryos) or DN ezrin (orange, N = 9 embryos) mRNA. Data are represented as mean ± SEM. Time, post-NEBD (hh:mm), except for **a**, where 00:00 is 68 h post-hCG-injection (hh:mm). Scale bars, **a**,**d** – 20 µm, **c** – 10 µm.

A cell’s fate is determined by its position within the embryo

Apolar blastomeres in 16-cell stage embryo can repolarize and adopt TE fate

When the dynamics of cellular behavior and the apical domain were tracked by live imaging, for embryos undergoing 8-to-16-cell stage divisions, I noted that upon asymmetric divisions, some apolar daughter cells stayed on, or moved to, the surface of the embryo and eventually acquired an apical domain ($N = 21$ cells in 16 embryos; Fig. 4.9a). The majority of these cells eventually turned on *Cdx2* expression, albeit later than the polar cells formed as a direct result of 8-to-16-cell stage division ($N = 11$ out of 13 cells in 8 embryos; Fig. 4.9b,d). This could explaining the cell-to-cell heterogeneity of Cdx2 expression observed in 16-cell stage embryos (Dietrich and Hiiragi, 2007; Ralston and Rossant, 2008). The proportion of apolar cells that acquired the apical domain at the 16-cell stage was 26% ($N = 21$ of 80 apolar cells in 16 embryos examined), indicating that the 8-to-16-cell division pattern alone cannot determine the cell fate, in agreement with recent studies (Watanabe et al., 2014; McDole et al., 2011; Yamanaka, Lanner and Rossant, 2010). This rate of repolarization is higher than that (1%, $N = 1$ out of 101 cells examined) reported in another recent study (Anani et al., 2014), possibly due to the difference in the spatiotemporal resolution of live images and in mRNA injection or transgenic mice used. Regardless of the proportions the observation made here indicates that cells in the 16-cell stage embryo can repolarize.

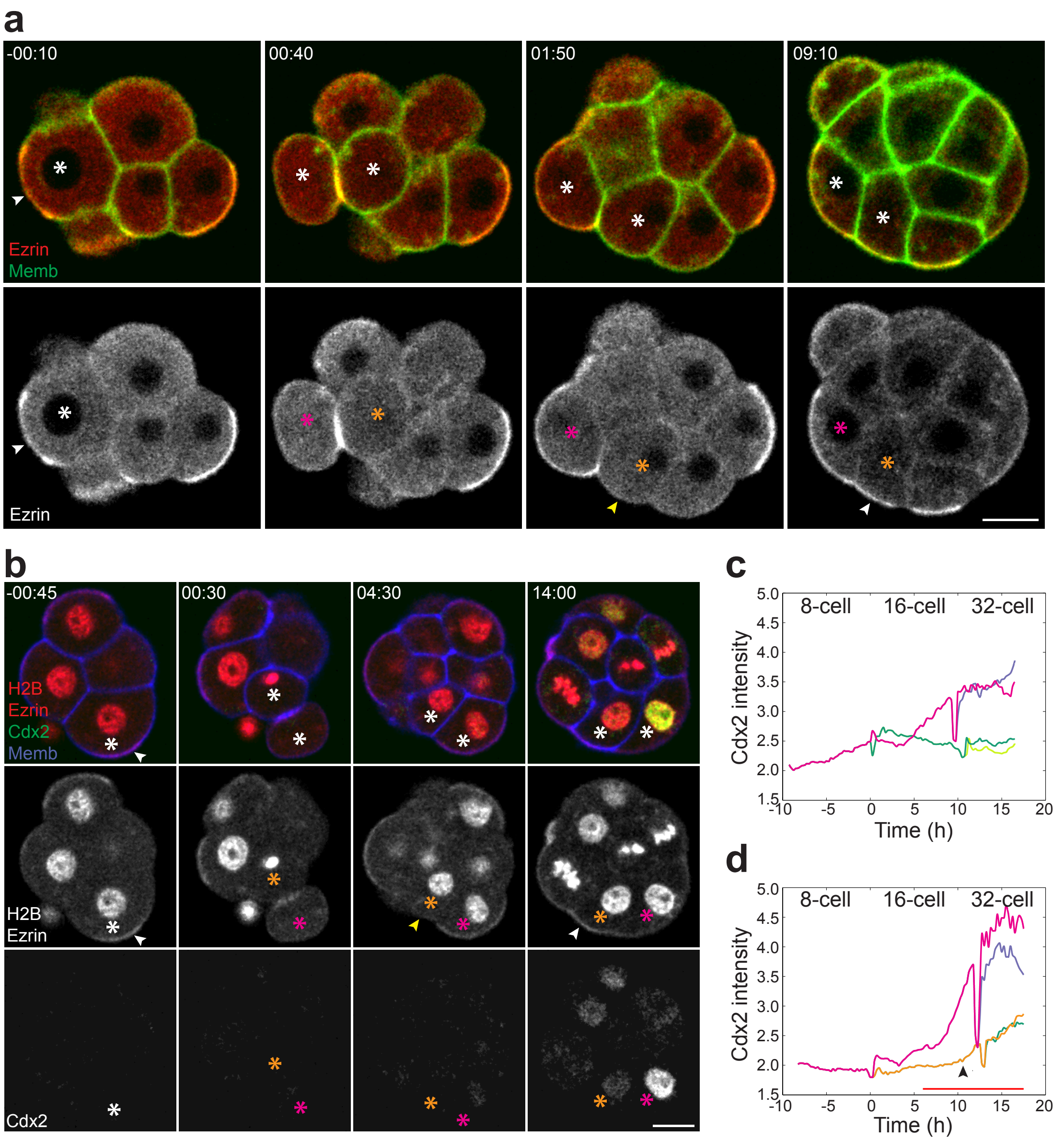
a
-00:10
00:40
01:50
09:10
Ezrin
Memb
Ezrin
b
-00:45
00:30
04:30
14:00
H2B
Ezrin
Cdx2
Memb
H2B
Ezrin
Cdx2
c
8-cell
16-cell
32-cell
Cdx2 intensity
Time (h)
5.0
4.5
4.0
3.5
3.0
2.5
2.0
1.5
-10
-5
0
5
10
15
20
d
8-cell
16-cell
32-cell
Cdx2 intensity
Time (h)

Figure 4.9: Cell positioning outside the embryo induces acquisition of the apical domain, which in turn induces Cdx2 expression.

a-b Time-lapse images of asymmetric 8-to-16-cell division in the mouse embryo. An apolar cell acquires the apical domain during the 16-cell stage (**a**,**b**) and up-regulates Cdx2 expression (**b**). White arrowhead indicates the apical domain, yellow arrowheads mark apolar cells that stay outside the embryo, asterisks label cells undergoing asymmetric division and their progeny: magenta asterisks label polar daughters, orange asterisks label apolar cells. Time, post-NEBD (hh:mm). Scale bars, 20 µm. **c-d,** Dynamics of Cdx2 expression in an 8-cell blastomere and its progenies. **c,** Apolar cell goes inside the embryo and has low level of Cdx2 expression. **d,** Cdx2 expression is up-regulated (black arrowhead) after an apolar cell acquires the apical domain (red underline).

The spatial context influences repolarization frequency

To test whether the repolarization frequency of apolar blastomeres observed in the 16-cell stage embryo is an intrinsic property of the cells, we examined the proportion of repolarizing cells in half (or 8/16th) embryos. When 4 blastomeres were removed from the 8-cell stage embryo to form the 4/8th-embryo and the cellular behavior was monitored following the 8-to-16-cell stage divisions (Fig. 4.10a), the rate of change from apolar to polar cells was higher (52%, $N = 22$ of 42 polar cells in 12 embryos; Fig. 4.10b) compared to the whole embryo. This result suggests that the cell position rearrangement is dependent not only on the intrinsic property of the cell, but also on the spatial context.

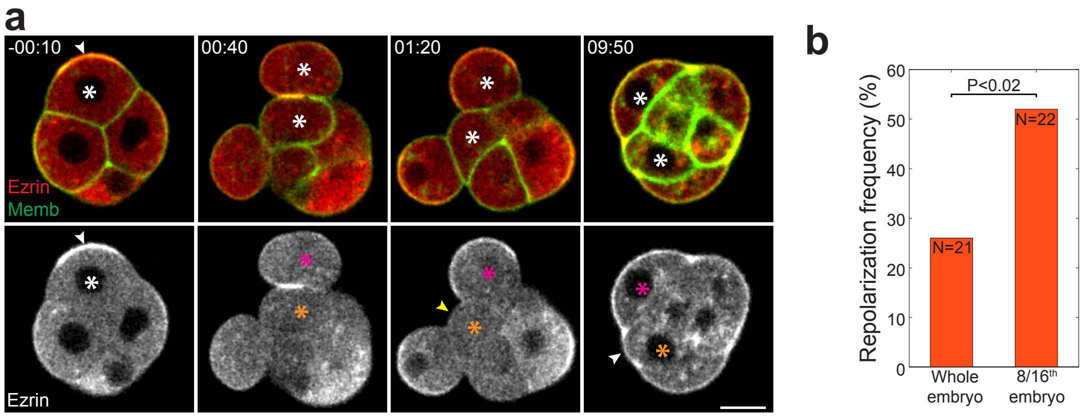

Figure 4.10: Spatial context influences repolarization rate.

a, Time-lapse images of the 4/8th mG embryo, microinjected with Ezrin-mCherry mRNA, in which an apolar cell acquires the apical domain during the 8/16th-cell stage. Time, post-NEBD (hh:mm). Scale bar, 20 µm. **b**, Repolarization frequency of apolar blastomeres at the 16-cell stage. The ratio of initially apolar cells that acquire the apical domain depends on the spatial context.

In summary, cell fate is not determined by the division pattern, but rather by its position within the embryo, which is influenced by the spatial context. When the cell is positioned to the embryo surface, it acquires the apical domain that in turn induces Cdx2 expression and TE differentiation.

Requirement and sufficiency of the apical domain for TE fate specification

The data described so far suggest the apical domain as TE cell fate driver. Thus, I decided to test whether it is indeed required and sufficient for TE cell fate specification.

Disruption of the apical domain results in a failure to form trophectoderm

Firstly, I confirmed that the apical domain is required for TE cell fate specification by examining the effect of its disruption on the early mouse development. When zygotes were injected with plasmid encoding shRNA against Pard6b, Pard6b protein was not detectable in the outside cells of the 32-cell embryos as determined by immunofluorescence staining (Fig. 4.11a). These embryos failed to form proper trophectoderm and Cdx2 expression was down-regulated (Fig. 4.11b,c,d), which is agreement with previously published data (Alarcon, 2010). Thus, the apical-basal polarity is required for TE differentiation.

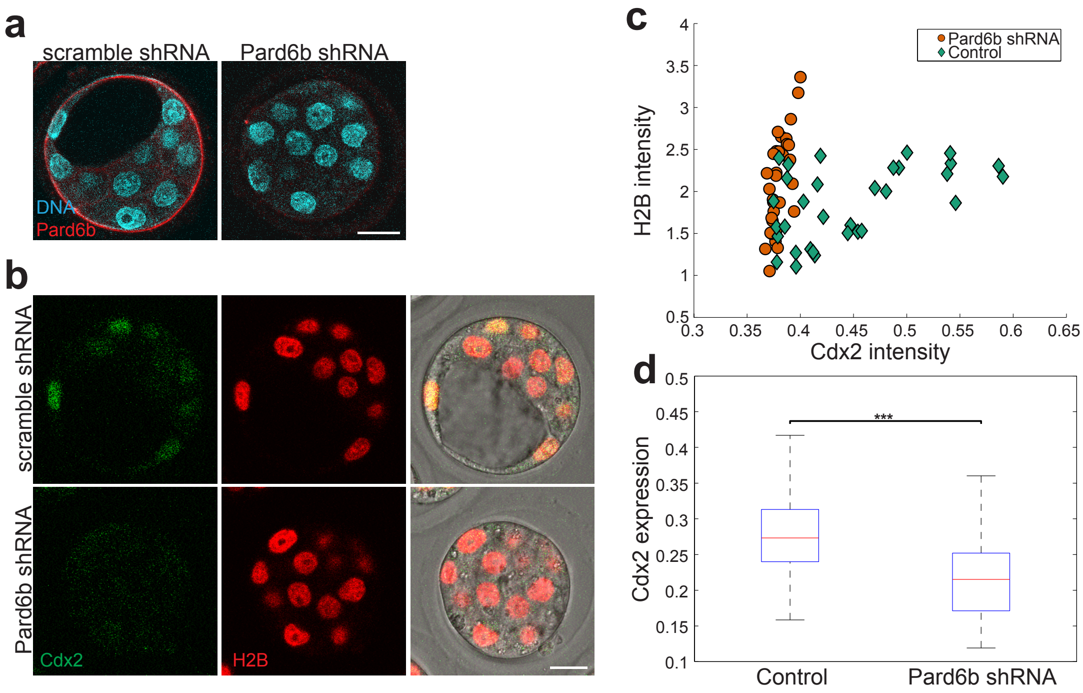
a
scramble shRNA
Pard6b shRNA
DNA
Pard6b
b
scramble shRNA
Pard6b shRNA
Cdx2
H2B
c
H2B intensity
Cdx2 intensity
Pard6b shRNA
Control
0.5
1
1.5
2
2.5
3
3.5
4
0.3
0.35
0.4
0.45
0.5
0.55
0.6
0.65
d
Cdx2 expression
0.1
0.15
0.2
0.25
0.3
0.35
0.4
0.45
0.5
***
Control
Pard6b shRNA

Figure 4.11: Apical-basal polarity is required for specifying TE cell fate.

a, Pard6b shRNA effectively suppresses the expression of Pard6b protein, as shown by immunofluorescence staining of the blastocyst for Pard6b. **b,** Cdx2 expression is suppressed in the blastocyst in which Pard6b was knock-down by shRNA. Scale bars, 20 µm. **c,** Cdx2 and H2B expression level for all individual cells in one control and one Pard6b knock-down embryo. **d,** Cdx2 expression down-regulation in embryos with suppressed Pard6b expression for a collection of all cells of several embryos (*N* = 3 embryos for each condition).

Induction of the apical domain in an apolar 1/8th blastomere

Finally, I wished to experimentally test whether the acquisition of the apical domain is sufficient for predicting and inducing the TE fate. The interplay between cell polarity and cell-cell adhesion in the whole embryo so far had precluded researchers from testing the sufficiency of a potential factor for TE fate specification. Here, I took an advantage of the self-organizing system of 1/8th blastomere development, and attempted to induce an apical domain in an as-yet apolar cell, in order to examine whether this induced apical domain is sufficient to drive the asymmetric division and TE fate specification as was observed in the development of normal 1/8th blastomeres.

To induce an apical domain in an apolar 1/8th blastomere I tried to directly manipulate molecules involved in the establishment of the apical domain, such as PI(4,5)P_2, Cdc42, Ras homolog gene family member A (RhoA) and Ezrin. First, I attempted to locally increase the concentration of PI(4,5)P_2 by employing light-inducible ("caged") version of PI(4,5)P_2. The local elevation in PI(4,5)P_2 concentration on the plasma membrane of apolar 1/8th blastomere led to increased polymerization of actin at the site of uncaging that resembled initiation of the apical domain formation (Fig. 4.12a). The local uncaging of 1,2-POG, used as a control, showed no effect on actin polymerization. Unfortunately, none of the treated blastomeres survived for longer than 30 min. Another approach I used was photoactivation of Cdc42 and RhoA employing the phytochrome system. However, while NIH-3T3 cells stably transfected with pHR-PhyB-mCherry-CAAX and pHR-iSH-YFP-Pif, used as control, developed protrusions at the activation site, this approach has not provided desired result in the 1/8th blastomeres in the same conditions (Fig. 4.12b,c). Finally, I learned from Takeshi Matsui that in fibroblasts PLL coated beads can recruit Ezrin-Radixin-Moesin proteins to the contact site with the bead and facilitate their phosphorylation. Hence, I used PLL coated beads to attempt to induce Ezrin clustering in an apolar 1/8th blastomere. Surprisingly, contact with such beads did not recruit Ezrin, but directed the formation of the apical domain systematically to the opposite side, away from the contact (Fig. 4.12d).

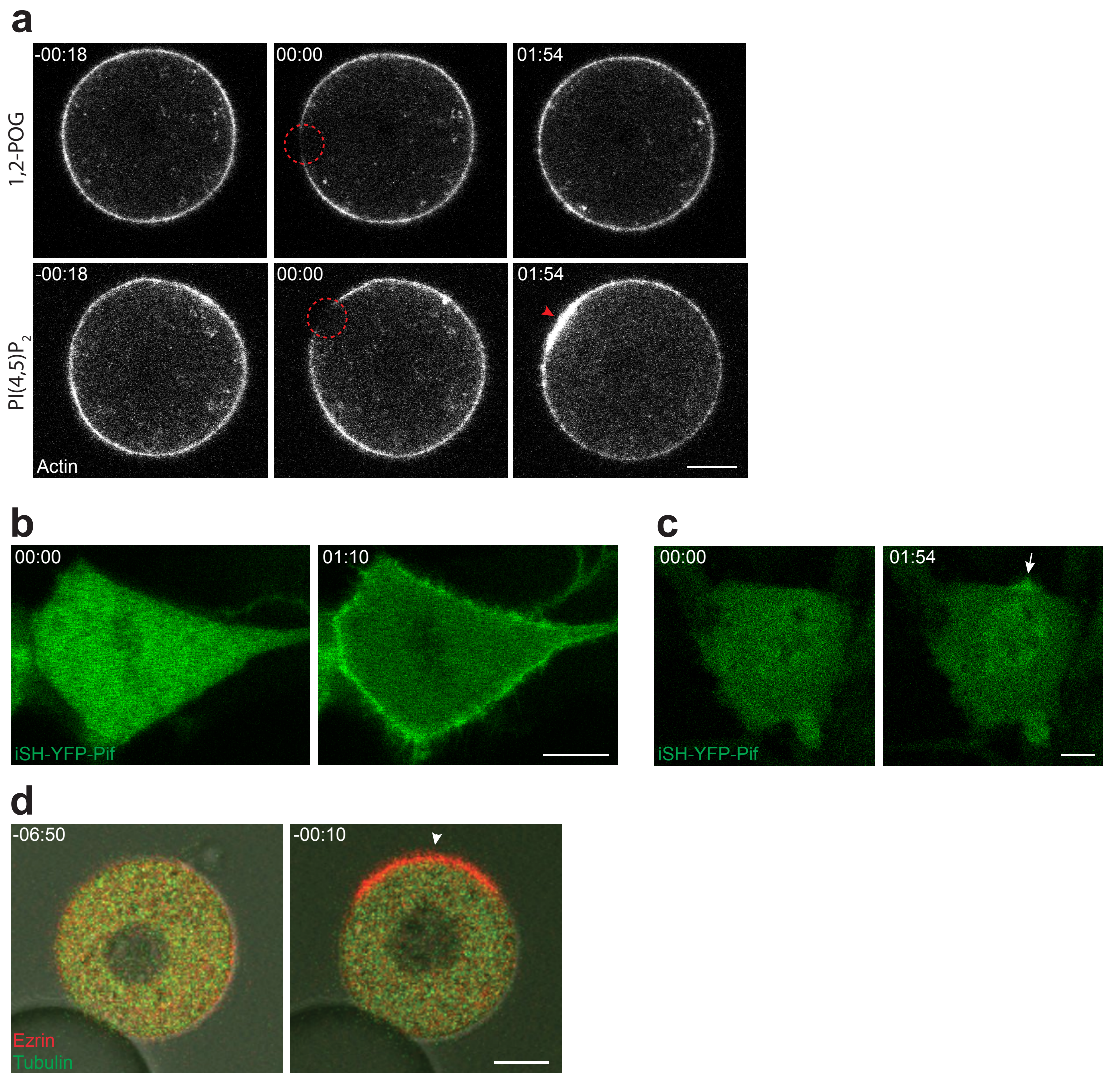
a
1,2-POG
PI(4,5)P2
-00:18
00:00
01:54
-00:18
00:00
01:54
Actin
b
00:00
01:10
iSH-YFP-Pif
c
00:00
01:54
iSH-YFP-Pif
d
-06:50
-00:10
Ezrin
Tubulin

Figure 4.12: Induction of the apical domain in an apolar 1/8th blastomere.

a, Local PI(4,5)P_2 and 1,2-POG uncaging in an apolar 1/8th blastomere expressing EGFP-hUtrCH. The site of uncaging is marked by a red circle. Red arrowhead marks the increased actin polymerization at the site of uncaging. **b,** Global activation of phosphoinositide 3-kinase (PI3K) in NIH-3T3 cells. **c,** Local activation of PI3K in NIH-3T3 cells. The white arrow marks the local accumulation of iSH-YFP-Pif and protrusion. **d,** PLL coated bead directs formation of the apical domain in 1/8th blastomere expressing Ezrin-mCherry and EGFP-tubulin away from the contact. The white arrowhead marks the apical domain. Time, **a** – post-uncaging (mm:ss), **b-c** – post-activation (mm:ss), **d** – post-NEBD (hh:mm). Scale bars, 10 µm.

Cdh1-independent cell contact facilitates and directs apical domain formation

Cell-cell contact is known to induce the formation of the apical domain opposite to the contact (Ziomek and Johnson, 1980). Moreover, in my experiments, PLL beads could direct the formation of the apical domain in the similar manner. Hence, in order to direct the formation of the apical domain, I developed an experimental system using cell-sized beads that by coating with specific molecules could mimic the cell-cell contact and allow spatiotemporal control of contact formation (Fig. 4.13).

Using a bead coated with Cdh1, I first confirmed that my experimental system can recapitulate the apical domain induction directed by cell-cell contact (Ziomek and Johnson, 1980). When compared to the 1/8th blastomeres developing without cell contact, contact with Cdh1-coated bead induced the formation of the apical domain more efficiently (84%, $N = 47$ of 56 cells, compared to 66%; Fig. 4.13a), indicating that cell contact facilitates the formation of apical-basal polarity (Ziomek and Johnson, 1980). To examine if induction of polarity by the cell contact is indeed mediated by Cdh1, mzCdh1$^{-/-}$ embryos (Stephenson, Yamanaka and Rossant, 2010) were used to prepare the 1/8th blastomeres. Unexpectedly, Cdh1-coated beads formed the contact with mzCdh1$^{-/-}$ 1/8th blastomeres, and this contact efficiently induced the apical domain formation on the side opposite to the contact (86%, $N = 12$ of 14 cells; Fig. 4.13b). This finding was confirmed by using another biologically inert bead made of PMMA that also maintained the contact to mzCdh1$^{-/-}$ blastomeres (86%, $N = 12$ of 14 cells; Fig. 4.13c). These findings demonstrate that the cell contact can facilitate cellular symmetry breaking of the 8-cell stage blastomere and the apical-basal polarization independently of Cdh1.

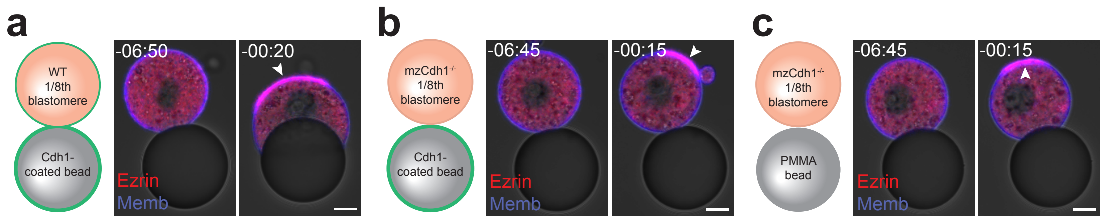
a
WT 1/8th blastomere
Cdh1-coated bead
-06:50
-00:20
Ezrin
Memb
b
mzCdh1-/- 1/8th blastomere
Cdh1-coated bead
-06:45
-00:15
Ezrin
Memb
c
mzCdh1-/- 1/8th blastomere
PMMA bead
-06:45
-00:15
Ezrin
Memb

Figure 4.13: Non-Cdh1-mediated contact facilitates cellular symmetry breaking.

a, Cdh1-coated beads induce the apical domain opposite to the contact in WT 1/8th blastomeres, microinjected with Ezrin-mCherry and Myr-palm-IFP (Memb) mRNAs. **b,** mzCdh1$^{-/-}$ 1/8th blastomeres, expressing Ezrin-mCherry and Myr-palm-IFP, form apical domain opposite to the contact with Cdh1-coated beads. **c,** PMMA-bead induces the apical domain in mzCdh1$^{-/-}$ 1/8th blastomeres as shown by Ezrin-mCherry signal. White arrowheads mark apical domain. Time, post-NEBD (hh:mm). Scale bars, 10 µm.

Induced apical domain predicts spindle orientation and TE-fate specification

When 1/8th blastomeres were placed in a contact with PMMA-beads, cell contact induced the apical domain formation in any surface area but excluding the contact and preferentially in the opposite hemisphere (N = 24, P < 0.001; Fig. 4.14a,b). Like apical domain formed without the contact, the induced apical domain was differentially segregated during 1/8th-to-2/16th-cell stage division (N = 17 of 26 cells; Fig. 4.14a,c). Moreover, in all blastomeres that inherited the apical domain the level of Cdx2 expression was higher compared to their sister blastomeres (N = 20 cells; Fig. 4.15). Thus, contact directs the position of the apical domain, which induces TE fate in the daughter cell inheriting it after asymmetric division.

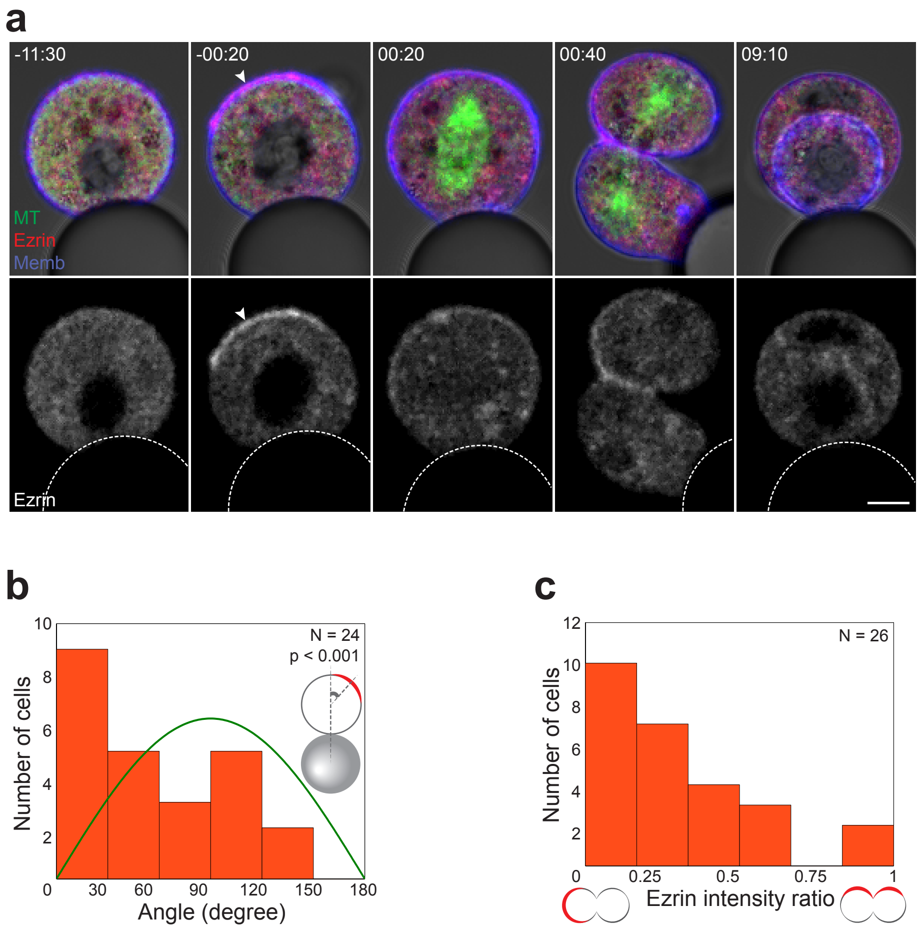

Figure 4.14: Contact with the PMMA bead directs formation of the apical domain and its differential segregation.

a, Time-lapse images of the 1/8th blastomere, derived from an R26-EGFP-Tuba (MT) embryo and microinjected with Ezrin-mCherry and Myr-palm-IFP (Memb) mRNAs, developing in contact with a PMMA-bead. Time, post-NEBD (hh:mm). Scale bar, 10 µm. **b,** Apical domain forms preferentially within the hemisphere opposite to the cell contact, and induces its differential segregation. **c,** 1/8th blastomeres cultured in contact with the bead differentially segregate apical domain during 1/8th-to-2/16th-cell stage division.

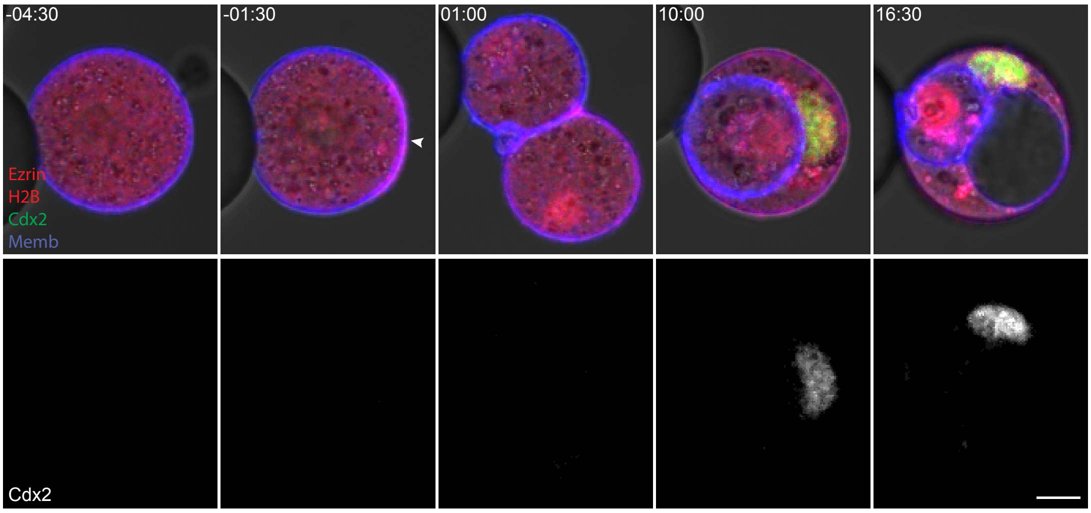

Figure 4.15: Induced apical domain predicts TE cell fate.

Time-lapse images of the 1/8th blastomere, derived from a Cdx2-EGFP x R26-H2B-mCherry embryo and microinjected with Ezrin-mCherry and Myr-palm-IFP (Memb) mRNAs, developing in contact with a PMMA-bead. Contact with the bead directs formation of the apical domain to the opposite side, away from the contact. Blastomere inheriting apical domain after asymmetric division up-regulates Cdx2 expression. Time, post-NEBD (hh:mm). Scale bar, 10 µm.

5. Discussion

In this study, I aimed to elucidate the symmetry breaking cue and the mechanism leading to differentiation of initially identical cells of the mouse pre-implantation embryo into two distinct cell types: ICM and TE. I showed that Cdh1-independent cell contact facilitates cellular symmetry breaking and directs the apical domain formation in the center of the contact-free surface. Apical domain, in turn, recruits MTOCs to the sub-apical region to form one of the spindle poles resulting in an asymmetric division. Cells inheriting apical domain after asymmetric division adopt TE fate, while apolar cells compete for the position inside the embryo and in those cells, that stay outside of the embryo, asymmetric cell contact induces apical domain formation and TE fate.

Cdh1-independent contact facilitates and directs the apical-basal polarization of the 1/8th blastomere

In the current study, I showed that the intrinsic ability of 1/8th blastomeres to self-polarize is facilitated and directed by local contact, in agreement with earlier studies (Johnson and Ziomek, 1981a; Ziomek and Johnson, 1980). The present results also show that induction of polarization by the cell contact does not require Cdh1, unlike in *C. elegance* embryo where E-cadherin plays an instructive role in the generation of cell polarity (Klompstra et al., 2015). Moreover, induction of 1/8th blastomere polarization by its attachment to the dish (data not shown) or any adhesive bead suggests the lack of molecular specificity in the nature of the inducing contact and that physical contact may be sufficient. Alternatively, specific extracellular molecules secreted by the blastomere may facilitate contact formation and cellular symmetry breaking. Thus, the nature of the contact and the mechanism by which the contact influencess the polarization of the 8-cell stage blastomeres is still unclear and awaits future studies.

Notably, 1/8th blastomeres develop the apical-basal polarity without any cell-cell, cell-extracellular matrix (ECM) or acellular contact in agreement with an earlier finding (Ziomek and Johnson, 1980). While this earlier study suggested the potential role of the remaining mid-body in induction of polarization, rendering the self-organization capacity of an isolated blastomere questionable, it is unlikely given that only one of the two daughter cells inherits the mid-body (Schiel, Childs and Prekeris, 2013), but 66% of 1/8th blastomeres derived from an embryo can polarize. Although the influence of cell history (e.g. previous cell contact) or localization of as-yet unidentified molecules cannot be excluded, it is conceivable to consider at this moment that 1/8th blastomeres can self-organize the apical-basal polarity.

Predominant asymmetric divisions of 8-cell stage blastomeres

Upon acquisition of the apical-basal polarity in the 8-cell stage blastomere, to our surprise, the majority of the cells aligns the spindle along the apical-basal axis and thus divides asymmetrically. Data presented here show that centrally positioned in the contact-free surface apical domain recruits MTOCs to the sub-apical region to form one of the spindle poles leading to an asymmetric division. Recruitment of MTOCs to the center of the apical domain at 8-cell stage was reported to depend on microtubules (Houliston, Pickering and Maro, 1987). At this stage microtubules accumulate at the apical side of the cell preceding MTOCs clustering. The microtubule accumulation might be driven by local nucleation of the microtubules or local increase in their stability mediated by apical domain. Further studies will elucidate the mechanism underlying asymmetric cell division in the 8-cell embryo and examine whether it is required for early mouse development.

While the finding that majority of 8-cell stage blastomeres divide asymmetrically is in agreement with several reports (Anani et al., 2014; Watanabe et al., 2014; Ziomek and Johnson, 1980), this may appear contradictory to other studies (Plusa, 2005; Bischoff, Parfitt and Zernicka-Goetz, 2008; Jedrusik et al., 2008) and to the cell polarity model in which the number of asymmetric divisions was proposed to determine the number of resultant inner cells (Johnson and Ziomek, 1981b). This apparent contradiction may be due to the difference in definition of asymmetric division. While in the current study asymmetric division is defined by differential segregation of the apical domain, many of the previous studies used the eventual position of the cell within the embryo to define the type of division. Namely, those divisions that give rise to two daughters, one located inside and the other outside of the embryo, were defined as an “asymmetric” division, while those generating two cells facing outside of the embryo as a “symmetric” division. My live-imaging at high spatiotemporal resolution revealed that many (26%) “symmetric” divisions, according to the earlier definition, actually result from asymmetric division, according to my new definition, followed by cell position rearrangement from inside to outside of the embryo (see Fig. 4.9a). This finding thus offers that our data can be reconciled with previous understanding that lacked the temporal resolution.

Apical domain predicts TE fate

The experiments shown here indicate that cells inheriting the apical domain after 8-to-16-cell stage division always adopt TE fate. Moreover, apolar cells that develop apical domain when outside of the embryo at the 16-cell stage, up-regulate Cdx2 expression and eventually become TE cells suggesting that apical domain is a faithful predictor of TE fate. This finding is consistent with other studies linking apical-basal polarity to TE fate specification. It was shown that the disruption of apical-basal polarity suppresses Cdx2 expression and TE fate specification (Alarcon, 2010). The underlying mechanism of Cdx2 expression control by apical-basal polarity is still not completely understood, but might be linked to the down-regulation of Hippo pathway activity through sequestering Amot from basolateral adherens junctions in outside cells (Hirate et al., 2013). Furthermore, it remains unclear whether apical domain is sufficient for the TE fate specification.

A cell's fate is specified according to its position within the embryo

The finding that as many as 26% of apolar cells repolarize and differentiate into TE indicates that cell fate is specified, not by the division pattern *per se*, but according to its eventual position within the embryo, i.e. the absence (inside) or presence (outside) of contact-free surface in which the apical domain emerges. This result indicate that the "inside-outside" model (Tarkowski and Wróblewska, 1967) can override the cell polarity model (Johnson and Ziomek, 1981b) and suggests contact to be the crucial cue to differentiate the "outside" and "inside" cells and also explains the cell-to-cell TE-gene (e.g. *Cdx2*) expression heterogeneity in morula (Dietrich and Hiiragi, 2007; Ralston and Rossant, 2008).

The eventual cell position and thus the percent of repolarizing apolar cells in the 16-cell stage embryo depends on the spatial context. Due to the high number of asymmetric divisions the number of apolar cells as a result of 8-to-16-cell stage divisions is higher than 0-5 cells that can be accommodated within the 16-cell stage embryo (Anani et al., 2014; Dietrich and Hiiragi, 2007). Those apolar cells would compete for the inside positions, and some of them be relocated to the surface of the embryo. Characterization of this cell competition and sorting mechanism, likely involving cell mechanics (Anani et al., 2014; Maitre et al., 2012), will help to fully understand the first cell lineage segregation in the mouse embryo.

In summary, cell fate in the pre-implantation embryo is specified in several consecutive steps. First, all blastomeres of the 8-cell stage embryo develop apical-basal polarity and the majority of them divide asymmetrically. Polar daughter cells adopt TE fate, while apolar sisters compete for the limited space available inside the embryo. Those apolar cells that get the inside position differentiate into ICM, whereas apolar cells that stayed outside repolarize and hence become TE (Fig. 5.1).

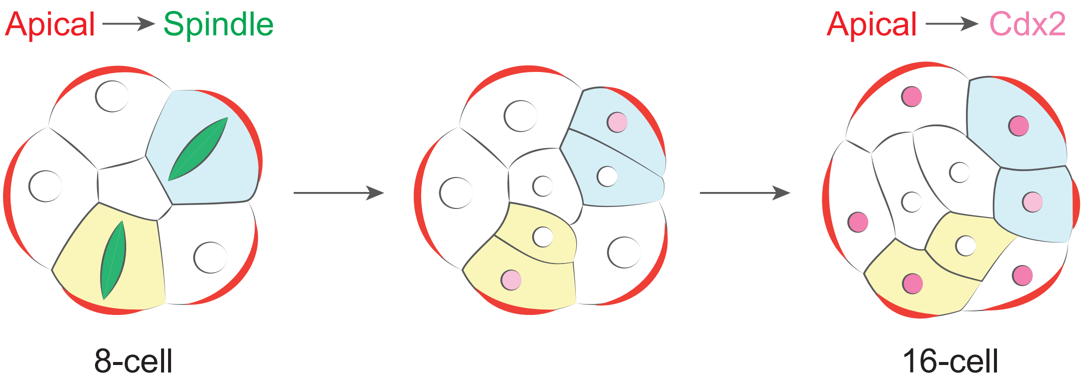

Figure 5.1: Refined model of the mouse pre-implantation development.

The apical domain directs spindle orientation in the 8-cell stage embryo, so that the majority of cells undergo asymmetric division. Polar cells become TE, as marked by Cdx2 expression, whereas apolar cells have not chosen their fate yet. At the 16-cell stage apolar cells compete for the inside position and those cells that are pushed to the surface of the embryo acquire the apical domain and adopt TE fate, while those that stay inside become ICM.

Perspectives

Taken together this study suggests that Cdh1-independent contact can direct cellular symmetry breaking and apical-basal polarization, and induces the first cell fate decision in the mouse. These data refine our understanding of the mouse pre-implantation development, as well as raise new exciting questions:

What is the mechanism of apical-basal polarization in the 8-cell stage embryo?

First, it would be interesting to know what allows blastomeres in the mouse embryo to polarize *de novo* at the 8-cell stage, but not before. It was shown that protein synthesis inhibition at the 4-cell stage (Levy et al., 1986) as well as injection of constitutively active form of RhoA (V14Rho) or Cdc42 (V12Cdc42) into 4-cell stage embryo lead to premature, appropriately oriented but aberrantly organized, polarization (Clayton, Hall and Johnson, 1999). These results suggest that already at the 4-cell stage, the embryo has all the material required for polarization and that the initiation of polarization at earlier stages is inhibited. Identification of this inhibitor will allow understanding how the timing of apical domain emergence is controlled and to identify the following cascade of events involved in apical-basal polarity establishment.

Another important aspect of apical-basal polarity establishment is how it is influenced by contact. While 1/8th blastomeres have the ability to self-polarize, I discovered that non-Cdh1-mediated contact facilitates cellular symmetry breaking and directs the apical-basal polarization in the 8-cell blastomere. The molecular identity of “contact” remains to be identified. In the future, we aim to identify the mechanism by which the “contact” induces and directs formation of the apical-basal polarity. This might involve integrin-mediated cell-ECM adhesion (specific integrins and ECM molecules are expressed at the 8-cell stage; Roberts et al., 2009; Cooper and MacQueen, 1983; Sherman et al., 1980), the physical cue of the cell contact (e.g. local block of the periodic contractile waves; Maître et al., 2015, *in press*), or a local deformation of the cell shape. “Reduced” experimental system presented in this study will be an excellent tool to address this question, as it allows full molecular and spatiotemporal control over cellular polarization.

How does a cell recognize its position within the embryo?

My study showed that cell fate is specified not by the division pattern *per se*, but according to its eventual position within the embryo. Therefore, it would be very important to understand the mechanism by which cells recognize their position within the embryo, inside or outside. Available data suggest that asymmetry in cell-cell contact may be the crucial cue to differentiate the “outside” from “inside” cells, with the presence of contact-free surface inducing the formation of apical domain and hence differentiation into TE. Therefore, we will investigate the mechanism by which apical domain formation is inhibited at the contact, with the eventual goal of inducing the apical domain in the inside cell by blocking the specific apical domain inhibitory signal coming from the cell contact.

Identification of the mechanism inhibiting apical domain formation at the contact will also provide us with an excellent basis for identification of the ICM fate inducing cue. It was shown that neither of Oct4, Nanog nor Sox2 is necessary for the ICM specification defined by expression of other ICM markers (Frum et al., 2013; Messerschmidt and Kemler, 2010; Wicklow et al., 2014). Now, my study suggests that the full cell contact, or the lack of contact-free surface, may be the crucial cue to drive the ICM differentiation. We will therefore test this hypothesis by providing contact on the whole cell surface, based on its molecular identification, and testing whether it is sufficient to drive the ICM differentiation.

What is the mechanism underlying de novo formation of epithelial polarity?

Cells in the pre-implantation mouse embryo lack cell polarity up to the early 8-cell stage and during the following days of development they progressively establish mature epithelial polarity (Collins and Fleming, 1995). This provides a unique opportunity to study *de novo* formation of epithelial polarity in a system, where the whole process can be observed under physiological conditions, using live imaging microscopy, and easily manipulated by genetics and micromanipulations.

6. References

Abe, T., Kiyonari, H., Shioi, G., Inoue, K.-I., Nakao, K., Aizawa, S. and Fujimori, T. (2011) 'Establishment of conditional reporter mouse lines at ROSA26 locus for live cell imaging.', *Genesis*, 49(7), pp. 579–590. doi: 10.1002/dvg.20753.

Aceto, D., Beers, M. and Kemphues, K. J. (2006) 'Interaction of PAR-6 with CDC-42 is required for maintenance but not establishment of PAR asymmetry in C. elegans.', *Developmental Biology*, 299(2), pp. 386–397. doi: 10.1016/j.ydbio.2006.08.002.

Akhtar, N. and Streuli, C. H. (2013) 'An integrin-ILK-microtubule network orients cell polarity and lumen formation in glandular epithelium.', *Nature Cell Biology*, 15(1), pp. 17–27. doi: 10.1038/ncb2646.

Alarcon, V. B. (2010) 'Cell Polarity Regulator PARD6B Is Essential for Trophectoderm Formation in the Preimplantation Mouse Embryo.', *Biology of Reproduction*, 83(3), pp. 347–358. doi: 10.1095/biolreprod.110.084400.

Altschuler, S. J., Angenent, S. B., Wang, Y. and Wu, L. F. (2008) 'On the spontaneous emergence of cell polarity.', *Nature*, 454(7206), pp. 886–889. doi: 10.1038/nature07119.

Anani, S., Bhat, S., Honma-Yamanaka, N., Krawchuk, D. and Yamanaka, Y. (2014) 'Initiation of Hippo signaling is linked to polarity rather than to cell position in the pre-implantation mouse embryo', *Development*, 141, pp. 2813-2824. doi:10.1242/dev.107276.

Atwood, S. X., Chabu, C., Penkert, R. R., Doe, C. Q. and Prehoda, K. E. (2007) 'Cdc42 acts downstream of Bazooka to regulate neuroblast polarity through Par-6 aPKC.', *Journal of Cell Science*, 120(18), pp. 3200–3206. doi: 10.1242/jcs.014902.

Beddington, R. and Robertson, E. J. (1999) 'Axis Development and Early Asymmetry in Mammals', *Cell*, 96(2), pp. 195–209. doi:10.1016/S0092-8674(00)80560-7.

Behringer, R. R., Eakin, G. S. and Renfree, M. B. (2006) 'Mammalian diversity: gametes, embryos and reproduction.', *Reproduction, fertility, and development*, 18(1-2), pp. 99–107. doi:10.1071/RD05137.

Benton, R. and St Johnston, D. (2003) 'Drosophila PAR-1 and 14-3-3 inhibit Bazooka/PAR-3 to establish complementary cortical domains in polarized cells.', *Cell*, 115(6), pp. 691–704. doi:10.1016/S0092-8674(03)00938-3.

Betschinger, J., Mechtler, K. and Knoblich, J. A. (2006) 'Asymmetric Segregation of the Tumor Suppressor Brat Regulates Self-Renewal in Drosophila Neural Stem Cells', *Cell*, 124(6), pp. 1241–1253. doi: 10.1016/j.cell.2006.01.038.

Betschinger, J. and Knoblich, J. A. (2004) 'Dare to be different: asymmetric cell division in Drosophila, C. elegans and vertebrates.', *Current Biology*, 14(16), pp. R674–85. doi: 10.1016/j.cub.2004.08.017.

Biggers, J. D., McGinnis, L. K. and Raffin, M. (2000) 'Amino acids and preimplantation development of the mouse in protein-free potassium simplex optimized medium.', *Biology of Reproduction*, 63(1), pp. 281–293. doi: 10.1095/biolreprod63.1.281.

Bischoff, M., Parfitt, D. E. and Zernicka-Goetz, M. (2008) 'Formation of the embryonic-abembryonic axis of the mouse blastocyst: relationships between orientation of early cleavage divisions and pattern of symmetric/asymmetric divisions', *Development*, 135(5), pp. 953–962. doi: 10.1242/dev.014316.

Boussadia, O., Kutsch, S., Hierholzer, A., Delmas, V. and Kemler, R. (2002) 'E-cadherin is a survival factor for the lactating mouse mammary gland.', *Mechanisms of development*, 115(1-2), pp. 53–62. doi:10.1016/S0925-4773(02)00090-4.

Bowman, S. K., Neumüller, R. A., Novatchkova, M., Du, Q. and Knoblich, J. A. (2006) 'The Drosophila NuMA Homolog Mud regulates spindle orientation in asymmetric cell division.', *Developmental Cell*, 10(6), pp. 731–742. doi: 10.1016/j.devcel.2006.05.005.

Brawand, D., Wahli, W. and Kaessmann, H. (2008) 'Loss of egg yolk genes in mammals and the origin of lactation and placentation.', *PLoS Biology*, 6(3), p. e63. doi: 10.1371/journal.pbio.0060063.

Burkel, B. M., Dassow, von, G. and Bement, W. M. (2007) 'Versatile fluorescent probes for actin filaments based on the actin-binding domain of utrophin.', *Cell motility and the cytoskeleton*, 64(11), pp. 822–832. doi: 10.1002/cm.20226.

Capecchi, M. R. (2005) 'Gene targeting in mice: functional analysis of the mammalian genome for the twenty-first century.', *Nature Reviews Genetics*, 6(6), pp. 507–512. doi: 10.1038/nrg1619.

Chant, J., Corrado, K., Pringle, J. R. and Herskowitz, I. (1991) 'Yeast BUD5, encoding a putative GDP-GTP exchange factor, is necessary for bud site selection and interacts with bud formation gene BEM1.', *Cell*, 65(7), pp. 1213–1224. doi:10.1016/0092-8674(91)90016-R.

Chau, A. H., Walter, J. M., Gerardin, J., Tang, C. and Lim, W. A. (2012) 'Designing Synthetic Regulatory Networks Capable of Self-Organizing Cell Polarization.', *Cell*, 151(2), pp. 320–332. doi: 10.1016/j.cell.2012.08.040.

Cheeks, R. J., Canman, J. C., Gabriel, W. N., Meyer, N., Strome, S. and Goldstein, B. (2004) 'C. elegans PAR proteins function by mobilizing and stabilizing asymmetrically localized protein complexes.', *Current Biology*, 14(10), pp. 851–862. doi: 10.1016/j.cub.2004.05.022.

Chen, L., Wang, D., Wu, Z., Ma, L. and Daley, G. Q. (2010) 'Molecular basis of the first cell fate determination in mouse embryogenesis.', *Cell research*, 20(9), pp. 982–993. doi: 10.1038/cr.2010.106.

Clark, A., Meignin, C. and Davis, I. (2007) 'A Dynein-dependent shortcut rapidly delivers axis determination transcripts into the Drosophila oocyte.', *Development*, 134(10), pp. 1955–1965. doi: 10.1242/dev.02832.

Clayton, L., Hall, A. and Johnson, M. H. (1999) 'A role for Rho-like GTPases in the polarisation of mouse eight-cell blastomeres.', *Developmental Biology*, 205(2), pp. 322–331. doi: 10.1006/dbio.1998.9117.

Collins, J. E. and Fleming, T. P. (1995) 'Epithelial differentiation in the mouse preimplantation embryo: making adhesive cell contacts for the first time.', *Trends in biochemical sciences*, 20(8), pp. 307–312. doi:10.1016/S0968-0004(00)89057-X.

Cook, H. A., Koppetsch, B. S., Wu, J. and Theurkauf, W. E. (2004) 'The Drosophila SDE3 homolog armitage is required for oskar mRNA silencing and embryonic axis specification.', *Cell*, 116(6), pp. 817–829. doi:10.1016/S0092-8674(04)00250-8.

Cooper, A. R. and MacQueen, H. A. (1983) 'Subunits of laminin are differentially synthesized in mouse eggs and early embryos.', *Developmental Biology*, 96(2), pp. 467–471. doi:10.1016/0012-1606(83)90183-5.

Courtois, A., Schuh, M., Ellenberg, J. and Hiiragi, T. (2012) 'The transition from meiotic to mitotic spindle assembly is gradual during early mammalian development.', *The Journal of Cell Biology,* 198(3), pp. 357-370. doi: 10.1083/jcb.201202135.

Couwenbergs, C., Labbé, J.-C., Goulding, M., Marty, T., Bowerman, B. and Gotta, M. (2007) 'Heterotrimeric G protein signaling functions with dynein to promote spindle positioning in C. elegans.', *The Journal of Cell Biology*, 179(1), pp. 15–22. doi: 10.1083/jcb.200707085.

Cramer, L. P. (2010) 'Forming the cell rear first: breaking cell symmetry to trigger directed cell migration.', *Nature Cell Biology*, 12(7), pp. 628–632. doi: 10.1038/ncb0710-628.

Cuenca, A. A., Schetter, A., Aceto, D., Kemphues, K. and Seydoux, G. (2003) 'Polarization of the C. elegans zygote proceeds via distinct establishment and maintenance phases.', *Development*, 130(7), pp. 1255–1265. doi: 10.1242/dev.00284.

Danielian, P. S., Muccino, D., Rowitch, D. H., Michael, S. K. and McMahon, A. P. (1998) 'Modification of gene activity in mouse embryos in utero by a tamoxifen-inducible form of Cre recombinase.', *Current Biology*, 8(24), pp. 1323–1326. doi:10.1016/S0960-9822(07)00562-3

Dard, N., Le, T., Maro, B. and Louvet-Vallée, S. (2009) 'Inactivation of aPKClambda reveals a context dependent allocation of cell lineages in preimplantation mouse embryos.', *PLoS ONE*, 4(9), p. e7117. doi: 10.1371/journal.pone.0007117.t004.

de Vries, W. N., Binns, L. T., Fancher, K. S., Dean, J., Moore, R., Kemler, R. and Knowles, B. B. (2000) 'Expression of Cre recombinase in mouse oocytes: a means to study maternal effect genes.', *Genesis*, 26(2), pp. 110–112. doi: 10.1002/(SICI)1526-

968X(200002)26:2<110::AID-GENE2>3.0.CO;2-8.

Delanoue, R., Herpers, B., Soetaert, J., Davis, I. and Rabouille, C. (2007) ‘Drosophila Squid/hnRNP helps Dynein switch from a gurken mRNA transport motor to an ultrastructural static anchor in sponge bodies.’, *Developmental Cell*, 13(4), pp. 523–538. doi: 10.1016/j.devcel.2007.08.022.

Dietrich, J. E., Panavaite, L., Gunther, S., Wennekamp, S., Groner, A., Pigge, A., Salvenmoser, S., Trono, D., Hufnagel, L. and Hiiragi, T. (2015) ‘Venus-trap in the mouse embryo reveals distinct molecular dynamics underlying specification of first embryonic lineages.’, *EMBO reports,* in revision.

Dietrich, J. E. and Hiiragi, T. (2007) ‘Stochastic patterning in the mouse pre-implantation embryo’, *Development*, 134(23), pp. 4219–4231. doi: 10.1242/dev.003798.

Doe, C. Q., Chu-LaGraff, Q., Wright, D. M. and Scott, M. P. (1991) ‘The prospero gene specifies cell fates in the Drosophila central nervous system.’, *Cell*, 65(3), pp. 451–464. doi:10.1016/0092-8674(91)90463-9.

Donnison, M., Beaton, A., Davey, H. W., Broadhurst, R., L'Huillier, P. and Pfeffer, P. L. (2005) ‘Loss of the extraembryonic ectoderm in Elf5 mutants leads to defects in embryonic patterning.’, *Development*, 132(10), pp. 2299–2308. doi: 10.1242/dev.01819.

Drubin, D. G. and Nelson, W. J. (1996) ‘Origins of Cell Polarity’, *Cell*, 84(3), pp. 335–344. doi:10.1016/S0092-8674(00)81278-7.

Ducibella, T., Ukena, T., Karnovsky, M. and Anderson, E. (1977) ‘Changes in cell surface and cortical cytoplasmic organization during early embryogenesis in the preimplantation mouse embryo.’, *The Journal of Cell Biology*, 74(1), pp. 153–167. doi: 10.1083/jcb.74.1.153.

Foe, V. E. and Alberts, B. M. (1983) ‘Studies of nuclear and cytoplasmic behaviour during the five mitotic cycles that precede gastrulation in Drosophila embryogenesis.’, *Journal of Cell Science*, 61, pp. 31-70.

Frum, T., Halbisen, M. A., Wang, C., Amiri, H. and Robson, P. (2013) ‘Oct4 Cell-Autonomously Promotes Primitive Endoderm Development in the Mouse Blastocyst.’, *Developmental Cell*, 25(6), pp. 610–622. doi:10.1016/j.devcel.2013.05.004.

Gaj, T., Gersbach, C. A. and Barbas, C. F. (2013) ‘ZFN, TALEN, and CRISPR/Cas-based methods for genome engineering.’, *Trends in biotechnology*, 31(7), pp. 397-405. doi:10.1016/j.tibtech.2013.04.004.

Goehring, N. W. and Grill, S. W. (2013) ‘Cell polarity: mechanochemical patterning.’, *Trends in cell biology*, 23(2), pp. 72–80. doi: 10.1016/j.tcb.2012.10.009.

Gordon, J. W. and Ruddle, F. H. (1981) ‘Integration and stable germ line transmission of genes injected into mouse pronuclei.’, *Science*, 214(4526), pp. 1244–1246. doi: 10.1126/science.6272397.

Gossler, A., Doetschman, T., Korn, R., Serfling, E. and Kemler, R. (1986) ‘Transgenesis by means of blastocyst-derived embryonic stem cell lines.’, *Proceedings of the National Academy of Sciences of the United States of America*, 83(23), pp. 9065–9069.

Gotta, M., Dong, Y., Peterson, Y. K., Lanier, S. M. and Ahringer, J. (2003) ‘Asymmetrically distributed C. elegans homologs of AGS3/PINS control spindle position in the early embryo.’, *Current Biology*, 13(12), pp. 1029–1037. doi:10.1016/S0960-9822(03)00371-3.

Gómez-López, S., Lerner, R. G. and Petritsch, C. (2014) ‘Asymmetric cell division of stem and progenitor cells during homeostasis and cancer.’, Cellular and Molecular Life Sciences, 71(4), pp. 575-597. doi: 10.1007/s00018-013-1386-1.

Grill, S. W., Gönczy, P., Stelzer, E. H. and Hyman, A. A. (2001) ‘Polarity controls forces governing asymmetric spindle positioning in the Caenorhabditis elegans embryo.’, *Nature*, 409(6820), pp. 630–633. doi: 10.1038/35054572.

Grill, S. W., Howard, J., Schäffer, E., Stelzer, E. and Hyman, A. A. (2003) ‘The Distribution of Active Force Generators Controls Mitotic Spindle Position’, Science, 301(5632), pp. 518-521. doi: 10.1126/science.1086560.

Guo, G., Huss, M., Tong, G. Q., Wang, C., Li Sun, L., Clarke, N. D. and Robson, P. (2010) ‘Resolution of cell fate decisions revealed by single-cell gene expression analysis from zygote to blastocyst.’, *Developmental Cell*, 18(4), pp. 675–685. doi: 10.1016/j.devcel.2010.02.012.

Halet, G., Viard, P. and Carroll, J. (2008) ‘Constitutive PtdIns(3,4,5)P3 synthesis promotes the development and survival of early mammalian embryos.’, *Development*, 135(3), pp. 425–429. doi: 10.1242/dev.014894.

Hao, Y., Boyd, L. and Seydoux, G. (2006) ‘Stabilization of cell polarity by the C. elegans RING protein PAR-2.’, *Developmental Cell*, 10(2), pp. 199–208. doi: 10.1016/j.devcel.2005.12.015.

Hillman, N., Sherman, M. I. and Graham, C. (1972) ‘The effect of spatial arrangement on cell determination during mouse development.’, *Journal of embryology and experimental morphology*, 28(2), pp. 263–278.

Hirate, Y., Hirahara, S., Inoue, K.-I., Suzuki, A., Alarcon, V. B., Akimoto, K., Hirai, T., Hara, T., Adachi, M., Chida, K., Ohno, S., Marikawa, Y., Nakao, K., Shimono, A. and Sasaki, H. (2013) ‘Polarity-dependent distribution of angiomotin localizes Hippo signaling in preimplantation embryos.’, *Current Biology*, 23(13), pp. 1181–1194. doi: 10.1016/j.cub.2013.05.014.

Hoege, C. and Hyman, A. A. (2013) ‘Principles of PAR polarity in Caenorhabditis elegans embryos.’, *Nature Reviews Molecular Cell Biology*, 14(5), pp. 315–322. doi: 10.1038/nrm3558.

Houliston, E., Pickering, S. J. and Maro, B. (1987) ‘Redistribution of microtubules and pericentriolar material during the development of polarity in mouse blastomeres.’, *The Journal of Cell Biology*, 104(5), pp. 1299–1308. doi: 10.1083/jcb.104.5.1299.

Hutterer, A., Betschinger, J., Petronczki, M. and Knoblich, J. A. (2004) ‘Sequential roles of Cdc42, Par-6, aPKC, and Lgl in the establishment of epithelial polarity during Drosophila embryogenesis.’, *Developmental Cell*, 6(6), pp. 845–854. doi: 10.1016/j.devcel.2004.05.003.

Huynh, J.-R. and St Johnston, D. (2004) ‘The origin of asymmetry: early polarisation of the Drosophila germline cyst and oocyte.’, *Current Biology*, 14(11), pp. R438–49. doi: 10.1016/j.cub.2004.05.040.

Ikeshima-Kataoka, H., Skeath, J. B., Nabeshima, Y., Doe, C. Q. and Matsuzaki, F. (1997) ‘Miranda directs Prospero to a daughter cell during Drosophila asymmetric divisions.’, *Nature*, 390(6660), pp. 625–629. doi: 10.1038/37641.

Irazoqui, J. E., Gladfelter, A. S. and Lew, D. J. (2003) ‘Scaffold-mediated symmetry breaking by Cdc42p.’, *Nature Cell Biology*, 5(12), pp. 1062–1070. doi: 10.1038/ncb1068.

Izumi, Y., Ohta, N., Hisata, K., Raabe, T. and Matsuzaki, F. (2006) ‘Drosophila Pins-binding protein Mud regulates spindle-polarity coupling and centrosome organization.’, *Nature Cell Biology*, 8(6), pp. 586–593. doi: 10.1038/ncb1409.

Jedrusik, A., Parfitt, D.-E., Guo, G., Skamagki, M., Grabarek, J. B., Johnson, M. H., Robson, P. and Zernicka-Goetz, M. (2008) ‘Role of Cdx2 and cell polarity in cell allocation and specification of trophectoderm and inner cell mass in the mouse embryo.’, *Genes & Development*, 22(19), pp. 2692–2706. doi: 10.1101/gad.486108.

Johnson, M. H. (2009) ‘From Mouse Egg to Mouse Embryo: Polarities, Axes, and Tissues.’, *Annual Review of Cell and Developmental Biology*, 25(1), pp. 483–512. doi: 10.1146/annurev.cellbio.042308.113348.

Johnson, M. H. and McConnell, J. M. L. (2004) ‘Lineage allocation and cell polarity during mouse embryogenesis.’, *Seminars in Cell & Developmental Biology*, 15(5), pp. 583–597. doi: 10.1016/j.semcdb.2004.04.002.

Johnson, M. H. and Ziomek, C. A. (1983) ‘Cell interactions influence the fate of mouse blastomeres undergoing the transition from the 16- to the 32-cell stage.’, *Developmental Biology*, 95(1), pp. 211-218. doi:10.1016/0012-1606(83)90019-2.

Johnson, M. H. and Ziomek, C. A. (1981a) ‘Induction of polarity in mouse 8-cell blastomeres: specificity, geometry, and stability.’, *The Journal of Cell Biology*, 91(1), pp. 303–308. doi: 10.1083/jcb.91.1.303.

Johnson, M. H. and Ziomek, C. A. (1981b) 'The foundation of two distinct cell lineages within the mouse morula.', *Cell*, 24(1), pp. 71-80. doi:10.1016/0092-8674(81)90502-X.

Johnson, M. H., Maro, B. and Takeichi, M. (1986) 'The role of cell adhesion in the synchronization and orientation of polarization in 8-cell mouse blastomeres.', *Journal of Embryology and Experimental Morphology*, 93, 239-255.

Kawagishi, R., Tahara, M., Sawada, K., Morishige, K., Sakata, M., Tasaka, K. and Murata, Y. (2004) 'Na+/H+ Exchanger-3 is involved in mouse blastocyst formation.', *Journal of Experimental Zoology*, 301A(9), pp. 767–775. doi: 10.1002/jez.a.90.

Kelly, S. J. (1977) 'Studies of the developmental potential of 4- and 8-cell stage mouse blastomeres.', *Journal of Experimental Zoology*, 200(3), pp. 365–376. doi: 10.1002/jez.1402000307.

Klompstra, D., Anderson, D. C., Yeh, J. Y., Zilberman, Y. and Nance, J. (2015) 'An instructive role for C. elegans E-cadherin in translating cell contact cues into cortical polarity.', *Nature Cell Biology*. doi: 10.1038/ncb3168.

Lee, C.-Y., Wilkinson, B. D., Siegrist, S. E., Wharton, R. P. and Doe, C. Q. (2006) 'Brat is a Miranda cargo protein that promotes neuronal differentiation and inhibits neuroblast self-renewal.', *Developmental Cell*, 10(4), pp. 441–449. doi: 10.1016/j.devcel.2006.01.017.

Lehtonen, E. (1980) 'Changes in cell dimensions and intercellular contacts during cleavage-stage cell cycles in mouse embryonic cells.', *Journal of embryology and experimental morphology*, 58, pp. 231–249.

Levy, J. B., Johnson, M. H., Goodall, H. and Maro, B. (1986) 'The timing of compaction: control of a major developmental transition in mouse early embryogenesis.', *Journal of embryology and experimental morphology*, 95, pp. 213–237.

Li, R. and Gundersen, G. G. (2008) 'Beyond polymer polarity: how the cytoskeleton builds a polarized cell.', *Nature Reviews Molecular Cell Biology*, 9(11), pp. 860–873. doi: 10.1038/nrm2522.

Liu, H., Wu, Z., Shi, X., Li, W., Liu, C., Wang, D., Ye, X., Liu, L., Na, J., Cheng, H. and Chen, L. (2013) 'Atypical PKC, regulated by Rho GTPases and Mek/Erk, phosphorylates Ezrin during eight-cell embryo compaction.', *Developmental Biology*, 375(1), pp. 13–22. doi: 10.1016/j.ydbio.2013.01.002.

Lois, C., Hong, E. J., Pease, S., Brown, E. J. and Baltimore, D. (2002) 'Germline transmission and tissue-specific expression of transgenes delivered by lentiviral vectors.', *Science*, 295(5556), pp. 868–872. doi: 10.1126/science.1067081.

Louvet, S., Aghion, J., Santa-Maria, A., Mangeat, P. and Maro, B. (1996) 'Ezrin becomes restricted to outer cells following asymmetrical division in the preimplantation mouse embryo.', *Developmental Biology*, 177(2), pp. 568–579. doi: 10.1006/dbio.1996.0186.

Lu, B., Rothenberg, M., Jan, L. Y. and Jan, Y. N. (1998) 'Partner of Numb colocalizes with Numb during mitosis and directs Numb asymmetric localization in Drosophila neural and muscle progenitors.', *Cell*, 95(2), pp. 225–235. doi:10.1016/S0092-8674(00)81753-5.

Maître, JL., Niwayama, R., Turlier, H., Nédélec, F., Hiiragi, T. (2015) 'Pulsatile cell-autonomous contractility drives compaction in the mouse embryo.', *Nature Cell Biology* (in press).

Maitre, J. L., Berthoumieux, H., Krens, S. F. G., Salbreux, G., Julicher, F., Paluch, E. and Heisenberg, C. P. (2012) 'Adhesion Functions in Cell Sorting by Mechanically Coupling the Cortices of Adhering Cells', *Science*, 338(6104), pp. 253–256. doi: 10.1126/science.1225399.

Manejwala, F. M., Cragoe, E. J. and Schultz, R. M. (1989) 'Blastocoel expansion in the preimplantation mouse embryo: Role of extracellular sodium and chloride and possible apical routes of their entry.', *Developmental Biology*, 133(1), pp. 210-220. doi:10.1016/0012-1606(89)90312-6.

Marco, E., Wedlich-Soldner, R., Li, R., Altschuler, S. J. and Wu, L. F. (2007) 'Endocytosis optimizes the dynamic localization of membrane proteins that regulate cortical polarity.', *Cell*, 129(2), pp. 411–422. doi: 10.1016/j.cell.2007.02.043.

Mazumdar, A. and Mazumdar, M. (2002) 'How one becomes many: Blastoderm cellularization in Drosophila melanogaster.', *Bioessays*, 24(11), pp. 1012-22. doi : 10.1002/bies.10184.

McDole, K. and Zheng, Y. (2012) 'Generation and live imaging of an endogenous Cdx2 reporter mouse line.', *genesis*, 50(10), pp. 775–782. doi: 10.1002/dvg.22049.

McDole, K., Xiong, Y., Iglesias, P. A. and Zheng, Y. (2011) 'Lineage mapping the pre-implantation mouse embryo by two-photon microscopy, new insights into the segregation of cell fates.', *Developmental Biology*, 355(2), pp. 239–249. doi: 10.1016/j.ydbio.2011.04.024.

Messerschmidt, D. M. and Kemler, R. (2010) 'Nanog is required for primitive endoderm formation through a non-cell autonomous mechanism.', *Developmental Biology*, 344(1), pp. 129–137. doi: 10.1016/j.ydbio.2010.04.020.

Meyer, M., de Angelis, M. H., Wurst, W. and Kühn, R. (2010) 'Gene targeting by homologous recombination in mouse zygotes mediated by zinc-finger nucleases.', *Proceedings of the National Academy of Sciences*, 107(34), pp. 15022–15026. doi: 10.1073/pnas.1009424107.

Mitsui, K., Tokuzawa, Y., Itoh, H., Segawa, K. and Murakami, M. (2003) 'The Homeoprotein Nanog Is Required for Maintenance of Pluripotency in Mouse Epiblast and ES Cells.', *Cell,* 113, pp. 631–642. doi:10.1016/S0092-8674(03)00393-3.

Mogilner, A., Allard, J. and Wollman, R. (2012) 'Cell polarity: quantitative modeling as a tool in cell biology.', *Science*, 336(6078), pp. 175–179. doi: 10.1126/science.1216380.

Morin, X. and Bellaïche, Y. (2011) 'Mitotic Spindle Orientation in Asymmetric and Symmetric Cell Divisions during Animal Development.', *Developmental Cell*, 21(1), pp. 102–119. doi: 10.1016/j.devcel.2011.06.012.

Mouse Genome Sequencing Consortium, Waterston, R. H., Lindblad-Toh, K., Birney, E., Rogers, J., Abril, J. F., Agarwal, P., Agarwala, R., Ainscough, R., Alexandersson, M., An, P., Antonarakis, S. E., Attwood, J., Baertsch, R., Bailey, J., Barlow, K., Beck, S., Berry, E., Birren, B., Bloom, T., Bork, P., Botcherby, M., Bray, N., Brent, M. R., Brown, D. G., Brown, S. D., Bult, C., Burton, J., Butler, J., Campbell, R. D., Carninci, P., Cawley, S., Chiaromonte, F., Chinwalla, A. T., Church, D. M., Clamp, M., Clee, C., Collins, F. S., Cook, L. L., Copley, R. R., Coulson, A., Couronne, O., Cuff, J., Curwen, V., Cutts, T., Daly, M., David, R., Davies, J., Delehaunty, K. D., Deri, J., Dermitzakis, E. T., Dewey, C., Dickens, N. J., Diekhans, M., Dodge, S., Dubchak, I., Dunn, D. M., Eddy, S. R., Elnitski, L., Emes, R. D., Eswara, P., Eyras, E., Felsenfeld, A., Fewell, G. A., Flicek, P., Foley, K., Frankel, W. N., Fulton, L. A., Fulton, R. S., Furey, T. S., Gage, D., Gibbs, R. A., Glusman, G., Gnerre, S., Goldman, N., Goodstadt, L., Grafham, D., Graves, T. A., Green, E. D., Gregory, S., Guigó, R., Guyer, M., Hardison, R. C., Haussler, D., Hayashizaki, Y., Hillier, L. W., Hinrichs, A., Hlavina, W., Holzer, T., Hsu, F., Hua, A., Hubbard, T., Hunt, A., Jackson, I., Jaffe, D. B., Johnson, L. S., Jones, M., Jones, T. A., Joy, A., Kamal, M., Karlsson, E. K., Karolchik, D., Kasprzyk, A., Kawai, J., Keibler, E., Kells, C., Kent, W. J., Kirby, A., Kolbe, D. L., Korf, I., Kucherlapati, R. S., Kulbokas, E. J., Kulp, D., Landers, T., Leger, J. P., Leonard, S., Letunic, I., Levine, R., Li, J., Li, M., Lloyd, C., Lucas, S., Ma, B., Maglott, D. R., Mardis, E. R., Matthews, L., Mauceli, E., Mayer, J. H., McCarthy, M., McCombie, W. R., McLaren, S., McLay, K., McPherson, J. D., Meldrim, J., Meredith, B., Mesirov, J. P., Miller, W., Miner, T. L., Mongin, E., Montgomery, K. T., Morgan, M., Mott, R., Mullikin, J. C., Muzny, D. M., Nash, W. E., Nelson, J. O., Nhan, M. N., Nicol, R., Ning, Z., Nusbaum, C., O'Connor, M. J., Okazaki, Y., Oliver, K., Overton-Larty, E., Pachter, L., Parra, G., Pepin, K. H., Peterson, J., Pevzner, P., Plumb, R., Pohl, C. S., Poliakov, A., Ponce, T. C., Ponting, C. P., Potter, S., Quail, M., Reymond, A., Roe, B. A., Roskin, K. M., Rubin, E. M., Rust, A. G., Santos, R., Sapojnikov, V., Schultz, B., Schultz, J., Schwartz, M. S., Schwartz, S., Scott, C., Seaman, S., Searle, S., Sharpe, T., Sheridan, A., Shownkeen, R., Sims, S., Singer, J. B., Slater, G., Smit, A., Smith, D. R., Spencer, B., Stabenau, A., Stange-Thomann, N., Sugnet, C., Suyama, M., Tesler, G., Thompson, J., Torrents, D., Trevaskis, E., Tromp, J., Ucla, C., Ureta-Vidal, A., Vinson, J. P., Niederhausern, Von, A. C., Wade, C. M., Wall, M., Weber, R. J., Weiss, R. B., Wendl, M. C., West, A. P., Wetterstrand, K., Wheeler, R., Whelan, S., Wierzbowski, J., Willey, D., Williams, S., Wilson, R. K., Winter, E., Worley, K. C., Wyman, D., Yang, S., Yang, S.-P., Zdobnov, E. M., Zody, M. C. and Lander, E. S. (2002) 'Initial sequencing and comparative analysis of the mouse genome.', *Nature*, 420(6915), pp. 520–562. doi: 10.1038/nature01262.

Munro, E. and Bowerman, B. (2009) ‘Cellular symmetry breaking during Caenorhabditis elegans development.’, *Cold Spring Harbor Perspectives in Biology*, 1(4), p. a003400. doi: 10.1101/cshperspect.a003400.

Munro, E., Nance, J. and Priess, J. R. (2004) ‘Cortical flows powered by asymmetrical contraction transport PAR proteins to establish and maintain anterior-posterior polarity in the early C. elegans embryo.’, *Developmental Cell*, 7(3), pp. 413–424. doi: 10.1016/j.devcel.2004.08.001.

Muzumdar, M. D., Tasic, B., Miyamichi, K., Li, L. and Luo, L. (2007) ‘A global double-fluorescent Cre reporter mouse.’, *Genesis*, 45(9), pp. 593–605. doi: 10.1002/dvg.20335.

Nagashima, H., Matsui, K., Sawasaki, T. and Kano, Y. (1984) ‘Production of monozygotic mouse twins from microsurgically bisected morulae.’, *Journal of reproduction and fertility*, 70(1), pp. 357–362.

Nance, J. and Zallen, J. A. (2011) ‘Elaborating polarity: PAR proteins and the cytoskeleton.’, *Development*, 138(5), pp. 799–809. doi: 10.1242/dev.053538.

Nguyen-Ngoc, T., Afshar, K. and Gönczy, P. (2007) ‘Coupling of cortical dynein and Gα proteins mediates spindle positioning in Caenorhabditis elegans.’, *Nature Cell Biology*, 9(11), pp. 1294–1302. doi: 10.1038/ncb1649.

Nichols, J., Zevnik, B., Anastassiadis, K. and Niwa, H. (1998) ‘Formation of Pluripotent Stem Cells in the Mammalian Embryo Depends on the POU Transcription Factor Oct4.’, *Cell*, 95(3), pp. 379-91. doi:10.1016/S0092-8674(00)81769-9

Nishioka, N., Inoue, K.-I., Adachi, K., Kiyonari, H., Ota, M., Ralston, A., Yabuta, N., Hirahara, S., Stephenson, R. O., Ogonuki, N., Makita, R., Kurihara, H., Morin-Kensicki, E. M., Nojima, H., Rossant, J., Nakao, K., Niwa, H. and Sasaki, H. (2009) ‘The Hippo signaling pathway components Lats and Yap pattern Tead4 activity to distinguish mouse trophectoderm from inner cell mass.’, *Developmental Cell*, 16(3), pp. 398–410. doi: 10.1016/j.devcel.2009.02.003.

O'Farrell, P. H., Stumpff, J. and Su, T. T. (2004) ‘Embryonic cleavage cycles: how is a mouse like a fly?’, *Current Biology*, 14(1), pp. R35–45. doi:10.1016/j.cub.2003.12.022.

Okada, Y., Takeda, S., Tanaka, Y., Izpisúa Belmonte, J.-C. and Hirokawa, N. (2005) ‘Mechanism of nodal flow: a conserved symmetry breaking event in left-right axis determination.’, *Cell*, 121(4), pp. 633–644. doi: 10.1016/j.cell.2005.04.008.

Pauken, C. M. and Capco, D. G. (2000) ‘The Expression and Stage-Specific Localization of Protein Kinase C Isotypes during Mouse Preimplantation Development.’, *Developmental Biology*, 223(2), pp. 411–421. doi: 10.1006/dbio.2000.9763.

Perona, R. M. and Wassarman, P. M. (1986) ‘Mouse blastocysts hatch in vitro by using a trypsin-like proteinase associated with cells of mural trophectoderm.', *Developmental Biology*, 114(1), pp. 42–52. doi:10.1016/0012-1606(86)90382-9.

Petricka, J. J., Van Norman, J. M. and Benfey, P. N. (2009) 'Symmetry breaking in plants: molecular mechanisms regulating asymmetric cell divisions in Arabidopsis.', *Cold Spring Harbor Perspectives in Biology*, 1(5), p. a000497. doi: 10.1101/cshperspect.a000497.

Petronczki, M. and Knoblich, J A (2001) 'DmPAR-6 directs epithelial polarity and asymmetric cell division of neuroblasts in Drosophila.', *Nature Cell Biology*, 3(1), pp. 43–49. doi: 10.1038/35050550.

Pickering, S. J., Maro, B., Johnson, M. H. and Skepper, J. N. (1988) 'The influence of cell contact on the division of mouse 8-cell blastomeres.', *Development*, 103(2), pp. 353–363.

Plusa, B. (2005) 'Downregulation of Par3 and aPKC function directs cells towards the ICM in the preimplantation mouse embryo.', *Journal of Cell Science*, 118(3), pp. 505–515. doi: 10.1242/jcs.01666.

Poser, I., Sarov, M., Hutchins, J. R. A., Hériché, J.-K., Toyoda, Y., Pozniakovsky, A., Weigl, D., Nitzsche, A., Hegemann, B., Bird, A. W., Pelletier, L., Kittler, R., Hua, S., Naumann, R., Augsburg, M., Sykora, M. M., Hofemeister, H., Zhang, Y., Nasmyth, K., White, K. P., Dietzel, S., Mechtler, K., Durbin, R., Stewart, A. F., Peters, J.-M., Buchholz, F. and Hyman, A. A. (2008) 'BAC TransgeneOmics: a high-throughput method for exploration of protein function in mammals.', *Nature Methods*, 5(5), pp. 409–415. doi: 10.1038/nmeth.1199.

Prehoda, K. E. (2009) 'Polarization of Drosophila neuroblasts during asymmetric division.', *Cold Spring Harbor Perspectives in Biology*, 1(2), p. a001388. doi: 10.1101/cshperspect.a001388.

Qiu, Z., Liu, M., Chen, Z., Shao, Y., Pan, H., Wei, G., Yu, C., Zhang, L., Li, X., Wang, P., Fan, H.-Y., Du, B., Liu, B., Liu, M. and Li, D. (2013) 'High-efficiency and heritable gene targeting in mouse by transcription activator-like effector nucleases.', *Nucleic acids research*, 41(11), p. e120. doi: 10.1093/nar/gkt258.

Ralston, A. and Rossant, J. (2008) 'Cdx2 acts downstream of cell polarization to cell-autonomously promote trophectoderm fate in the early mouse embryo.', *Developmental Biology*, 313(2), pp. 614–629. doi: 10.1016/j.ydbio.2007.10.054.

Ralston, A., Cox, B. J., Nishioka, N., Sasaki, H., Chea, E., Rugg-Gunn, P., Guo, G., Robson, P., Draper, J. S. and Rossant, J. (2010) 'Gata3 regulates trophoblast development downstream of Tead4 and in parallel to Cdx2.', *Development*, 137(3), pp. 395–403. doi: 10.1242/dev.038828.

Riechmann, V. and Ephrussi, A. (2001) 'Axis formation during Drosophila oogenesis.', *Current opinion in genetics & development*, 11(4), pp. 374-383. doi:10.1016/S0959-437X(00)00207-0.

Roberts, J. E., Nikolopoulos, S. N., Oktem, O., Giancotti, F., Oktay, K. and FACOG (2009) ‘Integrin beta-4 signaling plays a key role in mouse embryogenesis.’, *Reproductive Sciences*, 16(3), pp. 286–293. doi: 10.1177/1933719108325506.

Rose, L. S. and Kemphues, K. J. (1998) ‘Early patterning of the *C. Elegans* embryo.’, *Annual Review of Genetics*, 32, pp. 521-545. doi: 10.1146/annurev.genet.32.1.521.

Rossant, J. and Lis, W. T. (1979) ‘Potential of isolated mouse inner cell masses to form trophectoderm derivatives in vivo.’, *Developmental Biology*, 70(1), pp. 255–261. doi: 10.1016/0012-1606(79)90022-8.

Rossant, J. and Tam, P. P. L. (2009) ‘Blastocyst lineage formation, early embryonic asymmetries and axis patterning in the mouse.’, *Development*, 136(5), pp. 701–713. doi: 10.1242/dev.017178.

Rossant, J. and Vijh, K. M. (1980) ‘Ability of outside cells from preimplantation mouse embryos to form inner cell mass derivatives.’, *Developmental Biology*, 76(2), pp. 475-482. doi:10.1016/0012-1606(80)90395-4.

Roth, S. and Lynch, J. A. (2009) ‘Symmetry breaking during Drosophila oogenesis.’, *Cold Spring Harbor Perspectives in Biology*, 1(2), p. a001891. doi: 10.1101/cshperspect.a001891.

Sanson, B. (2001) ‘Generating patterns from fields of cells. Examples from Drosophila segmentation.’, *EMBO reports*, 2(12), pp. 1083–1088. doi: 10.1093/embo-reports/kve255.

Schaefer, M., Shevchenko, A., Shevchenko, A. and Knoblich, J. A. (2000) ‘A protein complex containing Inscuteable and the Galpha-binding protein Pins orients asymmetric cell divisions in Drosophila.’, *Current Biology*, 10(7), pp. 353–362. doi:10.1016/S0960-9822(00)00401-2

Schiel, J. A., Childs, C. and Prekeris, R. (2013) ‘Endocytic transport and cytokinesis: from regulation of the cytoskeleton to midbody inheritance.’, *Trends in cell biology*, 23(7), pp. 319–327. doi: 10.1016/j.tcb.2013.02.003.

Schober, M., Schaefer, M. and Knoblich, J A (1999) ‘Bazooka recruits Inscuteable to orient asymmetric cell divisions in Drosophila neuroblasts.’, *Nature*, 402(6761), pp. 548–551. doi: 10.1038/990135.

Schuldt, A. J., Adams, J. H., Davidson, C. M., Micklem, D. R., Haseloff, J., St Johnston, D. and Brand, A. H. (1998) ‘Miranda mediates asymmetric protein and RNA localization in the developing nervous system.’, *Genes & Development*, 12(12), pp. 1847–1857. doi: 10.1101/gad.12.12.1847.

Servant, G., Weiner, O. D., Herzmark, P., Balla, T., Sedat, J. W. and Bourne, H. R. (2000) ‘Polarization of chemoattractant receptor signaling during neutrophil chemotaxis.’, *Science*, 287(5455), pp. 1037–1040. doi: 10.1126/science.287.5455.1037.

Shen, C. P., Jan, L. Y. and Jan, Y. N. (1997) ‘Miranda is required for the asymmetric localization of Prospero during mitosis in Drosophila.’, *Cell*, 90(3), pp. 449–458. doi:10.1016/S0092-8674(00)80505-X.

Sherman, M. I., Gay, R., Gay, S. and Miller, E. J. (1980) ‘Association of collagen with preimplantation and peri-implantation mouse embryos.’, *Developmental Biology*, 74(2), pp. 470–478. doi:10.1016/0012-1606(80)90446-7.

Siegrist, S. E. and Doe, C. Q. (2007) ‘Microtubule-induced cortical cell polarity.’, *Genes & Development*, 21(5), pp. 483–496. doi: 10.1101/gad.1511207.

Siegrist, S. E. and Doe, C. Q. (2005) ‘Microtubule-Induced Pins/Gαi Cortical Polarity in Drosophila Neuroblasts.’, *Cell*, 123(7), pp. 1323–1335. doi: 10.1016/j.cell.2005.09.043.

Siller, K. H., Cabernard, C. and Doe, C. Q. (2006) ‘The NuMA-related Mud protein binds Pins and regulates spindle orientation in Drosophila neuroblasts.’, *Nature Cell Biology*, 8(6), pp. 594–600. doi: 10.1038/ncb1412.

Speck, O., Hughes, S. C., Noren, N. K., Kulikauskas, R. M. and Fehon, R. G. (2002) ‘Moesin functions antagonistically to the Rho pathway to maintain epithelial integrity.’, *Nature*, 421(6918), pp. 83–87. doi: 10.1038/nature01295.

Srinivasan, D. G., Fisk, R. M., Xu, H. and van den Heuvel, S. (2003) ‘A complex of LIN-5 and GPR proteins regulates G protein signaling and spindle function in C elegans.’, *Genes & Development*, 17(10), pp. 1225–1239. doi: 10.1101/gad.1081203.

Stephenson, R. O., Yamanaka, Y. and Rossant, J. (2010) ‘Disorganized epithelial polarity and excess trophectoderm cell fate in preimplantation embryos lacking E-cadherin.’, *Development*, 137(20), pp. 3383–3391. doi: 10.1242/dev.050195.

Strumpf, D., Mao, C.-A., Yamanaka, Y., Ralston, A., Chawengsaksophak, K., Beck, F. and Rossant, J. (2005) ‘Cdx2 is required for correct cell fate specification and differentiation of trophectoderm in the mouse blastocyst.’, *Development,* 132, pp. 2093-2102. doi: 10.1242/dev.01801.

Sulston, J. E., Schierenberg, E., White, J. G. and Thomson, J. N. (1983) ‘The embryonic cell lineage of the nematode Caenorhabditis elegans.’, *Developmental Biology*, 100(1), pp. 64–119. doi: 10.1016/0012-1606(83)90201-4.

Suwińska, A., Czołowska, R., Ożdżeński, W. and Tarkowski, A. K. (2008) ‘Blastomeres of the mouse embryo lose totipotency after the fifth cleavage division: Expression of Cdx2 and Oct4 and developmental potential of inner and outer blastomeres of 16- and 32-cell embryos.’, *Developmental Biology*, 322(1), pp. 133–144. doi: 10.1016/j.ydbio.2008.07.019.

Suzuki, A. and Ohno, S. (2006) ‘The PAR-aPKC system: lessons in polarity.’, *Journal of Cell Science*, 119(6), pp. 979–987. doi: 10.1242/jcs.02898.

Suzuki, A., Hirata, M., Kamimura, K., Maniwa, R., Yamanaka, T., Mizuno, K., Kishikawa, M., Hirose, H., Amano, Y., Izumi, N., Miwa, Y. and Ohno, S. (2004) 'aPKC acts upstream of PAR-1b in both the establishment and maintenance of mammalian epithelial polarity.', *Current Biology*, 14(16), pp. 1425–1435. doi: 10.1016/j.cub.2004.08.021.

Takaoka, K. and Hamada, H. (2011) 'Cell fate decisions and axis determination in the early mouse embryo.', *Development*, 139(1), pp. 3–14. doi: 10.1242/dev.060095.

Tarkowski, A. K. (1961) 'Mouse Chimæras Developed from Fused Eggs.', *Nature*, 190(4779), pp. 857–860. doi: 10.1038/190857a0.

Tarkowski, A. K. and Wróblewska, J. (1967) 'Development of blastomeres of mouse eggs isolated at the 4- and 8-cell stage.', *Journal of embryology and experimental morphology*, 18(1), pp. 155–180.

Testa, G., Zhang, Y., Vintersten, K., Benes, V., Pijnappel, W. W. M. P., Chambers, I., Smith, A. J. H., Smith, A. G. and Stewart, A. F. (2003) 'Engineering the mouse genome with bacterial artificial chromosomes to create multipurpose alleles.', *Nature biotechnology*, 21(4), pp. 443–447. doi: 10.1038/nbt804.

Thomas, K. R. and Capecchi, M. R. (1987) 'Site-directed mutagenesis by gene targeting in mouse embryo-derived stem cells.', *Cell*, 51(3), pp. 503–512. doi:10.1016/0092-8674(87)90646-5.

Thompson, B. J. (2012) 'Cell polarity: models and mechanisms from yeast, worms and flies.', *Development*, 140(1), pp. 13–21. doi: 10.1242/dev.083634.

Toettcher, J. E., Gong, D., Lim, W. A. and Weiner, O. D. (2011) 'Light Control of Plasma Membrane Recruitment Using the Phy-PIF System.', *Methods Enzymology,* 497, pp. 409–423. doi: 10.1016/B978-0-12-385075-1.00017-2.

Tsunoda, Y., Yasui, T., Nakamura, K., Uchida, T. and Sugie, T. (1986) 'Effect of cutting the zona pellucida on the pronuclear transplantation in the mouse.', *Journal of Experimental Zoology*, 240(1), pp. 119–125. doi: 10.1002/jez.1402400115.

Turing, A. M. (1952) 'The chemical basis of morphogenesis.', *Philos. Trans. R. Soc. Lond. B: Biol. Sci.*, 237 (1952), pp. 37–72.

Vanzo, N. F. and Ephrussi, A. (2002) 'Oskar anchoring restricts pole plasm formation to the posterior of the Drosophila oocyte.', *Development,* 129, pp. 3705-3714.

Vestweber, D., Gossler, A., Boller, K. and Kemler, R. (1987) 'Expression and distribution of cell adhesion molecule uvomorulin in mouse preimplantation embryos.', *Developmental Biology*, 124(2), pp. 451–456. doi:10.1016/0012-1606(87)90498-2.

Vinot, S., Le, T., Ohno, S., Pawson, T., Maro, B. and Louvet-Vallée, S. (2005) 'Asymmetric distribution of PAR proteins in the mouse embryo begins at the 8-cell stage during compaction.', *Developmental Biology*, 282(2), pp. 307–319. doi: 10.1016/j.ydbio.2005.03.001.

Wagner, T. E., Hoppe, P. C., Jollick, J. D., Scholl, D. R., Hodinka, R. L. and Gault, J. B. (1981) 'Microinjection of a rabbit beta-globin gene into zygotes and its subsequent expression in adult mice and their offspring.', *Proceedings of the National Academy of Sciences of the United States of America*, 78(10), pp. 6376–6380.

Wang, H. and Dey, S. K. (2006) 'Roadmap to embryo implantation: clues from mouse models.', *Nature Reviews Genetics*, 7(3), 185–199. doi:10.1038/nrg1808.

Wang, H., Yang, H., Shivalila, C. S., Dawlaty, M. M., Cheng, A. W., Zhang, F. and Jaenisch, R. (2013) 'One-step generation of mice carrying mutations in multiple genes by CRISPR/Cas-mediated genome engineering.', *Cell*, 153(4), pp. 910–918. doi: 10.1016/j.cell.2013.04.025.

Wang, X., Chen, X. and Yang, Y. (2012) 'Spatiotemporal control of gene expression by a light-switchable transgene system.', *Nature Methods*, 9(3), pp. 266–269. doi: 10.1038/nmeth.1892.

Watanabe, T., Biggins, J. S., Tannan, N. B. and Srinivas, S. (2014) 'Limited predictive value of blastomere angle of division in trophectoderm and inner cell mass specification.', *Development*, 141(11), pp. 2279–2288. doi: 10.1242/dev.103267.

Wedlich-Soldner, R. (2003) 'Spontaneous Cell Polarization Through Actomyosin-Based Delivery of the Cdc42 GTPase.', *Science*, 299(5610), pp. 1231–1235. doi: 10.1126/science.1080944.

Wedlich-Soldner, R. and Li, R. (2003) 'Spontaneous cell polarization: undermining determinism.', *Nature Cell Biology*. Nature Publishing Group, 5(4), pp. 267–270. doi: 10.1038/ncb0403-267.

Wennekamp, S., Mesecke, S., Nédélec, F. and Hiiragi, T. (2013) 'A self-organization framework for symmetry breaking in the mammalian embryo.', *Nature Reviews Molecular Cell Biology*, 14(7), pp. 452–459. doi: 10.1038/nrm3602.

Wicklow, E., Blij, S., Frum, T., Hirate, Y., Lang, R. A., Sasaki, H. and Ralston, A. (2014) 'HIPPO pathway members restrict SOX2 to the inner cell mass where it promotes ICM fates in the mouse blastocyst.', *PLoS genetics*, 10(10), p. e1004618. doi: 10.1371/journal.pgen.1004618.

Wilhelm, J. E., Hilton, M., Amos, Q. and Henzel, W. J. (2003) 'Cup is an eIF4E binding protein required for both the translational repression of oskar and the recruitment of Barentsz.', *The Journal of Cell Biology*, 163(6), pp. 1197–1204. doi: 10.1083/jcb.200309088.

Wodarz, A. (2005) 'Molecular control of cell polarity and asymmetric cell division in Drosophila neuroblasts.', *Current Opinion in Cell Biology*, 17(5), pp. 475–481. doi: 10.1016/j.ceb.2005.08.005.

Wodarz, A., Ramrath, A., Grimm, A. and Knust, E. (2000) ‘Drosophila atypical protein kinase C associates with Bazooka and controls polarity of epithelia and neuroblasts.’, *The Journal of Cell Biology*, 150(6), pp. 1361–1374. doi: 10.1083/jcb.150.6.1361.

Wodarz, A., Ramrath, A., Kuchinke, U. and Knust, E. (1999) ‘Bazooka provides an apical cue for Inscuteable localization in Drosophila neuroblasts.’, *Nature*, 402(6761), pp. 544–547. doi: 10.1038/990128.

Yamanaka, Y., Lanner, F. and Rossant, J. (2010) ‘FGF signal-dependent segregation of primitive endoderm and epiblast in the mouse blastocyst.’, *Development*, 137(5), pp. 715–724. doi: 10.1242/dev.043471.

Yamanaka, Y., Ralston, A., Stephenson, R. O. and Rossant, J. (2006) ‘Cell and molecular regulation of the mouse blastocyst.’, *Developmental Dynamics*, 235(9), pp. 2301–2314. doi: 10.1002/dvdy.20844.

Zaessinger, S., Busseau, I. and Simonelig, M. (2006) ‘Oskar allows nanos mRNA translation in Drosophila embryos by preventing its deadenylation by Smaug/CCR4.’, *Development*, 133(22), pp. 4573–4583. doi: 10.1242/dev.02649.

Ziomek, C. A. and Johnson, M. H. (1980) ‘Cell surface interaction induces polarization of mouse 8-cell blastomeres at compaction.’, *Cell,* 21(3), pp. 935-942. doi:10.1016/0092-8674(80)90457-2.

Acknowledgements

This thesis marks the end of my PhD study. It has been a hard journey, but full of exciting discoveries, both scientific and personal.

Here I would like to thank all the people who have helped me to go through this time and to make this work possible.

First of all I am truly grateful to Takashi Hiiragi for giving me the opportunity to work on this exciting project and for his constant support during this time.

I would like to thank Alexander Aulehla, Darren Gilmour and Oliver Gruss for being part of my PhD committee and for their precious advises.

I am extremely grateful to Aurélien and Ritsuya who immensely contributed to this work and helped me to move my first steps in the molecular biology work and a fancy image analysis. Also I want to thank them for being great lab mates, who would always bring a positive atmosphere in the lab!

I thank Sebastian for teaching me the mouse work, for his patience and for catching the mice that escaped me during this time.

I am indebted to Steffi and Ramona, for being not only great labmates, but also for their wonderful support in the lab and with my personal matters. Another big thank you goes to Steffi for making delicious birthday cakes!

I thank Jean-Leon, Laura and Rukshala for reading this manuscript and for their valuable feedback. I am extremely grateful to Björn for the help with translation of my summary into German. I am also thankful to them for being great lab mates!

I would like to thank all other former and current lab members –Yusuke, Jens, Kasia, Ivica, Herve, Manu, Judith and Petr for being great labmates, for interesting discussions, for their help and advices.

I also want to thank our collaborators from Dresden (Nicolas Berger, Ina Poser and Frank Buchholz), San Francisco (Delquin Gong and Orion Weiner) and EMBL (Andre Nadler, Antonio Politi) for sharing their expertise and great contribution to my work.

This study would not be possible without excellent work of transgenic and mouse facilities. Thus, I am very thankful to Yvonne and to all animal technicians who took care of hundreds of my mice.

I want to thank my fellow predocs and especially Aleksandra and Nils for making my time at EMBL unforgettable.

I thank my family for helping me to get where I am now and for their endless support, even when they are several thousand kilometers away.

Most importantly I would like to thank Dima for his love, patience, great care and constant support during all these years!

Thank you all! Without all of you, I would have never achieved this.